M. Claeys (Referee) magda.claeys@ua.ac.be
Received and published: 6 April 2015

General comments:

This is a very comprehensive and fine study on the formation of isoprene-derived SOA during an intensive field campaign carried out at Look Rock, a site in the Ozark Mountains in the Eastern USA, where isoprene emissions during summer are known to be high. The authors have combined on-line measurements using the Aerodyne Aerosol Chemical Speciation Monitor (ACSM) with off-line chemical measurements of a suite of isoprene-related SOA tracers. The isoprene-derived SOA tracers contributed with ~9% (up to 26%) to the organic aerosol (OA) mass, and almost exclusively were made up by IEPOX-related tracers. An interesting result is that using PMF analysis of the ACSM data an IEPOX-OA factor could be derived that correlates well with off-line measured concentrations of 2-methyltetrols, C5-alkene triols, and IEPOX-derived organosulfates. There is, however, a substantial gap between the IEPOX-OA factor mass (~25%, up to 47%) accounting for 32% of the total OA, whereas that estimated by off-line isoprene SOA tracer measurements is substantially lower, i.e. ~9%, which is at present not understood but suggesting that in addition to the IEPOX-related SOA tracers there are other isoprene-related SOA tracers that are not covered by the off-line measurements. As expected, good correlations were found between particle-sulfate with both IEPOXand MAE-derived SOA tracers and the IEPOX-OA factor, supporting the important role of sulfate in isoprene SOA formation. The authors have also successfully modeled the IEPOX-derived SOA tracers 2-methyltetrols and corresponding sulfates.

We thank Professor Claeys for her very careful review of our manuscript. Her comments have improved the clarity of our manuscript.

Specific comments:

Page 7369/7370 – lines 27 – 5: The only pathway considered for the formation of the sulfate ester of 2-methylglyceric acid is the methacrylic acid epoxide (MAE) pathway (Line et al., 2013b). There is sufficient evidence in my opinion that the pathway involving reactive uptake of methacrolein onto highly acidic aqueous aerosol and reaction with the sulfate radical anion should also be taken into account and mentioned. See, for example, Schindelka et al. (Faraday Discussions, 165, 237-259, 2013). The latter pathway allows to explain the formation of other C2-C5 isoprene-related organosulfates, for example, the sulfate ester of glycolic acid (MW 156), which is difficult to explain otherwise.

We have added this pathway and reference to the main text as follows:

"Under both high- and low-NO conditions, acid-catalyzed reactive uptake and multiphase chemistry of isoprene-derived epoxides (IEPOX and MAE) as well as aqueous reactions of MACR and methyl vinyl ketone (MVK) with sulfate radical anion are now known to enhance SOA formation from isoprene (Surratt et al., 2007b, Surratt et al., 2010, Lin et al., 2013b, Schindelka et al., 2013).

Page 7388 – line 1 (and Figure 5): The elemental composition of terpenylic acid (MW 172) should be C8H12O4, instead of C8H12NO4.

This has been corrected as suggested.

Page 7389 – lines 19-28: Here, oligomeric IEPOX-derived HULIS is mentioned and the suggestion is made that quantification of these compounds could help to close the IEPOX-OA mass budget. Is there already any evidence for the presence of these compounds in ambient fine aerosol from an isoprene-rich site? Other compounds that may help to close the isoprene SOA mass budget are the C2-C5 isoprene-related organosulfates, formed through aqueous-phase reactions of methacrolein or methyl vinyl ketone, first-generation gas-phase oxidation products of isoprene, with the sulfate radical anion (mentioned above).

Lin et al. (2014) reported IEPOX-derived HULIS observation at Look Rock and Centerville sites during 2013 SOAS campaign. These sites are characterized by high isoprene emissions, particularly at the Look Rock site.

To clarify this we have revised the text as:

"An interesting and potentially important observation is that oligomeric IEPOX-derived humic-like substances (HULIS) have been reported in both reactive uptake experiments onto acidified sulfate seed aerosol and in ambient fine aerosol collected from LRK and Centerville sites during the 2013 SOAS campaign (Lin et al. 2014)."

It is noted that we didn't include the C2-C5 organosulfates from aqueous reactions of methyl vinyl ketone or methacrolein in this discussion here since we were referring to IEPOX-derived SOA mass closure only.

Page 7390 – line 5: The statement "However, it should be noted that in all previous studies 2-methyltetrols and C5-alkene triols were quantified by surrogate standards structurally unrelated to the targeted analytes." is too general. Authentic standards are a better choice but a surrogate standard used in previous studies is the C4-tetrol erythritol, which is structurally related (homologous) to the 2-methyltetrols (e.g. Kourtchev et al., Plant Biology 10, 138-149, 2008; Claeys et al., ACP 10, 9319-9331, 2010). The situation is different for previous measurements of the sulfate esters of the 2- methyltetrols (MW 216), where indeed a surrogate standard that is unrelated to the analytes (i.e. n-propylsulfate) has been used.

We revised the sentence as follows:

"It should be noted that in all previous studies sulfate esters of 2-methyltetrol were quantified by surrogate standard structurally unrelated to the target analytes (i.e., sodium propyl sulfate). While in current study, a mixture of authentic 2-methyltetrol sulfate esters was used as a standard for quantifying IEPOX-derived organosulfates."

Technical corrections:

Page 7373 – line 13: . . .. a Nafion dryer . . ...

This has been changed as suggested.

Page 7377 – line 11: . . .. by using a T-piece in . . .. . .

This has been changed as suggested.

Page 7377 – line 27: the abbreviation "sLPM"should be defined.

We changed "sLpm" to "standard L min^{-1}".

Page 7384 – line 28: . . ... higher than those . . ...

This has been changed as suggested.

Page 7388 – line 27: . . .. the abundance of . . ..

This has been changed as suggested.

Page 7393 – line 3: . . .. in the predicted IEPOX SOA . . ...

This has been changed as suggested.

Page 7409 – line 8: 2-methylglyceric acid

This has been changed as suggested.

Supplement – page 3 – Table S2: . . ... and reference mass spectra [Note: the abbreviation "MS"stands for "mass spectrometry" and not for "mass spectra"].

We changed "MS" into "mass spectra".

Anonymous Referee #2
Received and published: 15 April 2015

This paper describes the results of a recent field campaign at the look-rock site during SOAS, investigating the formation of isoprene derived SOA through the PMF analysis of AMS data along with the measurement of select isoprene-OA tracers. The authors are able find that a significant amount of the OA measured at the site was from isoprene derived SOA (~30% based on the PMF analysis), but that the specific isoprene-SOA tracers measured accounted for only a small portion of this. The analysis performed in this paper seems well done, and overall this is a good paper. However, when all is said and done, it would seem that the results of this paper do not dramatically improve our state of knowledge when it comes to isoprene SOA. A significant fraction of isoprene SOA has been observed in other locations, and this paper simply reaffirms that this can be the case here as well. The expected correlations with other species (ie: SO4, ph, NOy) based upon known chemistry for isoprene SOA formation are not significantly observed, partly because of the complex nature of the air masses intercepting the site. The results generally do not fit what we think we know about isoprene SOA formation. As a result, this paper does not provide any major new insights, except for emphasizing how little we in fact understand about this chemistry. For this reason alone it should be publishable after some relatively minor issues are addressed and commented on as outlined below.

We thank the reviewer for their helpful comments as they have helped to improve the quality and clarity of the manuscript.

Introduction, pg 8: The authors mention that the results of this paper will help the regional modelling of isoprene SOA via better parameterizations, since they are currently under predicting this. However, right now what are models for this part of the USA using for isoprene SOA? I know that this group had modified CMAQ with some new isoprene chemistry, bit I did not think that explicit heterogeneous or liquid phase chemistry was included (but maybe they are??). If the current chemistry is insufficient for understanding field work, how can it be used to provide a better parameterization for a model?, If regional models are using a simple overall yield approach for isoprene SOA (under high or low NOx) then how will this work here be useful to them, and more importantly why are those models under predicting isoprene SOA in the first place? Some more information on the current model developments and issues would be useful here.

Heterogeneous liquid phase chemistry of IEPOX was added to a research version of CMAQ in the work of Pye et al. (2013, ES&T). The chemistry predicts the uptake of IEPOX (and MAE) via acid-catalyzed particle-phase reaction using many of the same parameters in simpleGAMMA, but with a slightly different approach. The publicly available version of CMAQv5.1, planned for release in Fall 2015, will include heterogeneous IEPOX chemistry for both research and regulatory simulations. The initial work of Pye et al. indicated that there were a number of uncertain parameters (such as the Henry's Law coefficient and particle-phase reaction rate constants) that affect the magnitude of IEPOX-OA. This work provides important insight into the effect of the magnitude of the Henry's law-coefficient and rate constants on IEPOX-derived SOA.

This work also provides insight into the contribution of species like 2-methyltetrols, which are explicitly predicted in CMAQv5.1, to total IEPOX-OA, which could be underpredicted by the bottom-up approach of models such as CMAQ and simpleGAMMA, since many IEPOX-derived constituents have not been identified (see Karambelas et al., 2014 ES&TL).

Pg 10: by this point we have a pretty good idea what PMF is. There is no need to repeat it all here, so I suggest it is put in the SI (or what you have in the SI is good enough).

We have greatly simplified the PMF section as suggested by the reviewer.

Pg 12, line 2: The CIMS does not measure MVK or MACR, so how is this done? It is not clear what you mean here.

The MVK and MACR were measured by PTR-TOF-MS. The sentence has been revised as follow:

"July CIMS data was corrected by comparing it to collocated MVK+MACR measured by PTR-TOF-MS (Section 2.4.2)…."

Pg 13, lines 5-10: What about wall loses for IEPOX and MAE in the chamber? I would expect there to be some losses. How do you account for this?

Wall loses for IEPOX and MAE in the chamber are 5.91×10^{-5} s^{-1} and 1.12×10^{-5} s^{-1}, respectively (Riedel et al., 2015). Over the course of calibration (~40 min), we expected to lose 14% and 3% of IEPOX and MAE, respectively.

We added this information to the main text as follows:

"During the course of the calibration experiments, we accounted for the fact that we would lose 14 and 3% of IEPOX and MAE, respectively. Wall loss rates for IEPOX and MAE have been measured in the chamber and are 5.91×10^{-5} s^{-1} and 1.12×10^{-5} s^{-1}, respectively (Riedel et al., 2015)."

Pg 13, line 28: typically I did not think a filter was used in front of a PTR-MS. How do you know that some gases are not also lost to the filter?

Practices vary as to employing a filter at the sample inlet when making PTR-MS measurements in ambient air. Below are a couple of additional references to studies where a filter was used. References to studies that did not use a filter can also be found in the literature. The argument for using a filter is that it will prevent particulate matter, which may contain semi-volatile organic compounds, from collecting on the walls of the sample lines. Any semi-volatile organic material that is deposited on the sample lines may later evaporate, leading to signals that could be attributed erroneously to gas phase species. In addition, organic material on the walls of the sample system may adsorb additional volatile or semi-volatile organic species from the gas phase, resulting in losses.

On the other hand, as the reviewer points out, losses of semi-volatile species on the filter itself are also possible, as is subsequent evaporation and detection of these species at a later time. One advantage of a filter is that its effects can be evaluated more easily (by changing or removing the filter) than the effects of deposition of particulate matter on the walls of the sample system. We have performed tests of the effect of the filter by monitoring gas phase concentrations with and without a filter and before and after filter changes and have observed no measurable loss of volatile species such as isoprene, methyl vinyl ketone, and methacrolein to the filter. The filter may have a more significant effect on compounds of lower volatility, however, such compounds are not reported in the current study.

References:

Park, J.-H., Goldstein, A. H., Timkovsky, J., Fares, S., Weber, R., Karlik, J., and Holzinger, R.: Eddy covariance emission and deposition flux measurements using proton transfer reaction – time of flight – mass spectrometry (PTR-TOF-MS): comparison with PTR-MS measured vertical gradients and fluxes, Atmos. Chem. Phys., 13, 1439-1456, doi:10.5194/acp-13-1439-2013, 2013.

Eerdekens, G., Ganzeveld, L., Vilà-Guerau de Arellano, J., Klüpfel, T., Sinha, V., Yassaa, N., Williams, J., Harder, H., Kubistin, D., Martinez, M., and Lelieveld, J.: Flux estimates of isoprene, methanol and acetone from airborne PTR-MS measurements over the tropical rainforest during the GABRIEL 2005 campaign, Atmos. Chem. Phys., 9, 4207-4227, doi:10.5194/acp-9-4207-2009, 2009.

Pg 22, lines 10-15: If indeed the CIMS data is partly or mostly ISOPOOH, what effect will this have on your hypothesis here?

The low correlation between gaseous IEPOX and IEPOX-OA factor was asserted due to time gap from IEPOX uptake and formation of IEPOX-OA. The lifetime of ISOPOOH will affect time series of IEPOX formation and thus the IEPOX-OA factor. CIMS sensitivities toward IEPOX and ISOPOOH were measured to be similar at 1.3×10^{-7} and 9.9×10^{-8} signal ppt^{-1}, respectively. We have investigated lowering the IEPOX mixing ratio by a constant factor between 100 and 10% of total *m/z* 177 signal. In this exercise, which will be reported in future study, we found that the model correlations are not sensitive and only tracers mass loadings vary with the IEPOX:ISOPOOH ratio. The inability to distinguish IEPOX from ISOPOOH is a limitation in our study.

We added this information to the main text as follows:
"We synthesized ISOPOOH (see Fig. S10 for nuclear magnetic resonance (NMR) data) and measured CIMS sensitivities toward ISOPOOH and IEPOX. Results indicated that response factors of both compounds were similar (see Fig. S11). Investigation of lowering the IEPOX mixing ratio by a constant factor of total *m/z* 177 signal, which will be reported in a future study, showed that SOA tracer model correlations are not sensitive to this and only tracers mass loadings vary with the IEPOX:ISOPOOH ratio. The inability to distinguish IEPOX from ISOPOOH is a limitation in our study."

Pg 23, lines 3-5: This may or may not make sense. On the one hand since MVK and MACR are formed very quickly from isoprene one would expect a diurnal profile for these products as well as isoprene. The lifetime of isoprene is very short, presumably making MVK etc...On the other hand there does seem to be a small diurnal profile to these species as well, but less than isoprene possibly for good reason. You would need to model the system to truly understand if the diurnal profile of these others should be as pronounced as isoprene. Based upon the figure alone I do not think you can make the assertion that it is all transported in.

What we meant in this is that the lack of diurnal variation of gaseous IEPOX and thus IEPOX-OA were due to continuous oxidation of isoprene emitted at the site (which was in a forest) and the surrounding forested areas, as well as from forests further upwind of the site. IEPOX reactive uptake, although it is only few hours, would mean that it could continue on given that there is aerosol sulfate (which is not formed on site).

To make this clearer, we have revised the text as follows:

"… IEPOX-OA was not only formed on site but could also transported from surrounding forested and isoprene-rich areas. Despite the strong diurnal profile of isoprene at the LRK site, diurnal variations of the gas-phase products of isoprene photooxidation, particularly IEPOX, were small during this campaign (Fig. 4). The lack of strong diurnal profile of IEPOX and the fact that reactive-uptake of IEPOX is influenced by aerosol sulfate (Lin et al., 2012) that is not formed on site, might explain the lack of significant diurnal variation (Fig. 3) of the IEPOX-OA factor at LRK. …"

Pg 23, lines 10-12: If both LV-OOA and the IEPOX-OA are both transported from elsewhere (as hypothesized), then why does the LV-OOA have a diurnal cycle of some kind and IEPOX-OA not? You need more analysis here on this issue.

We added more discussion on this issue as follow:

"…Diurnal profile of LV-OOA observed at LRK is similar to more-oxidized OOA (MO-OOA) observed at Centerville (Xu et al., 2015), suggesting their regional sources. At LRK average mixing ratios of monoterpenes and isoprene were <1 ppb and ~2 ppb (Fig. 4), respectively. Low anthropogenic emissions at LRK (<1 ppb; Fig. S16) suggests that BVOCs could be the source of LV-OOA (50% of OA) formation. Anthropogenic emissions as well as nitrate chemistry in the valley could also influence LV-OOA formation that oxidized during transport to the LRK site."

Pg 23, lines 17-29: I am not sure why this paragraph on terpenes is needed if this is a paper about isoprene SOA. Seems to stick out and does add much overall. I suggest it is removed or at least placed in the SI.

Part of this paragraph has been removed and placed into the SI.

We added in the text the following:

"Potential sources of 91Fac is discussed in more detail in the SI (Fig. S15) and its association with biogenic SOA chemistry will be the focus of future studies."

Pg 25, line 5: This is more than 100%. How is this possible?

There were some miscalculation and typos. This has been fixed as follows:

"In sum, IEPOX- and MAE-derived tracers contributed 96.6% and 3.4%, respectively, of total isoprene-derived SOA mass quantified from filter samples."

Pg 25,lines 9-10: This is a bit confusing here. In the above lines you say IEPOX and MAE derived tracers are ~97% of isoprene derived SOA, but here you say 25% of the IEPOX-OA factor mass...what is the difference between isoprene derived SOA and IEPOX-OA mass? I assume you mean one form offline and one from On-line AMS data? If so you need explicitly state that here.

Isoprene-derived SOA mass was measured by offline analysis, while IEPOX-OA factor mass was resolved by PMF analysis of OA fraction measured by ACSM. This has been changed as follows:

"…. Total IEPOX-derived tracers masses quantified from filter samples were on average 26.3% (maximum 48.5%) of the IEPOX-OA factor mass resolved by PMF…."

Pg 27, lines 1-5: it may also suggest that additional organics may result in the acidity being not accessible to the IEPOX eventually. This has been observed in some lab studies for other systems (although I do not recall the references), and may also explain why there is no diurnal profile, since the uptake occurred quickly then was slowed by this organic addition. You might also expect a moderate correlation with sulfate if this were to be occurring. Perhaps looking at the correlation between IEPOX-OA and the ratio of Org:SO4 might be helpful in this regard, as a means to isolate older vs local air masses, and possibly to get a hint if the added organics are self-limiting for this process.

IEPOX-OA shows no correlation with ratio of Org:SO4 as illustrated below. The average ratio Org:SO4 of 2.42 indicates that the air masses is mostly aged. No-correlation between IEPOX-OA and ratio of Org:SO4 might suggest a mix of local and non-local (aged) air masses.

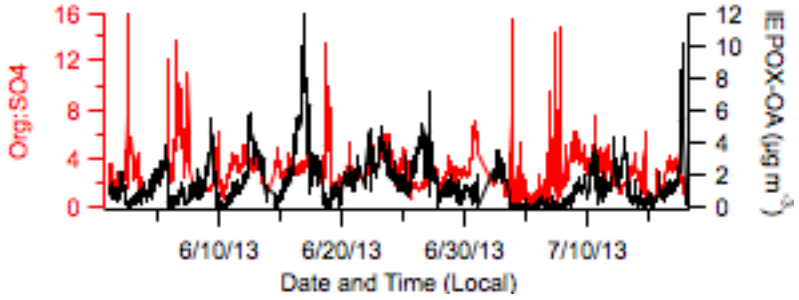

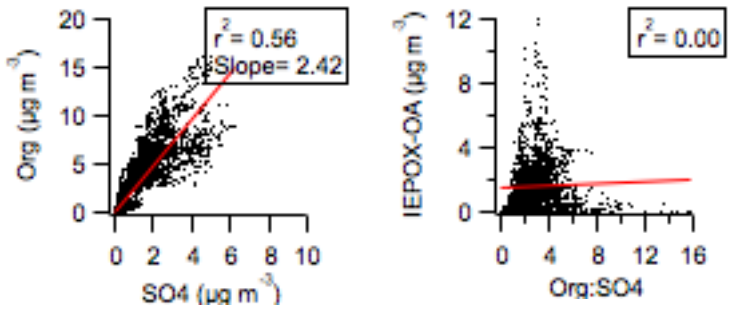

Pg 27, lines 15-16: And yet since the particles remained acidic why should it not be taken up? Again this may point to a particle phase issue; possibly viscosity/mass transfer limitations caused an organic barrier of some kind.

Our recent flow tube studies have shown that organic coatings with PEG-300 can suppress IEPOX uptake (Gaston et al., 2014), and thus, lowering the uptake coefficient by upwards of a factor of 2 at similar acidities. However, organic coatings of more complex mixtures and of atmospheric relevance have not been systematically studied. It is unclear at this time how coatings will affect IEPOX uptake in the atmosphere.

To clarify this section, we have revised this sentence as:

"Further complicating factors may be viscosity or morphology changes of the aerosol as IEPOX is taken up by heterogeneous reaction, and thus, slowing of uptake kinetics as the aerosol surface is coated with a hydrophobic organic layer (Gaston et al., 2014). Additionally, liquid-liquid phase separation is likely to occur in the atmosphere due to changes of relative humidity that affect particles water content (You et al., 2012). Moreover, the effects of aerosol viscosity and morphology on IEPOX uptake is not well understood and warrant further study using aerosol of complex mixtures and of atmospheric relevance."

Pg 28, lines 1-2: The NOx should also be from upwind, thus still correlated, and yet they are not. The fact that species of both high and low NOx seem to be not correlated to what is expected, seems to be a little odd. On the one hand you are saying that both are not formed locally, but it is non-local where the NOx is, so how can they both formed elsewhere and transported in? Unless they were from two separate regions, one with NOx and one without. This needs to be clearer here.

The NO_x was from urban areas upwind of the site. MAE/HMML could be formed in the urban areas since they are downwind of forested areas where isoprene is emitted. We revised the sentence as follow:

"….The observation that neither the summed MAE/HMML tracers nor 2-MG correlated with NO_x, is consistent with the hypothesis that MAE/HMML is formed in urban areas upwind and transported to the sampling site. …"

Pg 29, line 9: typo – should be "a" subset. . ..

This has been changed as suggested.

Pg 29, line 27-28: Despite this consistency, a correlation does not exist with acidity in the measurements. The model does not include transport along a trajectory and processing along the way, and yet this is what the authors are asserting is happening. So how can one use initial inputs of IEPOX etc... from the site when the initial inputs should be from at the source? Therefore there is not much reason to have faith in the so-called good correlation between box model and measurements since the model output is for 12 hrs of local emissions and the measurements are of processed SOA from elsewhere. It would seem then that the correlation is just fortuitous. In fact, it is not clear what the point of running this model was in the first place, especially if you didn't expect it to agree anyways. The authors need to justify this model's use, and at the very least explain the reasons for trying to do this at all.

We were justified in using gas-phase IEPOX concentrations measured model inputs because atmospheric lifetime of IEPOX is a few hours (Gaston et al., 2014; and diurnal profile Fig. 4), meaning that it is all relatively local. Aerosol sulfate is regional, as indicated by the flat diurnal profile. Furthermore, measurements at all SOAS locations indicate highly acidic aerosol. Additional support for our choice of local data as model inputs is that aerosol acidity is instantaneously determined by the local thermodynamic equilibrium, which for the aerosol we have at hand is less than 1 hour. Given this, and that water equilibrates on the order of seconds strongly suggests that all the relevant chemistry here is fast and using local initial conditions of IEPOX etc. is appropriate.

Our goal in using the model was to help reconcile what we know about the chemical mechanism of IEPOX-OA formation, as represented in simpleGAMMA (which includes dependence on aerosol acidity, aerosol liquid water, sulfate, and ammonium content), with the apparent lack of expected correlation with acidity and aerosol liquid water. The model results provide estimated IEPOX SOA mass loadings, which we compare to observed concentrations. We feel that the demonstrated model-data agreement shows that the observations are consistent with the known chemical mechanisms, despite the lack of correlation between acidity and the tracers.

Figure 3: On my screen the black of IEPOX in the pie chart looks grey and different from the black below it. I presume this is not intended?

We have fixed the figure.

Figure 5: What is the purpose of this figure? Since the correlations are poor for everything, what is it telling you? I would sooner like to see the correlations of IEPOX-OA with NO.

We relocated Fig. 5 to SI since it is mainly utilized to explore possible sources of 91Fac instead of the isoprene-derived SOA factor. Further investigation of the sources of 91Fac will be conducted in a future study.

Anonymous referee #3

This manuscript describes results obtained at the ground site of Look Rock, TN, during the 2013 Southern Oxidant and Aerosol Study (SOAS). A large set of instruments was deployed to measure the particle chemical composition (with on-line and off-line techniques) and gas-phase compounds. Results reported in this manuscript concern mainly non-refractory submicron particles (NR-PM1) with an Aerodyne aerosol chemical speciation monitor (ACSM), isoprene-derived secondary organic aerosol (SOA) tracers from filter samplings, and gaseous compounds with a high-resolution time-of-flight chemical ionization mass spectrometer (HR-ToF-CIMS) and a proton transfer reaction time-of-flight mass spectrometer (PTR-ToF-MS).

The authors showed that isoprene-derived SOA contributed significantly to the total organic mass, and that almost all the tracers quantified with off-line techniques were isoprene epoxydiol (IEPOX)- derived compounds. Results obtained suggest that IEPOX-derived SOA was not formed locally but rather during long-range transport, during which anthropogenic and biogenic emissions mix and interact.

This manuscript is well written, fits the scope of the journal, and provides interesting information on the complex mechanisms leading to the formation of isoprene-derived SOA. I recommend its publication in Atmospheric Chemistry and Physics after minor revisions.

We thank the reviewer for their careful review of our manuscript and the suggestions made below that help with improving clarity of our manuscript.

Specific comments:

1) Section 2.1: A better description of the sampling site is needed to fully understand the rest of the manuscript. If the authors include just one figure with a map of the region and a wind rose plot for the entire campaign, it will help a lot to better understand the different air masses, where the anthropogenic influences come from, etc. Without this information, even the back-trajectories given in the supplementary material (Figures S12 and S13) are impossible to understand, because we have no idea on the locations of biogenic or anthropogenic sources.

As suggested by the reviewer, we have added maps and description of study location in the SI.

2) Section 2.2: According to results shown later (section 3.4.1, Figure 6a), particles seem rather acidic. In these conditions, the use of a constant collection efficiency (CE) of 0.5 for the ACSM is not appropriate. I suggest that the authors introduce a time-dependant CE using equation 4 in Middlebrook et al. (2012).

The CE of 0.5 was calculated using Equation 4 of Middlebrook et al. (2012). The calculated CE values were around 0.5 during the entire field campaign.

We added this information into the main text of the experimental section describing the ACSM as follows:

"A collection efficiency (CE) of 0.5 calculated using Eq. 4 of Middlebrook et al. (2012) was applied to the ACSM data in order to accommodate composition-dependent CE."

Reference:

Middlebrook, A. M., Bahreini, R., Jimenez, J. L., and Canagaratna, M. R.: Evaluation of Composition-Dependent Collection Efficiencies for the Aerodyne Aerosol Mass Spectrometer using Field Data, *Aerosol Sci. Technol.*, *46*, 258-271, 10.1080/02786826.2011.620041, 2012.

3) Section 3.2: Additional information is needed in the supplementary material to support the choice of the 3-factor solution. In particular, it would be important to show mass spectra of the PMF factors for the 2-, 4-, and eventually 5-factor solution, in order to see how the OOA split into different factors. In addition to that, it would be useful to show a few diagnostic plots, such as the correlation among the PMF factors based on time series and mass spectra (so the same graph as Figure S3, panel d) for the 2-, 4-, and eventually 5-factor solution.

Moreover, can the authors confirm that they do not resolve a hydrocarbon-like organic aerosol (HOA) factor, even if they go up to 10 factors? This is a bit surprising for a site which is supposed to have anthropogenic influences. This result, coupled to the low concentration of primary pollutants (BC, NOx, CO), suggests that anthropogenic influences were quite limited at the sampling site.

There was no primary anthropogenic emission at the site since it was located atop of a mountain located in the densely forested Great Smoky Mountain National Park. Some primary pollutants could be transported to the site from the valley, which is more populated, however it was still very low. Low concentration of primary OA did not show as distinct factor from PMF analysis. This could also be attributed to the 30-minute time resolution of the ACSM, preventing it from being sensitive enough to pick up low concentrations of primary OA plume.

We have added time series, mass spectra, and factor inter-correlation plots of 2-, 4-, and 5-factor solutions in the SI section. HOA factor was observed in the 4- and 5-factor solutions, however, its temporal variation could not be distinguished from other factors and it was not well correlated with primary pollutants (i.e., CO and NO_x). Therefore, we concluded that the ACSM could not resolve the HOA factor from the organic mass spectral data collected during this study.

4) Section 3.3: It seems there is a mistake in the percentages of isoprene-derived SOA tracers reported in this section. Thus, the contribution of IEPOX- (96.8%) and MAE- (8.8%) derived tracers to the total isoprene-derived SOA mass is higher than 100% (page 7389, line 5). Moreover, the sum of all the tracers given in Table 1 reaches 101.6%.

This has been corrected in Section 3.3 and in Table 1.

Technical corrections:

1) Page 7368, line 1: "methacrylic acid epoxide (MAE)". Actually, MAE appears for the first time 2 lines earlier (page 7367, line 27), so the abbreviation should be defined already there.

This has been changed as suggested.

2) Page 7384, line 28: "but higher than that those".

This has been corrected as: "but higher than those "

3) Page 7393, line 3: "decrease in the in predicted IEPOX SOA".

This has been corrected as: "decrease in the predicted IEPOX SOA"

4) Supplementary material, page 13, line 5: "organic aerosol mass (OM)"

This has been corrected as: "organic matter (OM)"

5) Supplementary material, page 15, line 2: "the 2014 2013 SOAS field study".

This has been corrected as: "the 2013 SOAS field study."

6) Supplementary material, page 16, line 1: "24-hr model during_the first".

This has been corrected as: "24-hr model during the first"

Examining the Effects of Anthropogenic Emissions on Isoprene-Derived Secondary Organic Aerosol Formation During the 2013 Southern Oxidant and Aerosol Study (SOAS) at the Look Rock, Tennessee, Ground Site

S. H. Budisulistiorini[1,6], X. Li[1], S. T. Bairai[2,†], J. Renfro[3], Y. Liu[4], Y. J. Liu[4], K. A. McKinney[4], S. T. Martin[4], V. F. McNeill[5], H. O. T. Pye[6], A. Nenes[7,8,9], M. E. Neff[10], E. A. Stone[10], S. Mueller[2,‡], C. Knote[11], S. L. Shaw[12], Z. Zhang[1], A. Gold[1], and J. D. Surratt[1]

[1] Department of Environmental Sciences and Engineering, Gillings School of Global Public Health, The University of North Carolina at Chapel Hill, Chapel Hill, NC, USA

[2] Tennessee Valley Authority, Muscle Shoals, AL, USA

[3] National Park Service, Gatlinburg, TN USA

[4] School of Engineering and Applied Sciences, Harvard University, Cambridge, MA USA

[5] Department of Chemical Engineering, Columbia University, NY, USA

[6] National Exposure Research Laboratory, US Environmental Protection Agency, Research Triangle Park, NC, USA

[7] School of Earth and Atmospheric Sciences, Georgia Institute of Technology, Atlanta, GA, USA

[8] School of Chemical and Biomolecular Engineering, Georgia Institute of Technology, Atlanta, GA, USA

[9] Foundation for Research and Technology, Hellas, Greece

[10] Department of Chemistry, University of Iowa, Iowa City, IA, USA

[11] Department of Experimental Meteorology, Ludwig Maximilian University of Munich, Munchen, Germany

[12] Electric Power Research Institute, Palo Alto, CA, USA

† Now at Battelle, Pueblo, CO, USA

‡ Now at Ensafe, Nashville, TN, USA

Correspondence to: J. D. Surratt (surratt@unc.edu)

Abstract

A suite of offline and real-time gas- and particle-phase measurements was deployed at Look Rock, Tennessee (TN), during the 2013 Southern Oxidant and Aerosol Study (SOAS) to examine the effects of anthropogenic emissions on isoprene-derived secondary organic aerosol (SOA) formation. High- and low-time resolution $PM_{2.5}$ samples were collected for analysis of known tracer compounds in isoprene-derived SOA by gas chromatography/electron ionization-mass spectrometry (GC/EI-MS) and ultra performance liquid chromatography/diode array detection-electrospray ionization-high-resolution quadrupole time-of-flight mass spectrometry (UPLC/DAD-ESI-HR-QTOFMS). Source apportionment of the organic aerosol (OA) was determined by positive matrix factorization (PMF) analysis of mass spectrometric data acquired on an Aerodyne Aerosol Chemical Speciation Monitor (ACSM). Campaign average mass concentrations of the sum of quantified isoprene-derived SOA tracers contributed to ~9% (up to 28%) of the total OA mass, with isoprene-epoxydiol (IEPOX) chemistry accounting for ~97% of the quantified tracers. PMF analysis resolved a factor with a profile similar to the IEPOX-OA factor resolved in an Atlanta study and was therefore designated IEPOX-OA. This factor was strongly correlated (r^2 > 0.7) with 2-methyltetrols, C_5-alkene triols, IEPOX-derived organosulfates, and dimers of organosulfates, confirming the role of IEPOX chemistry as the source. On average, IEPOX-derived SOA tracer mass was ~26% (up to 49%) of the IEPOX-OA factor mass, which accounted for 32% of the total OA. A low-volatility oxygenated organic aerosol (LV-OOA) and an oxidized factor with a profile similar to 91Fac observed in areas where emissions are biogenic-dominated were also resolved by PMF analysis, whereas no primary organic aerosol (POA) sources could be resolved. These findings were consistent with low levels of primary pollutants, such as nitric oxide (NO ~0.03 ppb), carbon monoxide (CO ~116

ppb), and black carbon (BC ~0.2 μg m^{-3}). Particle-phase sulfate is fairly correlated (r^2 ~0.3) with both methacrylic acid epoxide (MAE~~)~~)/hydroxymethyl-methyl-α-lactone (HMML)-(henceforth called methacrolein (MACR)-derived SOA tracers) and IEPOX-derived SOA tracers, and more strongly correlated (r^2 ~0.6) with the IEPOX-OA factor, in sum suggesting an important role of sulfate in isoprene SOA formation. Moderate correlation between the ~~MAE~~MACR-derived SOA tracer 2-methylglyceric acid with sum of reactive and reservoir nitrogen oxides (NO_y; r^2 = 0.38) and nitrate (r^2 = 0.45) indicates the potential influence of anthropogenic emissions through long-range transport. Despite the lack of a clear association of IEPOX-OA with locally estimated aerosol acidity and liquid water content (LWC), box model calculations of IEPOX uptake using the simpleGAMMA model, accounting for the role of acidity and aerosol water, predicted the abundance of the IEPOX-derived SOA tracers 2-methyltetrols and the corresponding sulfates with good accuracy (r^2 ~0.5 and ~0.7, respectively). The modeling and data combined suggest an anthropogenic influence on isoprene-derived SOA formation through acid-catalyzed heterogeneous chemistry of IEPOX in the southeastern U.S. However, it appears that this process was not limited by aerosol acidity or LWC at Look Rock during SOAS. Future studies should further explore the extent to which acidity and LWC as well as aerosol viscosity and morphology becomes a limiting factor of IEPOX-derived SOA, and their modulation by anthropogenic emissions.

1 Introduction

Atmospheric fine particulate matter ($PM_{2.5}$, aerosol with aerodynamic diameter $\leq$ 2.5 μm) can scatter and/or absorb solar and terrestrial radiation as well as influence cloud formation and as a result, can markedly affect regional and global climate (IPCC, 2013). It is now also established that exposure to $PM_{2.5}$ can have an adverse impact on human health (Dockery et al., 1993, Mauderly and Chow, 2008, Hsu et al., 2011). Organic matter (OM) comprises the largest mass fraction of $PM_{2.5}$ and is derived largely from secondary organic aerosol (SOA) formed through atmospheric oxidation of volatile organic compounds (VOCs). SOA formation has been modeled primarily within the framework of absorptive gas-to-particle partitioning (Pankow, 1994, Odum et al., 1996), with the products of volatile and semi-volatile organic precursors decreasing in volatility during multi-generational oxidation, and condensing onto pre-existing particles or creating new particles through nucleation. Recent work has demonstrated the importance of heterogeneous (or particle-phase) chemistry in SOA formation (Jang et al., 2002, Kalberer et al., 2004, Tolocka et al., 2004, Gao et al., 2004, Surratt et al., 2006); however, chemical transport models are only just beginning to incorporate explicit details of this chemistry for specific SOA precursors (Pye et al., 2013, Karambelas et al., 2014). Although much progress has been made in recent years in identifying key biogenic and anthropogenic SOA precursors, significant gaps still remain in our knowledge of the formation mechanisms, composition and properties of SOA (Hallquist et al., 2009).

Isoprene (2-methyl-1,3-butadiene, C_5H_8) is the most abundant non-methane VOC emitted into Earth's atmosphere at ~600 Tg yr^{-1} (Guenther et al., 2006). The southeastern U.S. during summer is a particularly strong source of isoprene, primarily through emissions by broad-leaf trees. Although isoprene is known to influence urban ozone (O_3) formation in the

southeastern U.S., only in the last decade has hydroxyl radical (OH)-initiated oxidation been recognized as leading to significant SOA formation, enhanced by the presence of anthropogenic pollutants such as nitrogen oxides (NO_x = NO + NO_2) and sulfur dioxide (SO_2) (Claeys et al., 2004, Edney et al., 2005, Surratt et al., 2006, Kroll et al., 2006, Surratt et al., 2010). Previously, the volatility of the photochemical oxidation products had been assumed to preclude formation of $PM_{2.5}$ from isoprene oxidation (Pandis et al., 1991, Kamens et al., 1982).

Recent studies have made significant strides in identifying critical intermediates in isoprene SOA formation by varying the levels of NO_x (Kroll et al., 2006, Surratt et al., 2006, Surratt et al., 2010) and acidity of sulfate aerosol (Surratt et al., 2006, Surratt et al., 2010, Lin et al., 2012, Lin et al., 2013a). The proposed role of isomeric isoprene epoxydiols (IEPOX) as key intermediates in the formation of isoprene SOA under low-nitric oxide (NO) conditions (Surratt et al., 2010, Paulot et al., 2009) has recently been confirmed in studies using authentic compounds (Lin et al., 2012, Gaston et al., 2014, Nguyen et al., 2014). Under high-NO conditions, isoprene SOA has been demonstrated to form primarily via oxidation of methacrolein (MACR) (Surratt et al., 2006) and methacryloyl peroxynitrate (MPAN) (Surratt et al., 2010) with methacrylic acid epoxide (MAE) (Lin et al., 2013b) and hydroxymethyl-methyl-α-lactone (HMML) (Nguyen et al., 2015) from the further oxidation of MACR demonstrated as ~~a~~ reactive ~~intermediate (Lin et al., 2013b).~~intermediates. Under both high- and low-NO conditions, acid-catalyzed reactive uptake and multiphase chemistry of isoprene-derived epoxides (IEPOX and MAE) as well as ~~reaction~~aqueous reactions of MACR and methyl vinyl ketone (MVK) with sulfate radical anion are now known to enhance SOA formation from isoprene (Surratt et al., 2007b, Surratt et al., 2010, Lin et al., 2013b, Schindelka et al., 2013). Recent flowtube studies on reactive uptake kinetics of *trans*-β-

IEPOX (Gaston et al., 2014), the predominant IEPOX isomer formed in the photochemical oxidation of isoprene (Bates et al., 2014), have estimated an atmospheric lifetime shorter than 5 h in the presence of highly acidic aqueous aerosol (pH $\leq$ 1). Since the predicted atmospheric lifetime of IEPOX for gas-phase oxidation is 8 – 33 hours at an average OH concentration of 10^6 molecules cm^{-3} (Jacobs et al., 2013, Bates et al., 2014) and 11 hours for deposition (Eddingsaas et al., 2010), reactive uptake of IEPOX onto highly acidic aqueous aerosol would be a competitive or potentially dominant fate of IEPOX in the atmosphere. Recent field data from sites across the southeastern U.S. collected by ~~Guo et al. (2014)~~ (Guo et al., 2015) yielded estimates that aerosol pH ranges from 0.5–2. Consistent with expectations based on the flowtube studies (Gaston et al., 2014, Riedel et al., 2015) and pH estimates from field data, IEPOX-derived SOA has been observed to account for up to 33% of the total fine organic aerosol (OA) mass collected during summer in downtown Atlanta, GA, by analysis of data acquired on an online Aerodyne Aerosol Chemical Speciation Monitor (ACSM) (Budisulistiorini et al., 2013). Similar level of isoprene-derived SOA has been recently observed at other field sites across the southeastern U.S. using the Aerodyne high-resolution time-of-flight aerosol mass spectrometer (HR-ToF-AMS) (Xu et al., 2015~~))~~). In offline chemical analysis of total fine OA mass at a rural site located in Yorkville, GA (Lin et al., 2013b), up to 20% of the OA mass could be attributed to the known IEPOX-derived SOA tracers, including the 2-methylterols (Claeys et al., 2004, Lin et al., 2012), C_5-alkene triols (Wang et al., 2005, Lin et al., 2012), *cis*- and *trans*-3-methyltetrahydrofuran-3,4-diols (Lin et al., 2012, Zhang et al., 2012b) and IEPOX-derived organosulfates (Surratt et al., 2007a, Surratt et al., 2010, Lin et al., 2012).

In addition to examining the effects of NO and aerosol acidity on isoprene SOA formation, the effect of varying relative humidity (RH) has recently been examined. In

chamber studies on the high-NO pathway under low-RH conditions, the isoprene SOA constituents 2-methylglyceric acid and corresponding oligoesters derived from MACR~~,~~ ~~MPAN, and MAE, were enhanced relative to higher RH conditions (Zhang et al., 2011, Nguyen et al., 2011).~~ and its associated SOA precursors (i.e., HMML and MAE), were influenced by RH conditions (Zhang et al., 2011, Nguyen et al., 2011, Nguyen et al., 2015). However, 2-methyltetrols, which are known to be major SOA constituents formed in the low-NO pathway and minor constituents in the high-NO pathway (Edney et al., 2005, Surratt et al., 2007b), did not vary significantly with RH (Zhang et al., 2011). While RH appears to have an effect on the formation of certain isoprene SOA constituents, recent flowtube studies demonstrated that aerosol acidity has a more pronounced effect on IEPOX- and MAE-derived SOA formation than RH (Gaston et al., 2014, Riedel et al., 2015). However, field studies have yielded mixed results. At Yorkville, GA, Lin et al. (2013a) observed no strong correlation of IEPOX-derived SOA with aerosol acidity, NH_3 levels or liquid water content (LWC), although there was a statistically significant enhancement of IEPOX-derived SOA under high SO_2-sampling scenarios. Similarly, no correlation between isoprene SOA tracers and aerosol pH or LWC was observed in the analysis of filter samples collected from field studies in Sacramento, CA, and Carson City, NV (Worton et al., 2013), and in the isoprene-derived PMF factor from field study in Centerville, AL (Xu et al., 2015). Another recent field study by Budisulistiorini et al. (2013) found weak correlation (r^2 = 0.22) between aerosol pH and an IEPOX-OA factor resolved by positive matrix factorization (PMF) from real-time organic aerosol mass spectra data acquired on an Aerodyne ACSM.

Although isoprene is now recognized as a major source of SOA, the exact manner in which isoprene-derived SOA is formed in the southeastern U.S. and how it is affected by anthropogenic pollutants (i.e., NO_x level, aerosol acidity, sulfate and primary aerosol

loadings) remains unclear. The gap in understanding has major public health and policy implications since isoprene is emitted primarily from terrestrial vegetation and is not controllable, whereas strategies to control anthropogenic pollutants can be implemented. Improving our fundamental understanding of the role of anthropogenic emissions in isoprene SOA formation will be key in improving existing air quality models, especially in the southeastern U.S. where models currently under-predict isoprene SOA formation (Foley et al., 2010, Carlton et al., 2010) and as a result will be critical to developing efficient control strategies for improving air quality. The study presented here is part of the 2013 Southeast Oxidant and Aerosol Study (SOAS) spanning 1 June – 17 July 2013 at the Look Rock (LRK), TN ground site (maps are provided in supplemental information (SI)). A major aim of SOAS was to address the issue of how exactly isoprene SOA formation occurs and the potential of anthropogenic emissions to enhance SOA formation. At the LRK ground site we approached this aim by examining the chemical composition of OA measured in real-time by the Aerodyne ACSM and subsequently applying PMF for source apportionment. We also collected $PM_{2.5}$ on filters and quantified tracers associated with isoprene chemistry to support the assignment of OA factors resolved from factor analyses of organic mass spectral data collected by the ACSM. We examined the potential influence of anthropogenic emissions on isoprene-derived SOA by correlation with temporal variation of anthropogenic markers monitored by collocated instruments. Finally, a photochemical box model was employed to further examine the potential interactions between SOA and anthropogenic emissions. The results of this study will help to improve model parameterizations required to bring model predictions closer to ambient observations of isoprene-derived SOA formation in the southeastern U.S.

2 Methods

2.1 Site Description

Fine aerosol was collected continuously from 1 June – 17 July 2013. LRK is a ridge-top site located on the northwestern edge of the Great Smoky Mountain National Park (GSMNP) downwind of Maryville and Knoxville and small farms with animal grazing areas (Figs. S1–S2). Up-slope flow carries pollutants emitted in the valley during early morning to the LRK site by mid-morning (Tanner et al., 2005). In the evening, down-slope flow accompanies a shift of wind direction to the south and east during summer that isolates the site from fresh primary emissions from the valley and allows aged-secondary species to accumulate (Tanner et al., 2005). As described in Tanner et al. (2005), particulate sulfate, black carbon (BC), organic carbon (OC), $PM_{2.5}$ and PM_{10} as well as gas-phase sulfur dioxide (SO_2), nitric oxide (NO), nitrogen dioxide (NO_2), and sum of reactive and reservoir nitrogen oxides (NO_y) were measured by a suite of collocated instruments throughout the campaign (Table S1). Meteorological measurements (RH, temperature, wind direction, and wind speed) and O_3 concentrations were acquired at a National Park Service (NPS) shelter across a secondary road opposite the LRK shelter.

2.2 ACSM NR-PM_1 Characterization

Fine ambient aerosol was sampled from the rooftop of the LRK site air-conditioned building during the SOAS campaign. The sampling inlet was approximately 6 m above the ground and equipped with a $PM_{2.5}$ cyclone. Sample was drawn at 3 L min^{-1} (residence time < 2 s) and dried using a Nafion drier (PD-200T-24SS, Perma Pure) to maintain RH below 10% and prevent condensation during sampling. ACSM operation parameters followed those of previous studies (Budisulistiorini et al., 2013, Budisulistiorini et al., 2014). Briefly, the

ACSM scanning rate was set at 200 ms amu^{-1} and data were averaged over 30 min intervals. Data were acquired using ACSM DAQ version 1438 and analyzed using ACSM Local version 1532 (Aerodyne Research, Inc.) within Igor Pro 6.3 (Wavemetrics). Calibrations for sampling flow rate, mass-to-charge ratio (*m/z*), response factor of nitrate (RF_{NO3}), and relative ionization efficiencies of both ammonium (RIE_{NH4}) and sulfate (RIE_{SO4}) were performed three times during the campaign. Mass resolution, heater bias and ionizer voltages, and amplifier zero settings were checked and adjusted daily. A collection efficiency (CE) of 0.5 calculated using Eq. 4 of Middlebrook et al. (2012~~))~~) was applied to the ACSM data in order to accommodate composition-dependent CE. Correlations of combined aerosol mass concentrations of ACSM non-refractory (NR)-PM_1 and collocated black carbon (BC) with aerosol volume concentrations of PM_1 measured by the Scanning Electrical Mobility System-Mixing Condensation Particle Counter (SEMS-MCPC, Brechtel Manufacturing Inc.) was strong (r^2 = 0.89) and suggested an aerosol density of 1.52 g cm^{-3} (Fig. ~~S2~~S3), close to that reported in previous studies in Pasadena, CA (Hayes et al., 2013) and Atlanta, GA (Budisulistiorini et al., 2014). If CE of 1 is used, the estimated aerosol density is 0.78 g cm^{-3}, which is much lower than suggested bulk organic and inorganic aerosol densities of 1.27 g cm^{-3} and 1.77 g cm^{-3}, respectively (Cross et al., 2007).

2.3 OA Source Characterization

OA fraction acquired by the ACSM was analysed using PMF (Paatero and Tapper, 1994) written in PMF Evaluation Tool (PET v2.4) (Ulbrich et al., 2009). In this study, uncertainty of a selected solution was investigated with Seeds (varied from 0 to 100, in steps of 5), 100 bootstrapping runs, and Fpeak parameters. Details of diagnostics for each PMF analysis are given in SI (Tables S2-S3 and Figs. S4-S8). Evaluation of Q/Q_{exp} time series and mass spectra and correlation of factor solutions at Fpeak 0 with collocated measurements

(Figs. S4–S5, Table S3) suggests that a 3-factor solution is optimum. We selected a 3-factor solution at Fpeak -0.09 based on the quality of PMF fits and interpretability when compared to tracer time series and reference mass spectra (Table S5). The mass spectrum of a factor designated IEPOX-OA conforms closely to the IEPOX-SOA factor resolved in Atlanta, GA (Budisulistiorini et al., 2013). The mass spectrum of the second factor correlates closely with the factor identified as LV-OOA in previous studies (Ulbrich et al., 2009, Ng et al., 2011). The third factor is designated 91Fac, based on the similarity of its mass spectrum to the factor 91Fac, an oxygenated factor resolved in areas dominated by biogenic emissions (Robinson et al., 2011, Chen et al., 2014).

2.4 Gas-phase Measurements

2.4.1 High-Resolution Time-of-Flight Chemical Ionization Mass Spectrometry (HR-ToF-CIMS) Measurements

Gaseous samples were measured through an approximately 1 m length of PTFE tubing (¼" outside diameter) from the sidewall of the building at flow rate of 2 L min^{-1}. The sampling line was placed to face the valley such that no structures or activity would compromise sampling. Instrument performance was maintained daily by baseline, threshold, and single ion area tuning as well as *m/z* calibration. The instrument was not operational during some periods of the field campaign (i.e., 13 – 16 June, 21 June – 4 July, and 14 – 16 July) due to power outage, broken components, and necessary maintenances. July HR-ToF-CIMS data was corrected by comparing it to collocated MVK+MACR measured by PTR-TOF-MS (~~section~~Section 2.4.2) and post-campaign calibration in order to derive a correction factor to account for decay in the micro-channel plate (MCP) detector.

The HR-ToF-CIMS instrument was operated in the negative ion mode using acetate ion chemistry for detection of isoprene-derived epoxides. It is henceforth referred as acetate CIMS. The acetate ion system efficiently detects small organic acids via deprotonation (Veres et al., 2008, Bertram et al., 2011), such as MAE, and some vicinal diol species, such as the IEPOX, as clusters with the reagent ion. MAE is detected as the $[C_4H_5O_3]^-$ ion at *m/z* 101, whereas IEPOX is detected as the $[CH_3COO{\cdot}C_5H_{10}O_3]^-$ ion at *m/z* 177 (Fig. S9). IEPOX and its gas-phase precursor, hydroxyhydroperoxides (ISOPOOH), were previously measured by CIMS with triple-quadrupole mass spectrometer that provides tandem mass spectra, as cluster ion with CF_3O^- at similar *m/z* and were distinguishable through their daughter ions using collision-induced dissociation (Paulot et al., 2009). Recent field and laboratory studies using acetate CIMS found that both ISOPOOH and IEPOX were observed at the same cluster ion at *m/z* 177~~, while the deprotonated form at *m/z* 117 could be attributed solely to IEPOX (D. K. Farmer, personal communication, 2015).~~. In our measurements, interferences of ISOPOOH to the cluster ion *m/z* 177 could not be differentiated because we could only observe the parent ions unlike Paulot et al. (2009~~))~~. ~~Moreover~~Our acetate CIMS sensitivities were measured to be relatively similar towards IEPOX and ISOPOOH at 10^{-7} and 9.9×10^{-8} signal ppt^{-1}, respectively. However, since we operated the acetate ~~ion chemistry HR-ToF-~~CIMS at different voltage settings than from Farmer et al. (personal communication, 2015), sensitivity of the deprotonated form of IEPOX is very low, and thus it could not be used to quantitatively measure IEPOX and/or to define the fractional contribution of IEPOX and ISOPOOH to the *m/z* 177 signal. ~~Therefore, we carefully note here that~~We synthesized ISOPOOH (see Fig. S10 for nuclear magnetic resonance (NMR) data) and measured CIMS sensitivities toward ISOPOOH and IEPOX. Results indicated that response factors of both compounds were similar (see Fig. S11). Investigation of lowering the IEPOX mixing ratio by a constant factor of total *m/z* 177 signal, which will be reported in a future study, showed that SOA tracer

Formatted: Tab stops: 15.24 cm, Left

model correlations are not sensitive to this and only tracers mass loadings vary with the IEPOX:ISOPOOH ratio. The inability to distinguish IEPOX from ISOPOOH is a limitation in our study. Therefore, we carefully note here that the *m/z* 177 ion measured during this study represents the upper limit of the IEPOX mixing ratio due to ISOPOOH interference at an unknown fraction of the signal.

Gaseous IEPOX and MAE were quantified with ~~HR-ToF-~~acetate CIMS by applying laboratory-derived calibration factors. All signals were normalized to acetate ion $[CH_3COO]^-$ at *m/z* 59 to take into account fluctuations in signal arising from changes in pressure during the course of field sampling and calibration. Calibrations were performed before and after the SOAS campaign using synthetic *trans-β*-IEPOX and MAE standards through dilution in a dark 10-m^3 indoor chamber at the University of North Carolina (UNC) (Lin et al., 2012). Synthetic procedures for *trans-β*-IEPOX and MAE have been described previously (Zhang et al., 2012b, Lin et al., 2013b). A known concentration of epoxide standard was injected into a 10-mL glass manifold using glass microliter syringes. The manifold was wrapped with heating tape and flushed with heated N_2 (g) at 5 L min^{-1} for at least 2 hours to the indoor chamber being sampled by the HR-ToF-CIMS until ion signals associated with MAE and IEPOX stabilized. We assumed unit injection efficiency of the epoxides through the glass chamber and into the chamber in calculating the chamber epoxide mixing ratios. Subsequently, we performed standard dilution of the ~~HR-ToF-~~acetate CIMS sample flow by using a T-piece in an N_2 (g) flow controlled by eight different micro-orifices to obtain an eight-point calibration curve. During the course of the calibration experiments, we accounted for the fact that we would lose 14 and 3% of IEPOX and MAE, respectively. Wall loss rates for IEPOX and MAE have been measured in the chamber and are 5.91×10^{-5} s^{-1} and 1.12×10^{-5} s^{-1}, respectively (Riedel et al., 2015). The chamber was sampled continuously at 2 L min^{-1}

for measurement of gaseous products by ~~HR-ToF-~~acetate CIMS and at 0.36 L min^{-1} for aerosol measurements by SEMS-MCPC to ensure that the chamber was particle free. Additionally, no particle nucleation events or significant particle loadings were observed over the course of calibrations. Normalized *m/z* 177 and 101 ions were plotted against epoxide mixing ratios of eight-point standards~~,~~; however, only four-point standards were used for IEPOX calibration due to non-linearity. Slopes of the fittings were used as calibration factors for the field measurements (Fig. ~~S10~~S12). Field calibrations were not performed due to the unavailability of IEPOX and MAE permeation tube systems.

2.4.2 Proton Transfer Reaction Time-of-Flight Mass Spectrometry (PTR-TOF-MS)

A proton-transfer-reaction time-of-flight mass spectrometer (PTR-TOF-MS 8000, Ionicon Analytik GmbH, Austria) equipped with switchable reagent ion capacity was used to measure the concentrations of gaseous organic species at the site. Ambient air was sampled from an inlet mounted on a tower ca. 2 m above the rooftop of the LRK site building through a 6.35 mm OD PFA sampling line at 4-5 standard L min^{-1}. A 2.0-µm pore size 47-mm diameter Zefluor teflon filter (Pall Corporation) at the inlet removed particles from the sample flow. The PTR-TOF-MS sub-sampled from this flow at a rate of 0.25 sLpm, resulting in a total inlet transit time of ca. 1-2 s.

PTR-TOF-MS has been described previously by Jordan et al. (2009a, 2009b~~))~~ and Graus et al. (2010~~))~~ and was operated in this study as described in Liu et al. (2013~~))~~. H_3O^+ reagent ions were used to selectively ionize organic molecules in the sample air. A high-resolution TOF detector (Tofwerk AG, Switzerland) was used to analyze the reagent and product ions and allowed for exact identification of the ion molecular formula (mass resolution >4000). The instrument was operated with a drift tube temperature of 80°C and a drift tube pressure of 2.35 mbar. In H_3O^+ mode, the drift tube voltage was set to 520 V,

resulting in an E/N of 120 Td (E, electric field strength; N, number density of air in the drift tube; unit, Townsend, Td; 1 Td = 10^{-17} V cm^2). PTR-TOF-MS spectra were collected at a time resolution of 10s. Mass calibration was performed every 2 min with data acquisition using the Tof-Daq v1.91 software (Tofwerk AG, Switzerland).

A calibration system was used to establish the instrument sensitivities to VOCs. Gas standards (Scott Specialty Gases) were added into a humidified zero air flow at controlled flow rates. Every 3 h the inlet flow was switched to pass through a catalytic converter (platinum on glass wool heated to 350°C) to remove VOCs and establish background intensities.

2.5 Filter Sampling Methods and Offline Chemical Analyses

$PM_{2.5}$ samples were collected on pre-baked Tissuquartz™ Filters (Pall Life Sciences, 8 × 10 in) with three high-volume $PM_{2.5}$ samplers (Tisch Environmental, Inc.). All high-volume $PM_{2.5}$ samplers were equipped with cyclones operated at 1 m^3 min^{-1}. One high-volume sampler collected $PM_{2.5}$ for 23 hours (08:00 to 07:00 the next day, local time), while the two remaining samplers collected $PM_{2.5}$ in two cycles. When the sampling schedules were daytime (08:00 – 19:00, local time) and nighttime (20:00 – 07:00, local time), the collection cycle and samples are defined as regular day-night sampling periods and samples. On selected days (10 – 12 June, 14 – 16 June, 29 – 30 June, and 9 – 16 July), when high levels of isoprene, sulfate (SO_4^{2-}), and NO_x were predicted at the LRK site by FLEXPART and MOZART model simulations (see SI), $PM_{2.5}$ were collected more frequently (08:00 – 11:00, 12:00 – 15:00, 16:00 – 19:00, and 20:00 – 07:00, local time) to capture the effects of anthropogenic pollution on isoprene SOA formation at higher time resolution by offline techniques. Such days are defined as intensive sampling periods and the samples as intensive samples. Forty-seven 23-

hour integrated and two sets of 64 intensive and 59 day-night filter samples were collected over the six-week period of the campaign and stored at -20°C until analysis. Field blanks were collected weekly by placing pre-baked quartz filters into the high-volume $PM_{2.5}$ samplers for 15 min and then removing and storing them under the same conditions as the field samples.

2.5.1 Instrumentation

Gas chromatography/electron ionization-mass spectrometry (GC/EI-MS) was performed on a Hewlett-Packard (HP) 5890 Series II Gas Chromatograph equipped with an Econo-Cap®-EC®-5 Capillary Column (30 m × 0.25 mm ID; 0.25 μm film thickness) coupled to an HP 5971A Mass Selective Detector. GC/EI-MS operating conditions and temperature program are provided in Surratt et al. (2010).

Ultra performance liquid chromatography/diode array detector-electrospray ionization high-resolution quadrupole time-of-flight mass spectrometry (UPLC/DAD-ESI-HR-QTOFMS) was performed on an Agilent 6500 series system equipped with a Waters Acquity UPLC HSS T3 column (2.1 × 100 mm, 1.8 μm particle size). UPLC/DAD-ESI-HR-QTOFMS operating conditions are described in Zhang et al. (2011).

2.5.2 Isoprene-derived SOA Tracer Quantification

Detailed filter extraction procedures are provided in Lin et al. (2013a). Briefly, from each filter two 37-mm punches (one for analysis by GC/EI-MS and one for UPLC/DAD-ESI-HR-QTOFMS analysis) were extracted in separate pre-cleaned scintillation vials with 20 mL high-purity methanol (LC-MS Chromasolv-grade®, Sigma Aldrich) by sonication for 45 min. Filter extracts were then filtered through 0.2-μm syringe filters (Acrodisc® PTFE membrane, Pall Life Sciences) to remove suspended filter fibers and insoluble particles, and then gently blown down to dryness under an N_2 (g) stream at room temperature.

The known IEPOX-derived SOA tracers, 2-methyltetrols (Claeys et al., 2004), C_5-alkene triols (Wang et al., 2005), *cis*- and *trans*-3-methyltetrahydrofuran-3,4-diols (3-MeTHF-3,4-diols) (Lin et al., 2013b), and IEPOX-derived dimers (Surratt et al., 2006), and the known MAE-derived SOA tracer, 2-methylglyceric acid (2-MG) (Edney et al., 2005), were identified by GC/EI-MS immediately following trimethylsilylation. Derivatization was performed by reaction with 100 μL of BSTFA + TMCS (99:1, v/v, Supelco) and 50 μL of pyridine (anhydrous, 99.8%, Sigma Aldrich) at 70°C for 1 hour. 1 μL of derivatized sample was directly analyzed. Base peak ions of the corresponding tracers, *m/z* 219 for 2-methyltetrols, *m/z* 231 for C_5-alkene triols, *m/z* 262 for 3-MeTHF-3,4-diols, *m/z* 335 for dimers, and *m/z* 219 for 2-MG, were quantified using authentic standards of 2-methyltetrols (50:50, v/v, 2-C-methylerythritol and 2-C-methylthreitol), *cis*- and *trans*-3-MeTHF-3,4-diols, and 2-MG. The C_5-alkene triols and dimers were quantified by the response factor obtained for the synthetic 2-methyltetrols. Synthetic procedures for *cis*- and *trans*-3-MeTHF-3,4-diols have been described previously by Zhang et al. (2012b). Synthesis of the tetrol mixture will be described in a forthcoming publication; the ^{1}H NMR trace (Figure ~~S11~~S13) shows a 1.2:1 2-C-methylerythritol and 2-C-methylthreitol of >99% purity.

Organosulfates, including the 2-methyltetrol sulfate esters ($[C_5H_{11}O_7S]^-$, *m/z* 215), IEPOX dimer sulfate esters ($[C_{10}H_{21}O_{10}S]^-$, *m/z* 333) (Surratt et al., 2008), and 2-MG sulfate ester ($[C_4H_7O_7S]^-$, *m/z* 199) (Lin et al., 2013b), were analyzed by UPLC/DAD-ESI-HR-QTOFMS. The UPLC/DAD-ESI-HR-QTOFMS was operated in both negative and positive ion modes; however, only the negative ion mode data is presented here since the positive ion mode data were recently described in Lin et al. (2014). Filter extract residues were reconstituted with 150 μL of a 50:50 (v/v) solvent mixture of methanol (LC-MS Chromasolv-grade, Sigma Aldrich) and laboratory Milli-q water and a 5 μL aliquot of each sample was

eluted with solvent of the same composition. IEPOX-derived sulfate esters (2-methyltetrol sulfate esters) were quantified using an authentic standard synthesized at UNC, while sodium propyl sulfate was used to quantify the remaining isoprene-derived organosulfates. The 2-methyltetrol sulfate ester standards were obtained and used as tetrabutylammonium salts. The synthetic procedure will be described in a forthcoming publication. The ^{1}H NMR trace (Fig. ~~S12~~S14) shows the purity of the sulfate ester mixture is >99%. The response factor of the authentic sulfate ester standards from several analyses is a factor of 2.25±0.13 lower than that of sodium propyl sulfate used in previous field studies (Lin et al., 2013a), suggesting that the IEPOX organosulfates likely make a contribution to mass concentration higher by a factor of ~2.3 than previously estimated at field sites. Table 1 summarized data for isoprene-derived SOA tracers quantified from 123 filter samples using the above techniques.

2.5.3 Filter Analysis of WSOC and OC Constituents

For analysis of water-soluble organic compound (WSOC) concentrations, additional filter punches (47 mm) were placed in pre-cleaned glass vials and extracted with 30 or 40 mL ultra pure water by sonication for 40 min at 1 kHz. Extracts were filtered through a syringe filter (0.45 µm, GE Heathcare UK Limited, UK) to remove insoluble particles. Samples were extracted batch-wise, with each batch containing 12-21 ambient samples, one lab blank, and one sample spiked with 1000 µgC L^{-1}. Total organic carbon (TOC) was analyzed using a 5310 C TOC Analyzer and 900 Inorganic Carbon Remover (ICR). The instrument was calibrated by single-point calibration with 1000 µgC L^{-1} of potassium hydrogen phthalate (KHP) and sodium carbonate. The calibration was verified with 1000 µgC L^{-1} of sucrose, and checked daily with a 1000 µgC L^{-1} of KHP standard. Standards and samples were run in triplicate; the first data point was rejected and the following two averaged.

Total OC and elemental carbon (EC) measurements from filter samples were conducted at the National Exposure Research Laboratory, U.S. Environmental Protection Agency, at Research Triangle Park, NC. A 1.5 cm^2 punch was taken from each filter for OC/EC analysis using the thermal-optical method (Birch and Cary, 1996) on a Sunset Laboratory (Tigard, OR) OC/EC instrument. Table S4 provides temperature and purge gas settings for the method. The instrument was calibrated internally using methane gas and the calibration was verified with sucrose solution at four mass concentrations.

2.6 Estimations of Aerosol pH and IEPOX-Derived SOA Tracers

The thermodynamic model, ISORROPIA-II (Fountoukis and Nenes, 2007, Nenes et al., 1999), is used to estimate aerosol pH. Inputs for the model include aerosol-phase sulfate, nitrate, and ammonium in μmol m^{-3}, measured by the ACSM under ambient conditions; RH and temperature obtained from National Park Service (NPS); and gas-phase ammonia obtained from Ammonia Monitoring Network (AMoN; TN01/Great Smoky Mountains National Park – Look Rock). ISORROPIA-II predicted particle hydronium ion concentration per volume of air (H^+_{air}, μg m^{-3}), aerosol water (LWC, μg m^{-3}), and aerosol aqueous phase mass concentration (μg m^{-3}). Aerosol pH is calculated by the following equation:

$$\text{pH} = -\log_{10} a_{H^+} = -\log_{10}\left(\frac{H^+_{air}}{LWC} \times \rho_{aer} \times 1000\right) \quad (4)$$

where a_{H^+} is H^+ activity in aqueous phase (mol L^{-1}), *LMASS* is the total liquid-phase aerosol mass (μg m^{-3}) and ρ_{aer} is aerosol density (g cm^{-3}). The ability of ISORROPIA to capture pH, LWC and gas-to-particle partitioning of inorganic volatiles (e.g., NH_3, HNO_3, HCl) has been the focus of other studies ~~(Fountoukis et al., 2009, Guo et al., 2014)~~ (Fountoukis et al., 2009, RW.ERROR - Unable to find reference:433) and is not further discussed here.

IEPOX-derived SOA tracers are estimated using simpleGAMMA (Woo and McNeill, 2015). It is a reduced version of GAMMA (Gas Aerosol Model for Mechanism Analysis), the detailed photochemical box model of aqueous aerosol SOA (aqSOA) formation developed by McNeill and coworkers (McNeill et al., 2012). GAMMA and simpleGAMMA represent aqSOA formation in terms of bulk aqueous uptake followed by aqueous-phase reaction (Schwartz, 1986). For this study, we utilized only the aqueous aerosol-phase chemistry of IEPOX to predict IEPOX-derived SOA constituents. We applied the Henry's law constant of 3×10^7 M atm^{-1} for IEPOX partitioning based on measurements by Nguyen et al. (2014) on deliquesced NaCl particles. Estimation of 2-methyltetrols and IEPOX-derived organosulfate masses in the aqueous phase was based on the Eddingsaas et al. (2010) mechanism:

$$\mathrm{IEPOX(aq)} \rightarrow (1-\square)\cdot 2\mathrm{methyltetrols} + \square \cdot \mathrm{IEPOXorganosulfate} \quad (5)$$

where β is a branching ratio between 2-methyltetrols and IEPOX-derived organosulfate concentration. We applied β = 0.4 based on the observation of Eddingsaas et al. (2010) for the most concentrated bulk solution they studied. The rate constant for reaction (5) (*ka*) is a function of $\square_{\square^+}$ and nucleophile concentrations (Eddingsaas et al., 2010), modified to include the possible protonation of IEPOX(aq) by ammonium (Nguyen et al., 2014):

$$\square\square = \square_{\square^+}\square_{\square^+} + \square_{\square\square_4^{2-}}[\square\square_4^{2-}]\square_{\square^+} + \square_{\square\square\square_4^-}[\square\square\square_4^-] + \square_{\square\square_4^+}[\square\square_4^+] \quad (6)$$

Here, $\square_{\square^+} = 5 \times 10^{-2}\square^{-1}$, $\square_{\square\square_4^{2-}} = 2 \times 10^{-4}\square^{-1}\square^{-1}$, and $\square_{\square\square\square_4^-} = 7.3 \times 10^{-4}\square^{-1}\square^{-1}$. The ammonium rate constant, $\square_{\square\square_4^+}$, was calculated using GAMMA and the results of the chamber study of Nguyen et al. (2014) to be $1.7 \times 10^{-5}\square^{-1}\square^{-1}$.

IEPOX uptake and formation of 2-methyltetrols and IEPOX-derived organosulfate was computed using simpleGAMMA with inputs of SO_4^{2-}, HSO_4^-, NH_4^+, LWC, $\square_{\square^+}$

concentrations (mol L^{-1}), and aerosol pH estimated by ISORROPIA-II simulation of field conditions, ambient temperature and RH, aerosol surface area (cm^2 cm^{-3}) obtained from SEMS-MCPC measurements, and IEPOX concentration (mol cm^{-3}) from ~~HR-ToF-~~acetate CIMS (Section 2.4). Masses of SOA tracers formed over 12 hours are compared with measurements in Section 3.4.2.

3 Results and Discussion

3.1 Fine Aerosol Component Mass Concentrations

Chemical measurements of fine aerosol made by the ACSM and collocated instruments are presented in Fig. 1. The ACSM measured a campaign average 7.6±4.7 µg m^{-3} of NR-PM_1, which is predominantly organic aerosol (64.1%). Sulfate aerosol (24.3%) is the most dominant inorganic aerosol component, followed by ammonium (7.7%), nitrate (3.8%), and chloride (0.1%). The NR-PM_1 mass measured at the site shows strong association (r^2 = 0.89) with the SEMS-MCPC PM_1 mass measurements (Figs. 1d and S3).

Moderate correlations, depicted in Fig. ~~S10,~~S15 were observed between ACSM OM and filter OC and WSOC (r^2 = 0.54, 0.39, respectively) as well as between filter OC and WSOC measurements (r^2 = 0.36), suggesting that fractions of OM and OC at LRK site are water-soluble as previously observed (Turpin and Lim, 2001). This water-soluble fraction may be associated with high isoprene emissions in this area (Zhang et al., 2012a). Lewis et al. (2004) reported that 56%-80% of total carbon in $PM_{2.5}$ samples collected during summer in Nashville, TN, was non-fossil carbon, supporting the importance of biogenic SOA in the southeastern U.S. during summer. It is potentially possible that some fraction of this non-fossil carbon is associated to biomass burning (Ke et al., 2007). A more recent study found that non-fossil carbon accounts for 50% of carbon at two urban sites and 70%–100% of

carbon at 10 near-urban or remote sites in the U.S. (Schichtel et al., 2008). In summer 2001, the fraction of non-fossil carbon was reported to vary from 66-80% of total carbon at the LRK, TN site, suggesting the importance of photochemical oxidation of biogenic VOCs (Tanner et al., 2004). The slope of the linear regression analysis on Fig. ~~S13a~~S15a indicates an OM:OC ratio of 2.34 and OM:WSOC ratio of 2.19. Using the Aiken et al. (2008) parameterization approach, we found an average (±1-σ) OM:OC ratio of 2.14 (±0.18). The LRK OM:OC ratios obtained from measurements and parameterization are consistent with a previous study at Look Rock (2.1) (Turpin and Lim, 2001), but higher than those measured at Centerville, AL (1.77) (Sun et al., 2011), probably ascribable to different atmospheric aerosol properties at the two sites.

Elemental analyses of ACSM unit-mass resolution data using the Aiken et al. (2008) parameterization results in an average O:C ratio of 0.77±0.12. This is within 0.6–1 of O:C ratio previously observed in the southeastern U.S. (Centerville, AL) (Sun et al., 2011, Xu et al., 2015~~))~~).

ACSM sulfate aerosol measurements (average of 1.85±1.23 µg m^{-3}) agree well (r^2 = 0.67, slope 1.08) with the collocated sulfate measurements (Table S1), demonstrating that ACSM performed well when compared to existing air quality monitoring instruments as previously reported (Budisulistiorini et al., 2014). Low nitrate concentration is expected due to the high summer temperatures (15–31°C) and low prevailing NO_x concentrations (0.1–2 ppb) measured at the site. In the absence of a significant source of chloride, chloride concentrations were predictably low (0.01±0.01 µg m^{-3}).

On average, mass concentration of BC was 0.23±0.14 µg m^{-3} or about 3% of total $PM_{2.5}$ measured at the site. The low relative contribution was consistent during the campaign except on 11 to 12 July when there was a significant increase during few hours overnight. EC

measured from filters was even lower at 0.06 μg m^{-3} on average and was only weakly correlated (r^2 = 0.32) with BC. Carbon monoxide (CO), another primary species measured at LRK, was also low (115.62±24.06 ppb on average) throughout the campaign. A previous study found that the level of primary species increased during mid-morning when the boundary layer height reached the site, and declined later in the day as a result of dilution (Tanner et al., 2005). In contrast, secondary species such as $PM_{2.5}$ and sulfate do not show significant diurnal variability, suggesting local meteorological conditions are less influential in determining concentrations of the long-lived species ~~(Tanner et al., 2005).~~(Tanner et al., 2005, Tanner et al., 2015). The overall low concentration of primary emissions at the site (Fig. ~~S14~~S16) is consistent with minimum local and/or regional primary emissions.

3.2 Source Apportionment of OA from the ACSM

PMF analysis was conducted on the ACSM OA mass spectral data in order to resolve factors (or source profiles) without a-priori assumptions. A 3-factor solution resolved from PMF analysis, as shown in Figs. 2 and 3, was selected as the best-fit (see SI for details of Q/Q_{exp}, fpeak, etc.), comprised of the known LV-OOA factor (Jimenez et al., 2009, Ulbrich et al., 2009), an IEPOX-OA factor (Budisulistiorini et al., 2013, Slowik et al., 2011, Robinson et al., 2011), and a factor similar to 91Fac, a factor previously observed in areas dominated by biogenic emissions (Robinson et al., 2011, Slowik et al., 2011, Chen et al., 2014).

The IEPOX-OA factor resolved from our dataset is more closely correlated to sulfate measured by the ACSM (r^2 = 0.58) than by the collocated instrument (r^2 = 0.31) (Table S5). Correlation of gaseous IEPOX measured by ~~HR-ToF-~~acetate CIMS with the IEPOX-OA factor is low (r^2 = 0.24), which may be a consequence of time gap from IEPOX uptake onto sulfate aerosol process which can take up ~5 hours in the presence of aqueous, highly acidic aerosol (pH ≤ 1) (Gaston et al., 2014). The time gap between formation of gaseous IEPOX

and IEPOX-OA factor could be wider due to ISOPOOH, which lifetime to OH is 3 – 5 hours ~~((~~Paulot et al., 2009~~))~~, interference on IEPOX signal measured by acetate ~~HR-ToF-~~acetate CIMS. Importantly, the IEPOX-OA factor correlates strongly with 2-methyltetrols (r^2 = 0.80), IEPOX-derived organosulfates (r^2 = 0.81), C_5-alkene triols (r^2 = 0.75), and dimers of organosulfates (r^2 = 0.73) (Table 2), giving an overall r^2 of 0.83 with sum of IEPOX-derived SOA tracers measured by offline techniques. The high correlation provides strong evidence that IEPOX chemistry gives rise to the PMF factor we have designated as the IEPOX-OA factor. The contribution of this factor to total OM is 32%, which is strikingly consistent with the contribution of the factor designated as the IEPOX-OA factor in the PMF analysis of fine organic aerosol collected in downtown Atlanta, GA (Budisulistiorini et al., 2013) and across other sites in this region (Xu et al., 2015). IEPOX-OA was not only formed on site but could also transported from surrounding forested and isoprene-rich areas. The reactive-uptake of IEPOX is influenced by aerosol sulfate (Lin et al., 2012) that is not formed on site, might explain the lack of significant diurnal variation (Fig. 3) of the IEPOX-OA factor at LRK. WSOC shows fair correlation with some IEPOX-OA tracers (r^2 = 0.3–0.4; Table S6) and IEPOX-OA factor (r^2 = 0.37; Table S5) the nature of which will be discussed in more detail below.

The LV-OOA factor contributes 50% of OM (Fig. 3). The average f_{44} = 0.22 is comparable to that of the standard LV-OOA profile (Ng et al., 2011), suggesting it is an oxidized (aged) aerosol. The LV-OOA correlated well with nitrate (r^2 = 0.62) but more weakly with sulfate (r^2 = 0.39) (Table S5). Correlation with nitrate as well as the high level of oxidation is consistent with the suggestion above that a fraction of OA originates ~~in~~from the valley. Located on a ridge top above the morning valley fog, LRK receives air masses from the valley as the boundary layer rises during the day (Tanner et al., 2005). ~~Xu et al.~~

(2015)Diurnal profile of LV-OOA observed less at LRK is similar to more-oxidized OA factor OOA (MO-OOA) observed at Centerville that was attributed to nitrate chemistry(Xu et al., 2015), suggesting their regional sources. At LRK average mixing ratios of monoterpenes. However, diurnal profiles of LV-OOA observed in Look Rock and Centervilleisoprene were significantly different. At Look Rock, LV-OOA increased during the day, and the opposite for Centerville. At Look Rock, monoterpenes was less than ≤1 ppb on average, whereas concentration of LV-OOA was and ~2 3 μg m^{-3}. Therefore, it is unlikely that monoterpenes was a main source of LV-OOA at Look Rock. BVOCs, including isoprene and monoterpenes, and ppb (Fig. 4), respectively. Low anthropogenic emissions at LRK (<1 ppb; Fig. S16) suggests that BVOCs could be the source of LV-OOA (50% of OA) formation. Anthropogenic emissions as well as nitrate chemistry in the valley, could be the source ofalso influence LV-OOA formation that oxidized during transport to the LRK site.

The 91Fac factor is characterized by a distinct ion at *m/z* 91. At LRK, the average f_{44} of 91Fac is 0.12, between the values 0.05 and 0.16 reported for standard SV-OOA and LV-OOA profiles, respectively (Ng et al., 2011), indicating that it is likely an oxygenated OA. The LRK 91Fac makes the smallest contribution to OM (18%) of the three factors resolved by PMF analysis. The 91Fac diurnal pattern shows slight increases during noon and night, suggesting that this factor might be affected by both photochemistry and nighttime chemistry. Potential sourcesources of 91Fac is provideddiscussed in more detail in the SI (Fig. S15S17) and its association of 91Fac with biogenic SOA chemistry will be the focus of future studies.

A source apportionment study of organic compounds in $PM_{2.5}$ at LRK during August 2002 using the chemical mass balance (CMB) model evaluated contributions by eight primary sources, chosen as representing the major contributors to fine primary OC in the southeast U.S. Primary sources, consisting largely of wood burning, were estimated to contribute ~14%

of the total OC at LRK (Ke et al., 2007). ^{14}C Analysis of the LRK $PM_{2.5}$ in the same study showed that during summer, ~84% of the OC was non-fossil carbon (Ke et al., 2007). By contrast, our current study resolved no POA by PMF analysis. However, in subsequent studies, we will investigate the influence of POA at LRK by examining the ^{14}C data from filter samples.

3.3 Identification and Quantification of Isoprene-derived SOA Tracers

2-Methylglyceric acid, 2-methyltetrols, C_5-alkene triols and IEPOX-derived organosulfates were detected in most filter samples (Table 1). Among all observed SOA tracers, 2-C-methylerythritol and 2-methylbut-3-ene-1,2,4-triol were the most abundant species identified by GC/EI-MS, contributing ~24.6% (120.7 ng m^{-3} on average) and ~20.1% (98.8 ng m^{-3} on average), respectively, of total quantified mass, while isomeric IEPOX-derived organosulfates accounted for ~34.5% (169.5 ng m^{-3} on average) of the mass detected by UPLC/DAD-ESI-HR-QTOFMS. Concentrations of the isomeric 3-MeTHF-3,4-diols were lower (≤ 18.8 ng m^{-3}), often at or below detection limits. Gaseous IEPOX was on average 1 ppb (maximum 5.8 ppb) significantly higher than gaseous MAE at 2.8×10^{-3} ppb on average (maximum 0.02 ppb). This explains the abundance of IEPOX-derived SOA tracers compared to MAE-derived tracers. It should be noted that IEPOX quantified here includes the interference of ISOPOOH on its signal; however, the overall measured IEPOX signal is still substantially higher than the MAE signal, even if we assume IEPOX only contributes to 1 – 10% of the *m/z* 177 intensity.

In sum, IEPOX- and MAE-derived tracers contributed 96.6% and 3.4%, respectively, of total isoprene-derived SOA mass quantified from filter samples. This observation is consistent with a previous field study in Yorkville, GA, which reported the summed IEPOX-derived SOA tracers comprised 97.5% of the quantified isoprene-derived SOA mass (Lin et

al., 2013a). Total IEPOX-derived tracers masses quantified from filter samples were on average 26.3% (maximum 48.5%) of the IEPOX-OA factor mass resolved by PMF. This is consistent with a recent laboratory study of isoprene photooxidation under high HO_2 conditions that suggested IEPOX isomers contributed about 50% of SOA mass formed (Liu et al., 2014).

Masses of IEPOX- and MAE-derived SOA tracers were fairly correlated (r^2 = 0.37 and 0.29, respectively) with WSOC (Fig. ~~S13c~~S15c). Around 26% of the WSOC mass might be explained by IEPOX-derived SOA tracer masses, which consist predominantly of 2-methyltetrols, C_5-alkene triols, and IEPOX-derived organosulfates. The tetrols and triols are hydrophilic compounds owing to the OH groups, and the organosulfates are ionic polar compounds (Gómez-González et al., 2008).

An interesting and potentially important observation is that oligomeric IEPOX-derived humic-like substances (HULIS) have been reported in both reactive uptake experiments onto acidified sulfate seed aerosol and in ambient fine aerosol from ~~Look Rock~~the LRK and Centerville sites during the SOAS campaign (Lin et al., 2014). The HULIS is a mixture of hydroxylated, sulfated as well as highly unsaturated, light-absorbing components which may partition between WSOC and water insoluble organic carbon (WISC) fractions (Lin et al., 2014). This finding might also in part explain the moderate correlation between WSOC and the IEPOX-OA factor. However, HULIS has not been quantified here due to the lack of authentic standards, but will likely help to close the IEPOX-OA mass budget once appropriate standards are developed and applied. As quantified by ACSM, summed isoprene-derived SOA tracers on average accounted for 0.5 μg m^{-3} or 9.4% (up to 4.4 μg m^{-3} or 28.1%) of the average organic aerosol mass of 5.1 μg m^{-3} (maximum 15.3 μg m^{-3}) during the campaign. This contribution is somewhat lower than reported at a different rural site in the southeast U.S.

(13.6% - 19.4%) (Lin et al., 2013a) but higher than reported at a forested site in central Europe (6.8%) (Kourtchev et al., 2009) and a rural site in south China (1.6%) (Ding et al., 2012). ~~However, it~~It should be noted that in all previous studies sulfate esters of 2-methyltetrol were quantified by surrogate standard structurally unrelated to the target analytes (i.e., sodium propyl sulfate). ~~In contrast to the~~While in current study, a mixture of authentic 2-methyltetrol sulfate esters was used as a standard for quantifying IEPOX-derived organosulfates. The use of structurally unrelated surrogate standards may account in part for discrepancies between this and previous studies in which total isoprene SOA mass may have been underestimated as a result of higher instrument response to surrogates and/or lower recovery in sample preparation. These possibilities warrant further investigation using the same analytical protocols and comparison of instrumental responses to authentic and surrogate standards.

3.4 Influence of Anthropogenic Emissions on Isoprene-Derived SOA Formation at Look Rock

3.4.1 Effects of aerosol acidity and nitrogen-containing species

The time series of aerosol pH estimated by ISORROPIA-II overlaid on the time series of the IEPOX-OA factor and IEPOX- and MAE-derived SOA tracers (Fig. 5a, Tables S5-S6) suggests that local aerosol acidity is not correlated with these measured variables. The correlation coefficients of the IEPOX-OA factor with ISORROPIA-II estimated pH and LWC bears out this conclusion (r^2 ~0; Table S5). These results are consistent with recent measurements reported by Xu et al. (2015~~))~~) across several sites in the southeastern U.S. Aerosol acidity can be expected to change during transport and aging. Further complicating factors may be ~~neutralization~~viscosity or morphology changes of the aerosol as IEPOX is

Formatted: Font color: Auto

Formatted: Font color: Auto

taken up by heterogeneous reaction, and thus, slowing of uptake kinetics as the aerosol surface is coated with a hydrophobic organic layer (Gaston et al., 2014). Additionally, liquid-liquid phase separation is likely to occur in the atmosphere due to changes of relative humidity that affect particles water content (You et al., 2012). Moreover, the effects of aerosol viscosity and morphology on IEPOX uptake is not well understood and warrant further study using aerosol of complex mixtures and of atmospheric relevance. Interpretation of the apparent lack of relationship between SOA and local aerosol acidity suggests that aerosol acidity is likely not the limiting factor in isoprene SOA formation at this site, especially since aerosol was consistently acidic during SOAS. The IEPOX-OA factor is moderately correlated with aerosol sulfate measured by ACSM (r^2 = 0.58), while IEPOX- and MAE-derived SOA tracers are less correlated (r^2 ~0.4) (Fig. 5b). Correlation between sulfate and IEPOX-OA factor is consistent with recent measurements by Xu et al. (2015), and suggests the need for aerosol surface area due to acidic sulfate for these heterogeneous reactions to occur leading to IEPOX-OA formation.

Formatted: Font color: Auto

Formatted: Font color: Auto

Formatted: Font color: Auto

Formatted: Font color: Auto

Correlation of IEPOX-OA and isoprene-derived SOA tracers with NO_x, NO_y, and reservoir species (NO_z = NO_y – NO_x) was also examined. None of the nitrogen species showed significant association with either the IEPOX-OA factor (r^2 < 0.1; Table S5) or the IEPOX-derived SOA tracers (r^2 < 0.3; Table S5). Absence of correlations suggest that: (1) the formation of isoprene SOA primarily through the low-NO pathway of isoprene photooxidation (Paulot et al., 2009, Surratt et al., 2010), (2) the isoprene oxidation did not happen locally, and (3) the gas-phase isoprene oxidation is not yet fully understood. Correlation plot of NO_y, a measure of total reactive nitrogen species including MPAN, with summed MAE tracers is shown in Fig. 5c and correlation values of NO_x with individual compounds are given in Table S6. Besides being derived solely from the hydrolysis of MAE,

2-MG is also proposed to be the hydrolysis product of hydroxymethyl-methyl-α-lactone (HMML~~) (Nguyen et al., 2015))~~ (Nguyen et al., 2015) and fair correlation between NO_y and 2-MG (r^2 = 0.38) is consistent with this hypothesis. The correlation of the high-NO_x isoprene SOA tracers (2-MG and its corresponding organosulfate) with NO_y is suggesting that other pathways like the uptake and hydrolysis of MAE could be a source, especially since the further oxidation of MACR has been shown to yield MAE directly (Lin et al., 2013b). The observation that neither the summed MAE/HMML-derived tracers nor 2-MG correlated with NO_x, is consistent with the hypothesis that MAE/HMML is formed in urban areas upwind and transported to the sampling site. Furthermore, it suggests that likely both HMML and MAE could be sources of these tracers.

In addition to the pattern of daily up-slope transport of air from the valley, air mass back-trajectory during high IEPOX-derived SOA episodes (Fig. ~~S16~~S18) indicated that air masses also originated west of LRK, in the direction of the urban areas of Knoxville and Nashville, TN. Yet further west of the LRK site are the Missouri Ozarks, a large source of isoprene emissions (referred to as the "isoprene volcano") (Guenther et al., 2006). During summer, isoprene emitted in the Ozarks could mix with anthropogenic emissions from Knoxville and Nashville, undergoing atmospheric processing during transport. As a consequence, long distance transport and accompanying oxidative processing may make a contribution to the IEPOX SOA ~~load~~loading at LRK. During low IEPOX-derived SOA periods (Fig. ~~S17~~S19) air masses originated predominantly from the south and southwest, which are densely forested, rural areas.

3.4.2 Box Modeling Supports the Impact of Aqueous Acidic Aerosol on IEPOX-Derived SOA

The IEPOX-derived SOA tracers (2-methyltetrols and IEPOX-derived organosulfate) predicted using simpleGAMMA, taking the locally measured IEPOX and aerosol parameters as inputs, show good correlation (r^2 = 0.5–0.7) with the tracers quantified from filter samples (Table 3, Fig. ~~S18~~S20). Slopes of the scatterplots show that the model overestimated the 2-methyltetrols and IEPOX-derived organosulfates by factors of 6.3 and 7.5, respectively. simpleGAMMA calculates Henry's Law gas-aqueous equilibration at each time step and decouples the subsequent aqueous-phase chemistry of IEPOX from dissolution (McNeill et al., 2012). In this study, we assumed an effective Henry's law constant, H*, of 3×10^7 M atm^{-1} for IEPOX, following the recent laboratory measurements of Nguyen et al. (2014), whereas previous studies assumed values which ranged one order of magnitude higher (1.3×10^8 M atm^{-1} (Eddingsaas et al., 2010)) or lower (2.7×10^6 M atm^{-1} (Pye et al., 2013)). Replacing the H* with that of Pye et al. (2013), the model underestimated the 2-methyltetrols and IEPOX-derived organosulfates by 56% and 43%, respectively. Decreasing the H* by one order of magnitude yielded a factor of ~10 decrease in the predicted IEPOX SOA tracers mass, which is consistent with Pye et al. (2013) observation in sensitivity studies that a factor of 7 increase in H* yielded a factor of ~5 increase in predicted IEPOX SOA yield. Similarly, summed masses of the modeled SOA tracers (Fig. 6) yielded a 141% (r^2 = 0.62) overestimate of the IEPOX-OA factor, whereas summed SOA tracers modeled by assuming H* of one order of magnitude lower yielded an 89% underestimate of the IEPOX-OA factor (r^2 = 0.62). simpleGAMMA predicts only a subset of IEPOX-derived SOA tracers, thus underestimation of the ~~predicted tracers to~~ IEPOX-OA factor is expected.

In addition to the uncertainty in the H* parameter, several other factors may also contribute to mass disagreement between the tracer estimated by simpleGAMMA and the field data. The box model simulations took locally measured IEPOX and aerosol parameters as inputs, and simulated 12 hours of reactive processing, rather than simulating uptake, reaction, and transport along a trajectory initiating in the valley. The locally measured IEPOX signal is noted above to have interference from ISOPOOH, thus the model outputs likely overestimate the measurements. Examination of IEPOX input variability to simpleGAMMA tracers estimation will be reported in a future study. Additionally, C_5-alkene triols, the third largest contributor to the IEPOX-derived SOA tracers, and oligomeric HULIS are not included in the simpleGAMMA model estimation. Neglect of the C_5-alkene triols and oligomers as well as yet unknown IEPOX-derived SOA formation pathways by this model could contribute to inaccuracy in estimation of the mass contribution of 2-methyltetrols and IEPOX-derived organosulfates to the total amount of IEPOX-derived SOA tracers and reduce the correlation. Finally, oxidative aging of IEPOX SOA tracers is not included in simpleGAMMA at this time due to current lack of availability of kinetic and mechanistic data. Overall, although mass disagreement persists, good correlation between model and field measurements of tracers suggest that the uptake mechanism of IEPOX is consistent with acid-catalyzed mechanism proposed from kinetic ~~((~~Eddingsaas et al., 2010, Pye et al., 2013~~)~~) and laboratory studies ~~((~~Lin et al., 2012, Nguyen et al., 2014~~)~~).

4 Conclusions

Offline chemical analysis of $PM_{2.5}$ samples collected from LRK, TN, during the 2013 SOAS campaign show a substantial contribution by IEPOX-derived SOA tracers to the total OA mass (~9% on average, up to 28%). A larger contribution (32%) to total OA mass is estimated by PMF analysis of the real-time ACSM OA mass spectrometric data. Overall, the

importance of IEPOX heterogeneous chemistry in this region is clearly demonstrable. No association was observed between the gas-phase constituents NO and NO_2 and the IEPOX-derived SOA tracers or the IEPOX-OA factor suggesting that IEPOX-derived SOA formed upwind or distant from the sampling site. Moderate association between NO_y and ~~MAE-/HMML~~MACR-derived SOA tracers was observed, consistent with the proposed involvement of oxidizing nitrogen compounds in ~~MAE-/HMML~~MACR-derived SOA formation ~~(Lin et al., 2013b, Nguyen et al., 2015)~~(Lin et al., 2013b, Nguyen et al., 2015). Particle-phase sulfate is fairly correlated (r^2 = 0.3–0.4) with both ~~MAE-/HMML~~MACR- and IEPOX-derived SOA tracers, and more strongly correlated (r^2 ~0.6) with the IEPOX-OA factor, overall suggesting that sulfate plays an important role in isoprene SOA formation. However, this association requires further analysis, in light of the proposed formation of IEPOX-derived SOA during transport to LRK from an upwind or down-slope origin. Several explanations may be proposed for the lack of a strong association between isoprene-derived SOA mass and particle acidity: 1) isoprene-derived SOA is not strongly limited by levels of predicted aerosol acidity and LWC even though these are in the favored ranges (pH < 2) to promote sufficient SOA production based on recent laboratory kinetic studies (Gaston et al., 2014, Riedel et al., 2015) and thus, other potentially unknown controlling factors in this region might need to be considered; 2) no strong correlation exists between SOA mass and local aerosol acidity which estimation is challenging due to changes in particle composition and characteristics during reactive uptake and 3) several key inter-related variables (LWC, aerosol surface area and aerosol acidity) control SOA yield and thus the correlation of aerosol acidity and SOA yield will be difficult to deconvolute from complex field data until modeling can better constrain these effects. Consistent with the suggestion that IEPOX-derived SOA forms during transport from distant locations, air mass back-trajectory indicated that westerly flow from potential sources of oxidation products where biogenic and anthropogenic emissions can mix, are likely

related to episodes of high levels of IEPOX-derived SOA measured at LRK. In contrast, when air masses originated mainly from forested and rural areas to the south and southeast of the site, high levels of IEPOX-derived SOA mass were not observed. Good correlation between SOA model outputs and field measurements suggests that gaps remain in our knowledge of isoprene-derived SOA formation. Laboratory studies are needed to reduce the uncertainty in the effective Henry's Law constant, H*, for IEPOX. Additional studies are needed to further quantify the condensed-phase mechanism and kinetics of SOA formation via the IEPOX pathway so that it may be represented in more detail in models. Notwithstanding, initial modeling results allow critical insight into how more explicit treatment of the reactions between anthropogenic pollutants and isoprene oxidation products may be incorporated into models of SOA formation. Importantly, by inclusion of explicit IEPOX- and MAE-derived SOA formation pathways in a model, Pye et al. (2013) recently demonstrated that by lowering SO_x emissions in the eastern U.S. by 25% could lower IEPOX- and MAE-derived SOA formation 35 to 40%. Future studies should attempt to improve model predictions of IEPOX-derived SOA formation and systematically examine effects of implementing stricter SO_x controls in this region.

Acknowledgements

This work was funded by the U.S. Environmental Protection Agency (EPA) through grant number 835404. The contents of this publication are solely the responsibility of the authors and do not necessarily represent the official views of the U.S. EPA. Further, the U.S. EPA does not endorse the purchase of any commercial products or services mentioned in the publication. The U.S. EPA through its Office of Research and Development collaborated in the research described here. It has been subjected to Agency review and approved for publication, but may not necessarily reflect official Agency policy. The author would also like

to thank the Electric Power Research Institute (EPRI) for their support. This study was supported in part by the National Oceanic and Atmospheric Administration (NOAA) Climate Program Office's AC4 program, award # NA13OAR4310064. We thank Bill Hicks of the Tennessee Valley Authority (TVA) for his assistance in collecting the collocated monitoring data at the LRK site. S. H. Budisulistiorini was supported by a Fulbright Presidential Fellowship (2010–2013) for attending the University of North Carolina at Chapel Hill and the UNC Graduate School Off-Campus Dissertation Research Fellowship, as well as partial appointment to the Internship/Research Participation Program at the Office of Research and Development, U.S. EPA, administered by the Oak Ridge Institute for Science and Education through an interagency agreement between the U.S. Department of Energy and EPA. M. Neff and E. A. Stone were supported by US EPA Science to Achieve Results (STAR) program grant number 835401. The authors thank Lynn Russell, Timothy Bertram and Christopher Cappa as well as their respective groups for their collaboration during the SOAS campaign at LRK. The authors thank Louisa Emmons for her assistance with forecasts made available during the SOAS campaign. The authors thank John Offenberg for providing access to Sunset OC/EC analysis instrument. The authors also thank Tianqu Cui for his assistance in helping deploy instrumentation from the UNC group, and Wendy Marth and Theran Riedel for their assistance in helping calibrate the ~~HR-ToF-~~ acetate CIMS. We would like to thank Annmarie Carlton, Joost deGouw, Jose Jimenez, and Allen Goldstein for helping to organize the SOAS campaign and coordinating communication between ground sites.

References

Aiken, A. C., DeCarlo, P.F., Kroll, J.H., Worsnop, D.R., Huffman, J.A., Docherty, K.S., Ulbrich, I.M., Mohr, C., Kimmel, J.R., Sueper, D., Sun, Y., Zhang, Q., Trimborn, A., Northway, M., Ziemann, P.J., Canagaratna, M.R., Onasch, T.B., Alfarra, M.R., Prevot, A.S.H., Dommen, J., Duplissy, J., Metzger, A., Baltensperger, U. and Jimenez, J.L.: O/C and OM/OC Ratios of Primary, Secondary, and Ambient Organic Aerosols with High-Resolution Time-of-Flight

Aerosol Mass Spectrometry, Environ. Sci. Technol., 42, 4478-4485, doi:10.1021/es703009q, 2008.

~~Alfarra, M. R., Prevot, A.S.H., Szidat, S., Sandradewi, J., Weimer, S., Lanz, V.A., Schreiber, D., Mohr, M. and Baltensperger, U.: Identification of the Mass Spectral Signature of Organic Aerosols from Wood Burning Emissions, Environ. Sci. Technol., 41, 5770-5777, doi:10.1021/es062289b, 2007.~~

Bates, K. H., Crounse, J.D., St. Clair, J.M., Bennett, N.B., Nguyen, T.B., Seinfeld, J.H., Stoltz, B.M. and Wennberg, P.O.: Gas Phase Production and Loss of Isoprene Epoxydiols, J. Phys. Chem. A, 118, 1237-1246, doi:10.1021/jp4107958, 2014.

Bertram, T. H., Kimmel, J.R., Crisp, T.A., Ryder, O.S., Yatavelli, R.L.N., Thornton, J.A., Cubison, M.J., Gonin, M. and Worsnop, D.R.: A field-deployable, chemical ionization time-of-flight mass spectrometer, Atmos. Meas. Tech., 4, 1471-1479, doi:10.5194/amt-4-1471-2011, 2011.

Birch, M. E. and Cary, R.A.: Elemental carbon-based method for occupational monitoring of particulate diesel exhaust: methodology and exposure issues, Analyst, 121, 1183-1190, doi:10.1039/AN9962101183", 1996.

Budisulistiorini, S. H., Canagaratna, M.R., Croteau, P.L., Baumann, K., Edgerton, E.S., Kollman, M.S., Ng, N.L., Verma, V., Shaw, S.L., Knipping, E.M., Worsnop, D.R., Jayne, J.T., Weber, R.J. and Surratt, J.D.: Intercomparison of an Aerosol Chemical Speciation Monitor (ACSM) with ambient fine aerosol measurements in downtown Atlanta, Georgia, Atmos. Meas. Tech., 7, 1929-1941, doi:10.5194/amt-7-1929-2014, 2014.

Budisulistiorini, S. H., Canagaratna, M.R., Croteau, P.L., Marth, W.J., Baumann, K., Edgerton, E.S., Shaw, S.L., Knipping, E.M., Worsnop, D.R., Jayne, J.T., Gold, A. and Surratt, J.D.: Real-Time Continuous Characterization of Secondary Organic Aerosol Derived from Isoprene Epoxydiols in Downtown Atlanta, Georgia, Using the Aerodyne Aerosol Chemical Speciation Monitor, Environ.Sci.Technol., 47, 5686-5694, doi:10.1021/es400023n, 2013.

Carlton, A. G., Bhave, P.V., Napelenok, S.L., Edney, E.O., Sarwar, G., Pinder, R.W., Pouliot, G.A. and Houyoux, M.: Model Representation of Secondary Organic Aerosol in CMAQv4.7, Environ.Sci.Technol., 44, 8553-8560, doi:10.1021/es100636q, 2010.

~~Chan, M. N., Surratt, J.D., Claeys, M., Edgerton, E.S., Tanner, R.L., Shaw, S.L., Zheng, M., Knipping, E.M., Eddingsaas, N.C., Wennberg, P.O. and Seinfeld, J.H.: Characterization and Quantification of Isoprene-Derived Epoxydiols in Ambient Aerosol in the Southeastern United States, Environ. Sci. Technol., 44, 4590-4596, doi:10.1021/es100596b, 2010.~~

Chen, Q., Farmer, D.K., Rizzo, L.V., Pauliquevis, T., Kuwata, M., Karl, T.G., Guenther, A., Allan, J.D., Coe, H., Andreae, M.O., P\oschl, U., Jimenez, J.L., Artaxo, P. and Martin, S.T.: Fine-mode organic mass concentrations and sources in the Amazonian wet season (AMAZE-08), Atmos. Chem. Phys. Discuss., 14, 16151-16186, doi:10.5194/acpd-14-16151-2014, 2014.

Claeys, M., Graham, B., Vas, G., Wang, W., Vermeylen, R., Pashynska, V., Cafmeyer, J., Guyon, P., Andreae, M.O., Artaxo, P. and Maenhaut, W.: Formation of Secondary Organic Aerosols Through Photooxidation of Isoprene, Science, 303, 1173-1176, doi:10.1126/science.1092805, 2004.

Cross, E. S., Slowik, J.G., Davidovits, P., Allan, J.D., Worsnop, D.R., Jayne, J.T., Lewis, D.K., Canagaratna, M. and Onasch, T.B.: Laboratory and Ambient Particle Density Determinations using Light Scattering in Conjunction with Aerosol Mass Spectrometry, Aerosol Sci. Technol., 41, 343-359, doi:10.1080/02786820701199736, 2007.

Ding, X., Wang, X., Gao, B., Fu, X., He, Q., Zhao, X., Yu, J. and Zheng, M.: Tracer-based estimation of secondary organic carbon in the Pearl River Delta, south China, J. Geophys. Res., 117, -D05313, doi:10.1029/2011JD016596, 2012.

Dockery, D. W., Pope, C.A., Xu, X., Spengler, J.D., Ware, J.H., Fay, M.E., Ferris, B.G. and Speizer, F.E.: An Association between Air Pollution and Mortality in Six U.S. Cities, N.Engl.J.Med., 329, 1753-1759, doi:10.1056/NEJM199312093292401, 1993.

Eddingsaas, N. C., VanderVelde, D.G. and Wennberg, P.O.: Kinetics and Products of the Acid-Catalyzed Ring-Opening of Atmospherically Relevant Butyl Epoxy Alcohols, J. Phys. Chem. A, 114, 8106-8113, doi:10.1021/jp103907c, 2010.

Edney, E. O., Kleindienst, T.E., Jaoui, M., Lewandowski, M., Offenberg, J.H., Wang, W. and Claeys, M.: Formation of 2-methyl tetrols and 2-methylglyceric acid in secondary organic aerosol from laboratory irradiated isoprene/NOX/SO2/air mixtures and their detection in ambient PM2.5 samples collected in the eastern United States, Atmos.Environ., 39, 5281-5289, doi:10.1016/j.atmosenv.2005.05.031, 2005.

Foley, K. M., Roselle, S.J., Appel, K.W., Bhave, P.V., Pleim, J.E., Otte, T.L., Mathur, R., Sarwar, G., Young, J.O., Gilliam, R.C., Nolte, C.G., Kelly, J.T., Gilliland, A.B. and Bash, J.O.: Incremental testing of the Community Multiscale Air Quality (CMAQ) modeling system version 4.7, Geosci. Model Dev., 3, 205-226, doi:10.5194/gmd-3-205-2010, 2010.

Fountoukis, C. and Nenes, A.: ISORROPIA II: a computationally efficient thermodynamic equilibrium model for K^+–Ca^{2+}–Mg^{2+}–NH_4^+–Na^+–SO_4^{2-}–NO_3^-–Cl^-–H_2O aerosols, Atmos. Chem. Phys., 7, 4639-4659, doi:10.5194/acp-7-4639-2007, 2007.

Fountoukis, C., Nenes, A., Sullivan, A., Weber, R., Van Reken, T., Fischer, M., Matias, E., Moya, M., Farmer, D. and Cohen, R.C.: Thermodynamic characterization of Mexico City aerosol during MILAGRO 2006, Atmos. Chem. Phys., 9, 2141-2156, doi:10.5194/acp-9-2141-2009, 2009.

Gao, S., Ng, N.L., Keywood, M., Varutbangkul, V., Bahreini, R., Nenes, A., He, J., Yoo, K.Y., Beauchamp, J.L., Hodyss, R.P., Flagan, R.C. and Seinfeld, J.H.: Particle Phase Acidity and Oligomer Formation in Secondary Organic Aerosol, Environ.Sci.Technol., 38, 6582-6589, doi:10.1021/es049125k, 2004.

Gaston, C. J., Riedel, T.P., Zhang, Z., Gold, A., Surratt, J.D. and Thornton, J.A.: Reactive Uptake of an Isoprene-Derived Epoxydiol to Submicron Aerosol Particles, Environ.Sci.Technol., 48, 11178-11186, doi:10.1021/es5034266, 2014.

Gómez-González, Y., Surratt, J.D., Cuyckens, F., Szmigielski, R., Vermeylen, R., Jaoui, M., Lewandowski, M., Offenberg, J.H., Kleindienst, T.E., Edney, E.O., Blockhuys, F., Van Alsenoy, C., Maenhaut, W. and Claeys, M.: Characterization of organosulfates from the photooxidation of isoprene and unsaturated fatty acids in ambient aerosol using liquid chromatography/(-) electrospray ionization mass spectrometry, J. Mass. Spectrom., 43, 371-382, doi:10.1002/jms.1329, 2008.

Graus, M., MÃ¼ller, M. and Hansel, A.: High resolution PTR-TOF: Quantification and formula confirmation of VOC in real time, J.Am.Soc.Mass Spectrom., 21, 1037-1044, doi:10.1016/j.jasms.2010.02.006, 2010.

Guenther, A., Karl, T., Harley, P., Wiedinmyer, C., Palmer, P.I. and Geron, C.: Estimates of global terrestrial isoprene emissions using MEGAN (Model of Emissions of Gases and Aerosols from Nature), Atmos. Chem. Phys., 6, 3181-3210, doi:10.5194/acp-6-3181-2006, 2006.

Guo, H., Xu, L., Bougiatioti, A., Cerully, K.M., Capps, S.L., Hite~~,~~ Jr., J.R., Carlton, A.G., Lee, S.-., Bergin, M.H., Ng, N.L., Nenes, A. and Weber, R.J.: ~~Particle~~Fine-particle water and pH in the southeastern United States, ~~Atmos. Chem. Phys. Discuss., 14, 27143-27193~~15, 5211-5228, doi:10.5194/~~acpd-14-27143-2014, 2014~~acp-15-5211-2015, 2015.

Hallquist, M., Wenger, J.C., Baltensperger, U., Rudich, Y., Simpson, D., Claeys, M., Dommen, J., Donahue, N.M., George, C., Goldstein, A.H., Hamilton, J.F., Herrmann, H., Hoffmann, T., Iinuma, Y., Jang, M., Jenkin, M.E., Jimenez, J.L., Kiendler-Scharr, A., Maenhaut, W., McFiggans, G., Mentel, T.F., Monod, A., Prevot, A.S.H., Seinfeld, J.H., Surratt, J.D., Szmigielski, R. and Wildt, J.: The formation, properties and impact of secondary organic aerosol: current and emerging issues, Atmos. Chem. Phys., 9, 5155-5236, doi:10.5194/acp-9-5155-2009, 2009.

Hayes, P. L., Ortega, A.M., Cubison, M.J., Froyd, K.D., Zhao, Y., Cliff, S.S., Hu, W.W., Toohey, D.W., Flynn, J.H., Lefer, B.L., Grossberg, N., Alvarez, S., Rappenglück, B., Taylor, J.W., Allan, J.D., Holloway, J.S., Gilman, J.B., Kuster, W.C., de Gouw, J.A., Massoli, P., Zhang, X., Liu, J., Weber, R.J., Corrigan, A.L., Russell, L.M., Isaacman, G., Worton, D.R., Kreisberg, N.M., Goldstein, A.H., Thalman, R., Waxman, E.M., Volkamer, R., Lin, Y.H., Surratt, J.D., Kleindienst, T.E., Offenberg, J.H., Dusanter, S., Griffith, S., Stevens, P.S., Brioude, J., Angevine, W.M. and Jimenez, J.L.: Organic aerosol composition and sources in Pasadena, California during the 2010 CalNex campaign, J. Geophys. Res., 118, 9233-9233, doi:10.1002/jgrd.50530, 2013.

Hsu, S. O. -., Ito, K. and Lippmann, M.: Effects of thoracic and fine PM and their components on heart rate and pulmonary function in COPD patients, J Expos Sci Environ Epidemiol, 21, 464-472, 2011.

IPCC 2013, *Climate Change 2013: The Physical Science Basis, Contribution of Working Group I to the Fifth Assessment Report to the Intergovernmental Panel on Climate Change*, Cambridge University Press, Cambridge, United Kingdom and New York, NY, USA.

Jacobs, M. I., Darer, A.I. and Elrod, M.J.: Rate Constants and Products of the OH Reaction with Isoprene-Derived Epoxides, Environ.Sci.Technol., 47, 12868-12876, doi:10.1021/es403340g, 2013.

Jang, M., Czoschke, N.M., Lee, S. and Kamens, R.M.: Heterogeneous Atmospheric Aerosol Production by Acid-Catalyzed Particle-Phase Reactions, Science, 298, 814-817, doi:10.1126/science.1075798, 2002.

Jimenez, J. L., Canagaratna, M.R., Donahue, N.M., Prevot, A.S.H., Zhang, Q., Kroll, J.H., DeCarlo, P.F., Allan, J.D., Coe, H., Ng, N.L., Aiken, A.C., Docherty, K.S., Ulbrich, I.M., Grieshop, A.P., Robinson, A.L., Duplissy, J., Smith, J.D., Wilson, K.R., Lanz, V.A., Hueglin, C., Sun, Y.L., Tian, J., Laaksonen, A., Raatikainen, T., Rautiainen, J., Vaattovaara, P., Ehn, M., Kulmala, M., Tomlinson, J.M., Collins, D.R., Cubison, M.J., E., Dunlea, J., Huffman, J.A., Onasch, T.B., Alfarra, M.R., Williams, P.I., Bower, K., Kondo, Y., Schneider, J., Drewnick, F., Borrmann, S.,

Weimer, S., Demerjian, K., Salcedo, D., Cottrell, L., Griffin, R., Takami, A., Miyoshi, T., Hatakeyama, S., Shimono, A., Sun, J.Y., Zhang, Y.M., Dzepina, K., Kimmel, J.R., Sueper, D., Jayne, J.T., Herndon, S.C., Trimborn, A.M., Williams, L.R., Wood, E.C., Middlebrook, A.M., Kolb, C.E., Baltensperger, U. and Worsnop, D.R.: Evolution of Organic Aerosols in the Atmosphere. Science, 326, 1525-1529, doi:10.1126/science.1180353, 2009.

Jordan, A., Haidacher, S., Hanel, G., Hartungen, E., Herbig, J., Märk, L., Schottkowsky, R., Seehauser, H., Sulzer, P. and Märk, T.D.: An online ultra-high sensitivity Proton-transfer-reaction mass-spectrometer combined with switchable reagent ion capability (PTR + SRI − MS), Int. J. Mass. Spectrom., 286, 32-38, doi:http://dx.doi.org/10.1016/j.ijms.2009.06.006, 2009a.

Jordan, A., Haidacher, S., Hanel, G., Hartungen, E., Märk, L., Seehauser, H., Schottkowsky, R., Sulzer, P. and Märk, T.D.: A high resolution and high sensitivity proton-transfer-reaction time-of-flight mass spectrometer (PTR-TOF-MS), Int. J. Mass. Spectrom., 286, 122-128, doi:http://dx.doi.org/10.1016/j.ijms.2009.07.005, 2009b.

Kalberer, M., Paulsen, D., Sax, M., Steinbacher, M., Dommen, J., Prevot, A.S.H., Fisseha, R., Weingartner, E., Frankevich, V., Zenobi, R. and Baltensperger, U.: Identification of Polymers as Major Components of Atmospheric Organic Aerosols, Science, 303, 1659-1662, 2004.

Kamens, R. M., Gery, M.W., Jeffries, H.E., Jackson, M. and Cole, E.I.: Ozone?isoprene reactions: Product formation and aerosol potential, Int J Chem Kinet, 14, 955-975, doi:10.1002/kin.550140902, 1982.

Karambelas, A., Pye, H.O.T., Budisulistiorini, S.H., Surratt, J.D. and Pinder, R.W.: Contribution of Isoprene Epoxydiol to Urban Organic Aerosol: Evidence from Modeling and Measurements, Environ. Sci. Technol. Lett., 1, 278-283, doi:10.1021/ez5001353, 2014.

Ke, L., Ding, X., Tanner, R.L., Schauer, J.J. and Zheng, M.: Source contributions to carbonaceous aerosols in the Tennessee Valley Region, Atmos.Environ., 41, 8898-8923, doi:10.1016/j.atmosenv.2007.08.024, 2007.

Kourtchev, I., Copolovici, L., Claeys, M. and Maenhaut, W.: Characterization of Atmospheric Aerosols at a Forested Site in Central Europe, Environ.Sci.Technol., 43, 4665-4671, doi:10.1021/es803055w, 2009.

Kroll, J. H., Ng, N.L., Murphy, S.M., Flagan, R.C. and Seinfeld, J.H.: Secondary Organic Aerosol Formation from Isoprene Photooxidation, Environ.Sci.Technol., 40, 1869-1877, 2006.

Lewis, C. W., Klouda, G.A. and Ellenson, W.D.: Radiocarbon measurement of the biogenic contribution to summertime PM-2.5 ambient aerosol in Nashville, TN, Atmos.Environ., 38, 6053-6061, doi:10.1016/j.atmosenv.2004.06.011, 2004.

Lin, Y. -., Knipping, E.M., Edgerton, E.S., Shaw, S.L. and Surratt, J.D.: Investigating the influences of SO_2 and NH_3 levels on isoprene-derived secondary organic aerosol formation using conditional sampling approaches, Atmos. Chem. Phys., 13, 3095-3134, doi:10.5194/acp-13-8457-2013, 2013a.

Lin, Y., Budisulistiorini, S.H., Chu, K., Siejack, R.A., Zhang, H., Riva, M., Zhang, Z., Gold, A., Kautzman, K.E. and Surratt, J.D.: Light-Absorbing Oligomer Formation in Secondary Organic Aerosol from Reactive Uptake of Isoprene Epoxydiols, Environ.Sci.Technol., 48, 12012-12021, doi:10.1021/es503142b, 2014.

Lin, Y., Zhang, H., Pye, H.O.T., Zhang, Z., Marth, W.J., Park, S., Arashiro, M., Cui, T., Budisulistiorini, S.H., Sexton, K.G., Vizuete, W., Xie, Y., Luecken, D.J., Piletic, I.R., Edney, E.O., Bartolotti, L.J., Gold, A. and Surratt, J.D.: Epoxide as a precursor to secondary organic aerosol formation from isoprene photooxidation in the presence of nitrogen oxides, Proc. Natl. Acad. Sci., doi:10.1073/pnas.1221150110, 2013b.

Lin, Y., Zhang, Z., Docherty, K.S., Zhang, H., Budisulistiorini, S.H., Rubitschun, C.L., Shaw, S.L., Knipping, E.M., Edgerton, E.S., Kleindienst, T.E., Gold, A. and Surratt, J.D.: Isoprene Epoxydiols as Precursors to Secondary Organic Aerosol Formation: Acid-Catalyzed Reactive Uptake Studies with Authentic Compounds, Environ. Sci. Technol., 46, 250-258, doi:10.1021/es202554c, 2012.

Liu, Y. J., Herdlinger-Blatt, I., McKinney, K.A. and Martin, S.T.: Production of methyl vinyl ketone and methacrolein via the hydroperoxyl pathway of isoprene oxidation, Atmos. Chem. Phys., 13, 5715-5730, doi:10.5194/acp-13-5715-2013, 2013.

Liu, Y., Kuwata, M., Strick, B.F., Thomson, R.J., Geiger, F.M., McKinney, K. and Martin, S.T.: Uptake of Epoxydiol Isomers Accounts for Half of the Particle-Phase Material Produced from Isoprene Photooxidation via the HO2 pathway, Environ.Sci.Technol., doi:10.1021/es5034298, 2014.

Mauderly, J. L. and Chow, J.C.: Health Effects of Organic Aerosols, Inhal.Toxicol., 20, 257-288, doi:10.1080/08958370701866008, 2008.

McNeill, V. F., Woo, J.L., Kim, D.D., Schwier, A.N., Wannell, N.J., Sumner, A.J. and Barakat, J.M.: Aqueous-Phase Secondary Organic Aerosol and Organosulfate Formation in Atmospheric Aerosols: A Modeling Study, Environ.Sci.Technol., 46, 8075-8081, doi:10.1021/es3002986, 2012.

Middlebrook, A. M., Bahreini, R., Jimenez, J.L. and Canagaratna, M.R.: Evaluation of Composition-Dependent Collection Efficiencies for the Aerodyne Aerosol Mass Spectrometer using Field Data, Aerosol Sci. Technol., 46, 258-271, doi:10.1080/02786826.2011.620041, 2012.

Nenes, A., Pandis, S.N. and Pilinis, C.: Continued development and testing of a new thermodynamic aerosol module for urban and regional air quality models, Atmos.Environ., 33, 1553-1560, doi:10.1016/S1352-2310(98)00352-5, 1999.

Ng, N. L., Canagaratna, M.R., Jimenez, J.L., Zhang, Q., Ulbrich, I.M. and Worsnop, D.R.: Real-Time Methods for Estimating Organic Component Mass Concentrations from Aerosol Mass Spectrometer Data, Environ. Sci. Technol., 45, 910-916, doi:10.1021/es102951k, 2011.

Nguyen, T. B., Coggon, M.M., Bates, K.H., ~~Crounse, J.D.,~~ Zhang, X., ~~Coggon, M.M.,~~ Schwantes, R.H., ~~Surratt, J.D., Kjaergaard, H.G., Seinfeld, J.H. and~~ Schilling, K.A., Loza, C.L., Flagan, R.C., Wennberg, P.O~~.: Mechanism of the hydroxyl radical (OH) oxidation of metharyoyl peroxynitrate (MPAN) and its saturated analogues: pathway for secondary organic~~, and Seinfeld, J.H.: Organic aerosol formation from the reactive uptake of isoprene ~~in anthropognically influenced areas, Phys.~~epoxydiols (IEPOX) onto non-acidified inorganic seeds, Atmos. Chem. ~~Chem. Phys., to be submitted, 2015~~Phys., 14, 3497-3510, doi:10.5194/acp-14-3497-2014, 2014.

~~Nguyen, T. B., Coggon, M.M., Bates, K.H., Zhang, X., Schwantes, R.H., Schilling, K.A., Loza, C.L., Flagan, R.C., Wennberg, P.O. and Seinfeld, J.H.: Organic aerosol formation from the reactive~~

~~uptake of isoprene epoxydiols (IEPOX) onto non-acidified inorganic seeds, Atmos. Chem. Phys., 14, 3497-3510, doi:10.5194/acp-14-3497-2014, 2014.~~

Nguyen, T. B., Roach, P.J., Laskin, J., Laskin, A. and Nizkorodov, S.A.: Effect of humidity on the composition of isoprene photooxidation secondary organic aerosol, Atmos. Chem. Phys., 11, 6931-6944, doi:10.5194/acp-11-6931-2011, 2011.

~~Norris, G., Vedantham, R., Wade, K., Brown, S., Prouty, J. and Foley, C.: EPA Positive Matrix Factorization (PMF) 3.0 Fundamentals and User Guide, Washington, DC, USA, 2008.~~

Nguyen, T. B., Bates, K.H., Crounse, J.D., Schwantes, R.H., Zhang, X., Kjaergaard, H., Surratt, J.D., Lin, P., Laskin, A., Seinfeld, J.H. and Wennberg, P.O.: Mechanism of the hydroxyl radical oxidation of methacryloyl peroxynitrate (MPAN) and its pathway toward secondary organic aerosol formation in the atmosphere, Phys.Chem.Chem.Phys., -, doi:10.1039/C5CP02001H", 2015.

Odum, J. R., Hoffmann, T., Bowman, F., Collins, D., Flagan, R.C. and Seinfeld, J.H.: Gas/Particle Partitioning and Secondary Organic Aerosol Yields, Environ. Sci. Technol., 30, 2580-2585, doi:10.1021/es950943+, 1996.

~~Paatero, P.: User's Guide for Positive Matrix Factorization Programs PMF2 and PMF3, University of Helsinki, Finland, 2007.~~

~~Paatero, P., Hopke, P.K., Song, X. and Ramadan, Z.: Understanding and controlling rotations in factor analytic models, Chemometrics Intellig.Lab.Syst., 60, 253-264, doi:10.1016/S0169-7439(01)00200-3, 2002.~~

Paatero, P. and Tapper, U.: Positive matrix factorization: A non-negative factor model with optimal utilization of error estimates of data values, Environmetrics, 5, 111-126, doi:10.1002/env.3170050203, 1994.

Pandis, S. N., Paulson, S.E., Seinfeld, J.H. and Flagan, R.C.: Aerosol formation in the photooxidation of isoprene and β-pinene, Atmos. Environ., 25, 997-1008, doi:http://dx.doi.org.libproxy.lib.unc.edu/10.1016/0960-1686(91)90141-S, 1991.

Pankow, J. F.: An absorption model of gas/particle partitioning of organic compounds in the atmosphere, Atmos.Environ., 28, 185-188, doi:10.1016/1352-2310(94)90093-0, 1994.

Paulot, F., Crounse, J.D., Kjaergaard, H.G., Kürten, A., St. Clair, J.M., Seinfeld, J.H. and Wennberg, P.O.: Unexpected Epoxide Formation in the Gas-Phase Photooxidation of Isoprene, Science, 325, 730-733, doi:10.1126/science.1172910, 2009.

Pye, H. O. T., Pinder, R.W., Piletic, I.R., Xie, Y., Capps, S.L., Lin, Y., Surratt, J.D., Zhang, Z., Gold, A., Luecken, D.J., Hutzell, W.T., Jaoui, M., Offenberg, J.H., Kleindienst, T.E., Lewandowski, M. and Edney, E.O.: Epoxide Pathways Improve Model Predictions of Isoprene Markers and Reveal Key Role of Acidity in Aerosol Formation, Environ.Sci.Technol., 47, 11056-11064, doi:10.1021/es402106h, 2013.

Riedel, T. P., Lin, Y., Budisulistiorini, S.H., Gaston, C.J., Thornton, J.A., Zhang, Z., Vizuete, W., Gold, A. and Surratt, J.D.: Heterogeneous reactions of isoprene-derived epoxides: reaction probabilities and molar secondary organic aerosol yield estimates, Environ. Sci. Technol. Lett., doi:10.1021/ez500406f, 2015.

Robinson, N. H., Hamilton, J.F., Allan, J.D., Langford, B., Oram, D.E., Chen, Q., Docherty, K., Farmer, D.K., Jimenez, J.L., Ward, M.W., Hewitt, C.N., Barley, M.H., Jenkin, M.E., Rickard, A.R., Martin, S.T., McFiggans, G. and Coe, H.: Evidence for a significant proportion of Secondary Organic Aerosol from isoprene above a maritime tropical forest, Atmos. Chem. Phys., 11, 1039-1050, doi:10.5194/acp-11-1039-2011, 2011.

Schichtel, B. A., Malm, W.C., Bench, G., Fallon, S., McDade, C.E., Chow, J.C. and Watson, J.G.: Fossil and contemporary fine particulate carbon fractions at 12 rural and urban sites in the United States, J. Geophys. Res., 113, D02311, doi:10.1029/2007JD008605, 2008.

Schindelka, J., Iinuma, Y., Hoffmann, D. and Herrmann, H.: Sulfate radical-initiated formation of isoprene-derived organosulfates in atmospheric aerosols, Faraday Discuss., 165, 237-259, doi:10.1039/C3FD00042G", 2013.

Schwartz, S.: Mass-Transport Considerations Pertinent to Aqueous Phase Reactions of Gases in Liquid-Water Clouds, 6, 415-471, doi:10.1007/978-3-642-70627-1_16, 1986.

Slowik, J. G., Brook, J., Chang, R.Y.-., Evans, G.J., Hayden, K., Jeong, C.-., Li, S.-., Liggio, J., Liu, P.S.K., McGuire, M., Mihele, C., Sjostedt, S., Vlasenko, A. and Abbatt, J.P.D.: Photochemical processing of organic aerosol at nearby continental sites: contrast between urban plumes and regional aerosol, Atmos. Chem. Phys., 11, 2991-3006, doi:10.5194/acp-11-2991-2011, 2011.

Sun, Y., Zhang, Q., Zheng, M., Ding, X., Edgerton, E.S. and Wang, X.: Characterization and Source Apportionment of Water-Soluble Organic Matter in Atmospheric Fine Particles (PM2.5) with High-Resolution Aerosol Mass Spectrometry and GC-MS, Environ.Sci.Technol., 45, 4854-4861, doi:10.1021/es200162h, 2011.

Surratt, J. D., Chan, A.W.H., Eddingsaas, N.C., Chan, M., Loza, C.L., Kwan, A.J., Hersey, S.P., Flagan, R.C., Wennberg, P.O. and Seinfeld, J.H.: Reactive intermediates revealed in secondary organic aerosol formation from isoprene, Proc. Natl. Acad. Sci., 107, 6640-6645, doi:10.1073/pnas.0911114107, 2010.

Surratt, J. D., Go□mez-Gonza□lez, Y., Chan, A.W.H., Vermeylen, R., Shahgholi, M., Kleindienst, T.E., Edney, E.O., Offenberg, J.H., Lewandowski, M., Jaoui, M., Maenhaut, W., Claeys, M., Flagan, R.C. and Seinfeld, J.H.: Organosulfate Formation in Biogenic Secondary Organic Aerosol, J Phys Chem A, 112, 8345-8378, doi:10.1021/jp802310p, 2008.

Surratt, J. D., Kroll, J.H., Kleindienst, T.E., Edney, E.O., Claeys, M., Sorooshian, A., Ng, N.L., Offenberg, J.H., Lewandowski, M., Jaoui, M., Flagan, R.C. and Seinfeld, J.H.: Evidence for Organosulfates in Secondary Organic Aerosol, Environ. Sci. Technol., 41, 517-527, doi:10.1021/es062081q, 2007a.

Surratt, J. D., Lewandowski, M., Offenberg, J.H., Jaoui, M., Kleindienst, T.E., Edney, E.O. and Seinfeld, J.H.: Effect of Acidity on Secondary Organic Aerosol Formation from Isoprene, Environ.Sci.Technol., 41, 5363-5369, doi:10.1021/es0704176, 2007b.

Surratt, J. D., Murphy, S.M., Kroll, J.H., Ng, N.L., Hildebrandt, L., Sorooshian, A., Szmigielski, R., Vermeylen, R., Maenhaut, W., Claeys, M., Flagan, R.C. and Seinfeld, J.H.: Chemical Composition of Secondary Organic Aerosol Formed from the Photooxidation of Isoprene, J Phys Chem A, 110, 9665-9690, doi:10.1021/jp061734m, 2006.

Formatted: Font: Baoli SC Regular

Formatted: Font: Baoli SC Regular

Tanner, R. L., Bairai, S.T. and Mueller, S.F.: Trends in concentrations of atmospheric gaseous and particulate species in rural eastern Tennessee as related to primary emissions reductions, Atmos. Chem. Phys. Discuss., 15, 13211-13262, doi:10.5194/acpd-15-13211-2015, 2015.

Tanner, R. L., Bairai, S.T., Olszyna, K.J., Valente, M.L. and Valente, R.J.: Diurnal patterns in PM2.5 mass and composition at a background, complex terrain site, Atmos.Environ., 39, 3865-3875, doi:10.1016/j.atmosenv.2005.03.014, 2005.

Tanner, R. L., Parkhurst, W.J. and McNichol, A.P.: Fossil Sources of Ambient Aerosol Carbon Based on 14C Measurements Special Issue of Aerosol Science and Technology on Findings from the Fine Particulate Matter Supersites Program, Aerosol Sci. Technol., 38, 133-139, doi:10.1080/02786820390229453, 2004.

Tolocka, M. P., Jang, M., Ginter, J.M., Cox, F.J., Kamens, R.M. and Johnston, M.V.: Formation of Oligomers in Secondary Organic Aerosol, Environ.Sci.Technol., 38, 1428-1434, doi:10.1021/es035030r, 2004.

Turpin, B. J. and Lim, H.J.: Species Contributions to PM2.5 Mass Concentrations: Revisiting Common Assumptions for Estimating Organic Mass, Aerosol Sci. Technol., 35, 602-610, doi:10.1080/02786820119445, 2001.

Ulbrich, I. M., Canagaratna, M.R., Zhang, Q., Worsnop, D.R. and Jimenez, J.L.: Interpretation of organic components from Positive Matrix Factorization of aerosol mas spectrometric data, Atmos. Chem. Phys., 9, 2891-2918, 2009.

Veres, P., Roberts, J.M., Warneke, C., Welsh-Bon, D., Zahniser, M., Herndon, S., Fall, R. and de Gouw, J.: Development of negative-ion proton-transfer chemical-ionization mass spectrometry (NI-PT-CIMS) for the measurement of gas-phase organic acids in the atmosphere, Int. J. Mass spectrom., 274, 48-55, doi:http://dx.doi.org/10.1016/j.ijms.2008.04.032, 2008.

Wang, W., Kourtchev, I., Graham, B., Cafmeyer, J., Maenhaut, W. and Claeys, M.: Characterization of oxygenated derivatives of isoprene related to 2-methyltetrols in Amazonian aerosols using trimethylsilylation and gas chromatography/ion trap mass spectrometry, Rapid Commun.Mass Spectrom., 19, 1343-1351, doi:10.1002/rcm.1940, 2005.

Woo, J. L. and McNeill, V.F.: simpleGAMMA ~~–a~~1.0 – A reduced model of secondary organic aerosol formation in the aqueous aerosol phase (aaSOA), Geosci. Model Dev~~. Disc.~~, 8, ~~463–482~~1821-1829, doi:10.5194/gmdd-8-463-2015, 2015.

Worton, D. R., Surratt, J.D., LaFranchi, B.W., Chan, A.W.H., Zhao, Y., Weber, R.J., Park, J., Gilman, J.B., de Gouw, J., Park, C., Schade, G., Beaver, M., Clair, J.M.S., Crounse, J., Wennberg, P., Wolfe, G.M., Harrold, S., Thornton, J.A., Farmer, D.K., Docherty, K.S., Cubison, M.J., Jimenez, J., Frossard, A.A., Russell, L.M., Kristensen, K., Glasius, M., Mao, J., Ren, X., Brune, W., Browne, E.C., Pusede, S.E., Cohen, R.C., Seinfeld, J.H. and Goldstein, A.H.: Observational Insights into Aerosol Formation from Isoprene, Environ.Sci.Technol., 47, 11403-11413, doi:10.1021/es4011064, 2013.

Xu, L., Guo, H., Boyd, C.M., Klein, M., Bougiatioti, A., Cerully, K.M., Hite, J.R., Isaacman-VanWertz, G., Kreisberg, N.M., Knote, C., Olson, K., Koss, A., Goldstein, A.H., Hering, S.V., de Gouw, J., Baumann, K., Lee, S., Nenes, A., Weber, R.J. and Ng, N.L.: Effects of anthropogenic emissions on aerosol formation from isoprene and monoterpenes in the southeastern United States, Proc. Natl. Acad. Sci., 112, 37-42, doi:10.1073/pnas.1417609112, 2015.

You, Y., Renbaum-Wolff, L., Carreras-Sospedra, M., Hanna, S.J., Hiranuma, N., Kamal, S., Smith, M.L., Zhang, X., Weber, R.J., Shilling, J.E., Dabdub, D., Martin, S.T. and Bertram, A.K.: Images reveal that atmospheric particles can undergo liquid–liquid phase separations, Proc. Natl. Acad. Sci., 109, 13188-13193, doi:10.1073/pnas.1206414109, 2012.

Zhang, H., Surratt, J.D., Lin, Y.H., Bapat, J. and Kamens, R.M.: Effect of relative humidity on SOA formation from isoprene/NO photooxidation: enhancement of 2-methylglyceric acid and its corresponding oligoesters under dry conditions, Atmos. Chem. Phys., 11, 6411-6424, doi:10.5194/acp-11-6411-2011, 2011.

Zhang, ~~Q. Q.: Understanding atmospheric organic aerosols via factor analysis of aerosol mass spectrometry: a review, Analyt. Bioanalyt. Chem., 401, 3045-3067, 2011.~~

~~Zhang,~~ X., Liu, Z., Hecobian, A., Zheng, M., Frank, N.H., Edgerton, E.S. and Weber, R.J.: Spatial and seasonal variations of fine particle water-soluble organic carbon (WSOC) over the southeastern United States: implications for secondary organic aerosol formation, Atmos. Chem. Phys., 12, 6593-6607, doi:10.5194/acp-12-6593-2012, 2012a.

Zhang, Z., Lin, Y.H., Zhang, H., Surratt, J.D., Ball, L.M. and Gold, A.: Technical Note: Synthesis of isoprene atmospheric oxidation products: isomeric epoxydiols and the rearrangement products cis- and trans-3-methyl-3,4-dihydroxytetrahydrofuran, Atmos. Chem. Phys., 12, 8529-8535, doi:10.5194/acp-12-8529-2012, 2012b.

1

Table 1. Summary of isoprene-derived SOA tracers measured by GC/EI-MS and UPLC/DAD-ESI-HR-QTOFMS

SOA Tracers	Retention Time (min)	# of Samples Detected[a]	Concentration (ng m^{-3}) Maximum	Concentration (ng m^{-3}) Mean	Average % among detected tracers
Tracers by GC/EI-MS					
trans-3-MeTHF-3,4-diol	20.5	55	18.8	2.7	0.~~6~~2%
cis-3-MeTHF-3,4-diol	21.1	29	5.7	1.7	0.~~4~~1%
2-methylglyceric acid	23.4	119	36.7	7.5	1.~~6~~5%
2-methylthreitol	32.9	122	329.8	42.4	8.~~8~~6%
2-methylerythritol	33.7	122	1269.7	120.7	~~25.2~~24.4%
(Z)-2-methylbut-3-ene-1,2,4-triol	25.6	121	260.0	29.1	~~6.1~~5.8%
2-methylbut-3-ene-1,2,3-triol	26.6	118	162.5	16.5	3.~~4~~2%
(E)-2-methylbut-3-ene-1,2,4-triol	26.9	122	1127.0	98.8	~~20.6~~19.9%
Tracers by UPLC/DAD-ESI-HR-QTOFMS tracers					
IEPOX-derived organosulfates	1.1–1.7	122	~~1087.4~~1135.3	~~161.2~~169.5	~~33~~34.2%
IEPOX-derived dimer organosulfate	2.8	~~70~~103	~~157.6~~14.0	~~17.2~~1.4	~~3.5~~0.2%
MAE-derived organosulfate	1.1	~~100~~114	~~30.6~~77.9	~~3.9~~10.0	~~0.8~~1.9%

[a] Total number of samples is 123

Table 2. Correlation (r^2) of PMF Factors with isoprene-derived SOA tracers measured by GC/EI-MS and UPLC/DAD-ESI-HR-QTOFMS

SOA Tracers	IEPOX-OA	LV-OOA	91Fac
3-methyltetrahydrofuran-3,4-diols	0.12	0.13	0.24
2-methyltetrols	0.80	0.20	0.38
C_5-alkene triols	0.75	0.19	0.44
2-methylglyceric ~~acids~~acid	0.38	0.44	0.44
IEPOX-derived organosulfates	0.~~78~~76	0.29	0.~~43~~42
IEPOX-derived dimer organosulfate	0.~~04~~71	0.~~00~~12	0.~~01~~34
MAE-derived organosulfate	0.~~34~~37	0.~~40~~44	0.~~50~~52

Table 3. Correlation (r^2) of modeled SOA tracers with measurements

H* (M atm^{-1})	2-methyltetrols r^2	2-methyltetrols Slope	IEPOX organosulfates r^2	IEPOX organosulfates Slope
3.0×10^7 [a]	0.45	9.61±0.91	0.~~65~~66	~~11.30~~10.65±0.~~78~~73
2.7×10^6 [b]	0.44	0.69±0.06	0.~~65~~66	0.~~95~~90±0.06

References: (a) Nguyen et al. (2014) and (b) Pye et al. (2013)

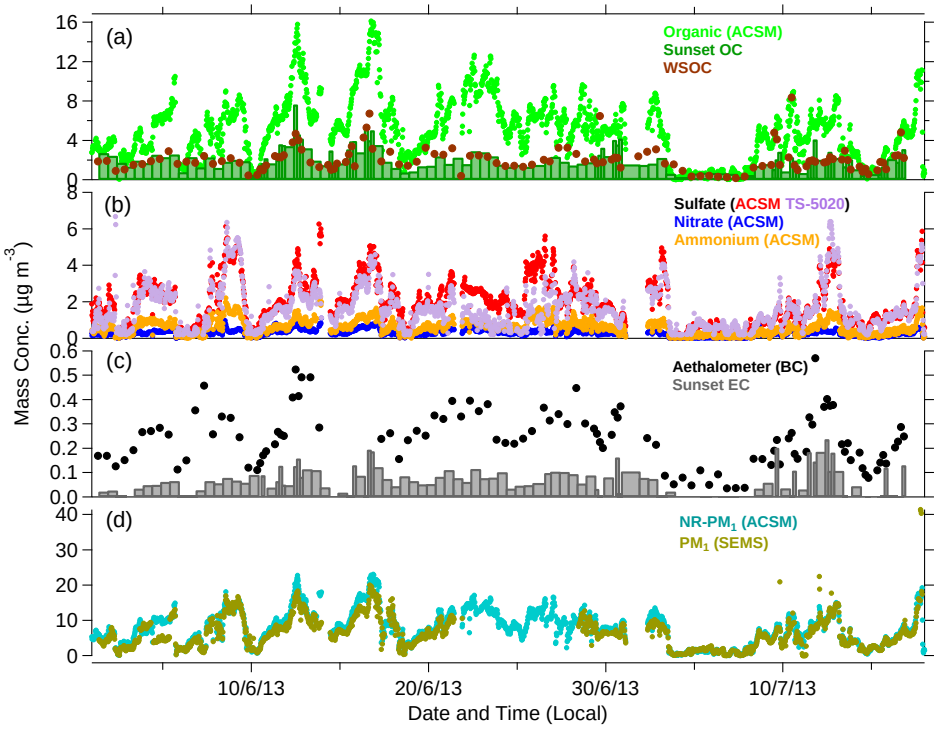

Figure 1. Time series mass concentration of (a) organic and (b) inorganics (excluding chloride) measured by ACSM, (c) black carbon (BC) measured by Aethalometer, and (d) NR-PM_1 and PM_1 mass concentrations measured by ACSM and SEMS-MCPC. Collocated sulfate aerosol measured by Thermo Scientific Sulfate Analyzer was plotted on (b). OC (bars) and WSOC (dots), both in unit of µgC m^{-3}, measured from filter samples were plotted on (a) with ACSM organic. EC (bars; in unit of µgC m^{-3}) measured from filter samples were plotted on (c) along with BC measurements.

Formatted: German (Germany)

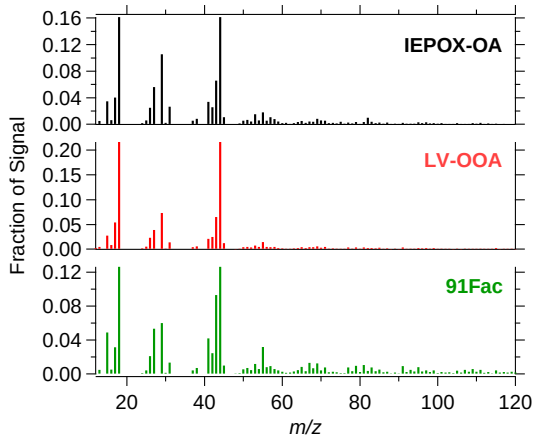

Figure 2. Mass spectra obtained for the 3-factor solution from PMF: IEPOX-OA, LV-OOA, and 91 Fac.

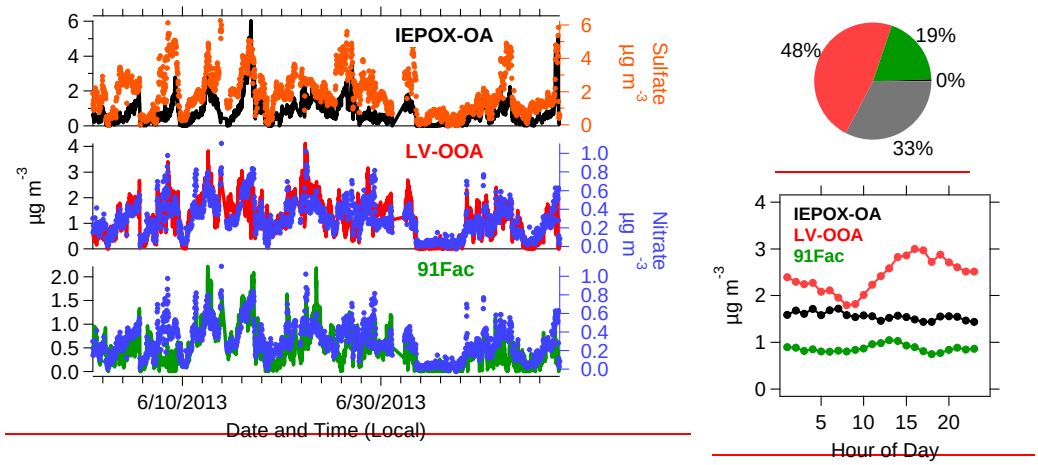

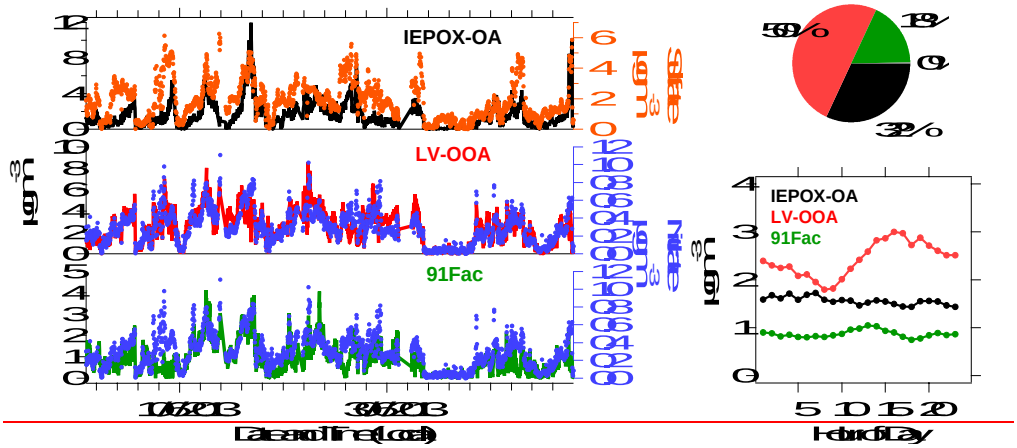

Figure 3. Left panel shows the PMF 3-factor solution time series mass contributions measured by ACSM. Top to bottom: left ordinate, IEPOX-OA (black), LV-OOA (red), and 91 Fac (green); right ordinate, sulfate (orange) and nitrate (blue). Right panel shows average mass contributions (top) and diurnal variation (bottom) of factors resolved by PMF.

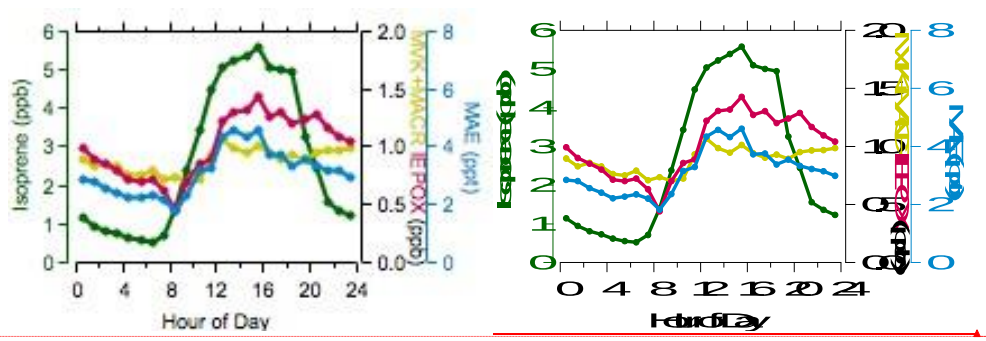

Figure 4. Diurnal variation of isoprene (left ordinate) as well as isoprene gaseous photooxidation products (right ordinates), i.e., MVK+MACR, IEPOX and MAE, measured at LRK site. It should be noted that ~~the right ordinates are on finer scale than the left ordinate~~IEPOX signal includes interference of ISOPOOH at unknown ratio, thus its mixing ratio represents an upper limit.

Formatted: German (Germany)
Formatted: Line spacing: single
Formatted: German (Germany)
Formatted: German (Germany)
Formatted: Indent: Left: 0 cm

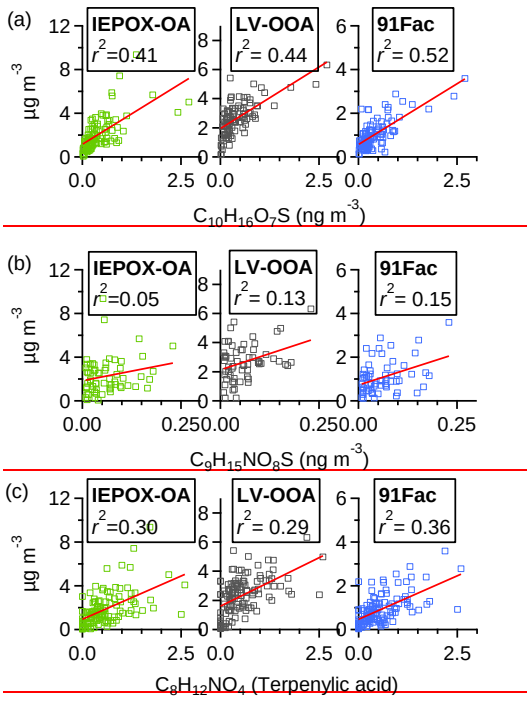

~~Figure 5.~~ ~~Correlation of PMF factors with α pinene derived organosulfate, $C_{10}H_{16}O_7S$ (a), nitrated organosulfates, $C_9H_{15}NO_8S$ (b), and terpenylic acid $C_8H_{12}NO_4$ (c).~~

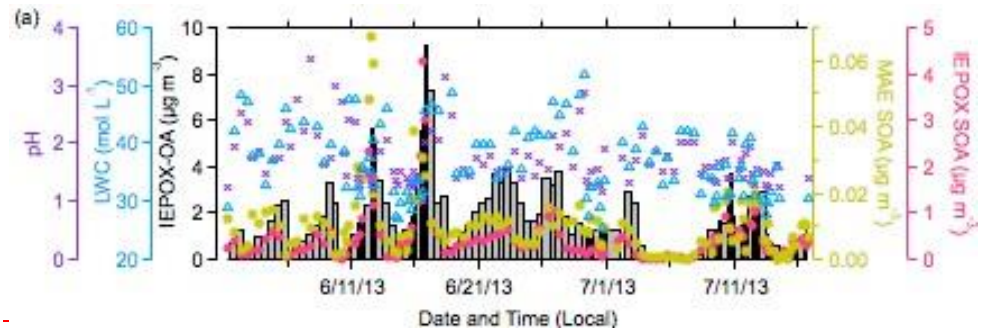

-

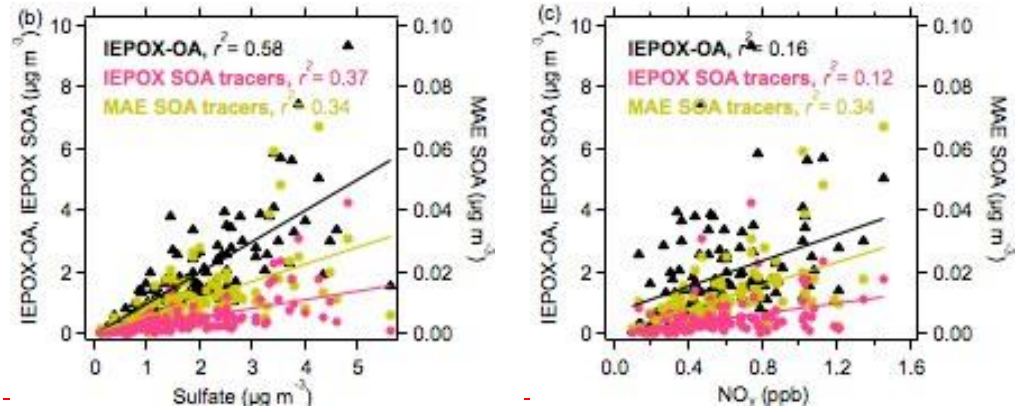

1 ~~Figure 6.~~

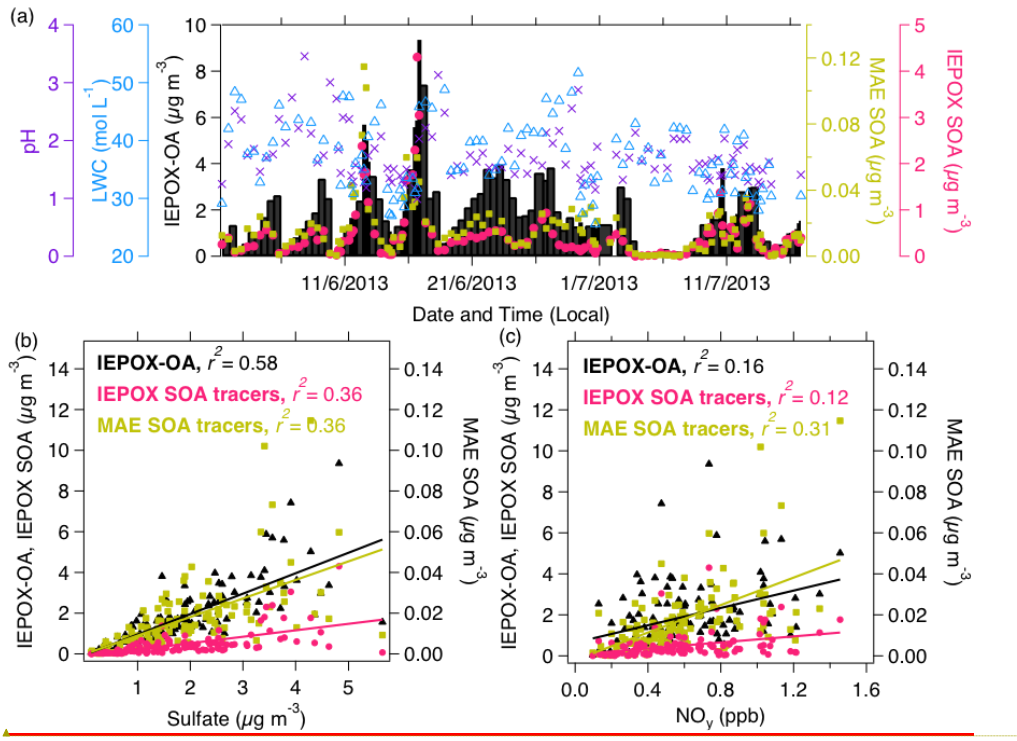

2

3 **Figure 5.** (a) Time series of IEPOX-OA factor (black bars; darker bars are intensive filter
4 sampling periods), sum of IEPOX-derived (pink circle) and MAE-derived (yellow square)
5 SOA tracers, aerosol pH (purple cross) and LWC (blue triangle) estimated by ISORROPIA-II
6 model. Campaign average pH and LWC are 1.78±0.53 and 38.71±7.43 mol L^{-1}, respectively.
7 Correlation plots between IEPOX-OA, summed of IEPOX- and MAE-derived SOA tracers
8 and (b) sulfate measurements by ACSM and (c) NO_y measurements from NPS.

Formatted: Font: Bold

Formatted: German (Germany)

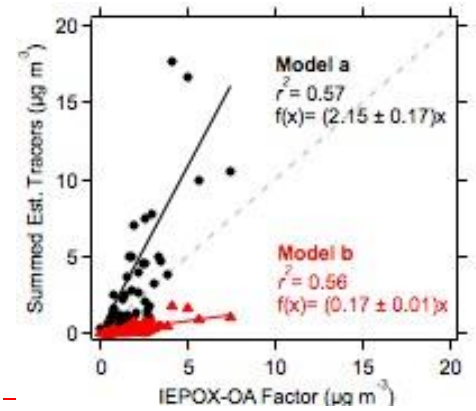

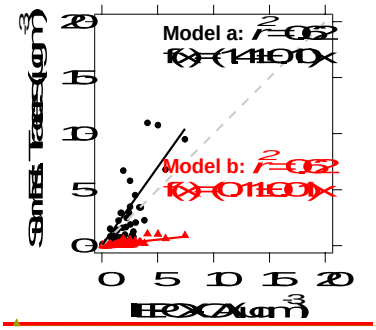

Formatted: Font: 16 pt, Bold, Kern at 14 pt

Figure ~~7~~6. Correlation of summed IEPOX-derived SOA tracers estimated by simpleGAMMA by assumming H* of 3.0 × 10^7 (Nguyen et al., 2014) (model a) and 2.7 × 10^6 (Pye et al., 2013) (model b) and IEPOX-OA factor from PMF analysis.

Supplementary Information

Examining the Effects of Anthropogenic Emissions on Isoprene-Derived Secondary Organic Aerosol Formation During the 2013 Southern Oxidant and Aerosol Study (SOAS) at the Look Rock, Tennessee, Ground Site

S. H. Budisulistiorini[1,6], X. Li[1], S. T. Bairai[2,†], J. Renfro[3], Y. Liu[4], Y. J. Liu[4], K. A. McKinney[4], S. T. Martin[4], V. F. McNeill[5], H. O. T. Pye[6], A. Nenes[7,8,9], M. E. Neff[10], E. A. Stone[10], S. Mueller[2,‡], C. Knote[11], S. L. Shaw[12], Z. Zhang[1], A. Gold[1], and J. D. Surratt[1]

[1] Department of Environmental Sciences and Engineering, Gillings School of Global Public Health, The University of North Carolina at Chapel Hill, Chapel Hill, NC, USA

[2] Tennessee Valley Authority, Muscle Shoals, AL, USA

[3] National Park Service, Gatlinburg, TN USA

[4] School of Engineering and Applied Sciences, Harvard University, Cambridge, MA USA

[5] Department of Chemical Engineering, Columbia University, NY, USA

[6] National Exposure Research Laboratory, US Environmental Protection Agency, Research Triangle Park, NC, USA

[7] School of Earth and Atmospheric Sciences, Georgia Institute of Technology, Atlanta, GA, USA

[8] School of Chemical and Biomolecular Engineering, Georgia Institute of Technology, Atlanta, GA, USA

[9] Foundation for Research and Technology, Hellas, Greece

[10] Department of Chemistry, University of Iowa, Iowa City, IA, USA

[11] Department of Experimental Meteorology, Ludwig Maximilian University of Munich, Munchen, Germany

[12] Electric Power Research Institute, Palo Alto, CA, USA

[†] Now at Battelle, Pueblo, CO, USA

[‡] Now at Ensafe, Nashville, TN, USA

Correspondence to: J. D. Surratt (surratt@unc.edu)

A. Sampling Site Location: Look Rock, Tennessee, USA

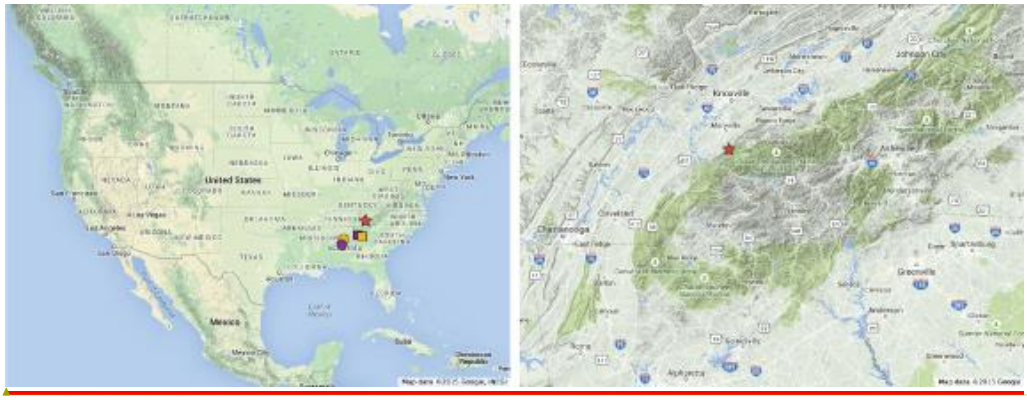

Figure S1. Maps of (a) United State of America, and (b) location of Look Rock, TN, (LRK) site. Courtesy by Google Maps.

The sampling site was located in Look Rock (LRK) site, Tennessee, USA, as marked in red star on left-panel Fig. S1. The circle marks are the other sampling sites participated in 2013 SOAS study located in Alabama, namely Centerville (purple) and Birmingham (yellow). The squares mark previous ambient aerosol measurements studies located in Atlanta, Georgia (yellow; Budisulistiorini et al., 2013) and Yorkville, Georgia (purple; Lin et al., 2013).

The right-panel of Fig. S1 illustrates area surrounding the LRK site. Knoxville, Maryville, Nashville, and Chattanooga urban areas are on the north to west of the site. The forested area of Great Smoky Mountains is stretched out from the northeast to the southwest of the site. As illustrated on Fig. S2, during the entire field campaign, the wind is coming mostly from the south and southeast of the site, as well as from the west. This would allow isoprene emitted from the forested area to be mixed with anthropogenic emissions from the urban areas. However, as the site is located at high elevation (~ 800 m above sea level), it is less likely that fresh emission could reach the site.

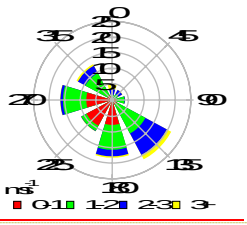

Formatted: Font: 16 pt, Bold, Font color: Auto, Kern at 14 pt

Formatted: Font color: Auto, Kern at 14 pt

Figure S2. Wind direction at sampling location

~~A.~~B. Ambient PM_1 and Collocated Measurements

Table S1. Collocated gas- and particle-phase measurements at LRK site.

Compound	Instrument	Analysis Method	Reporting Frequency
SO_2	Thermo Scientific 43i TLE	Pulsed fluorescence	1 hr
CO	Thermo Scientific 48i TLE	NDIR-GFC	1 hr
NO	Thermo Scientific 42c	Chemiluminescence	1 hr
NO_y	Thermo Scientific 42c	Chem./Mo converter	1 hr
NO_2	API 200EU	Chem./photolytic conv.	1 hr
BC	Magee AE 22	Optical absorption	1 hr
SO_4	Thermo Scientific 5020	Thermal/fluorescence	1 hr
$PM_{2.5}$	Met One BAM-1020	Beta attenuation	1 hr
PM_{10}	Met One BAM-1020	Beta attenuation	1 hr
O_3[a]	Thermo Scientific 49i	UV absorption	1 hr

[a]Ozone is measured at National Park Service shelter next to LRK shelter

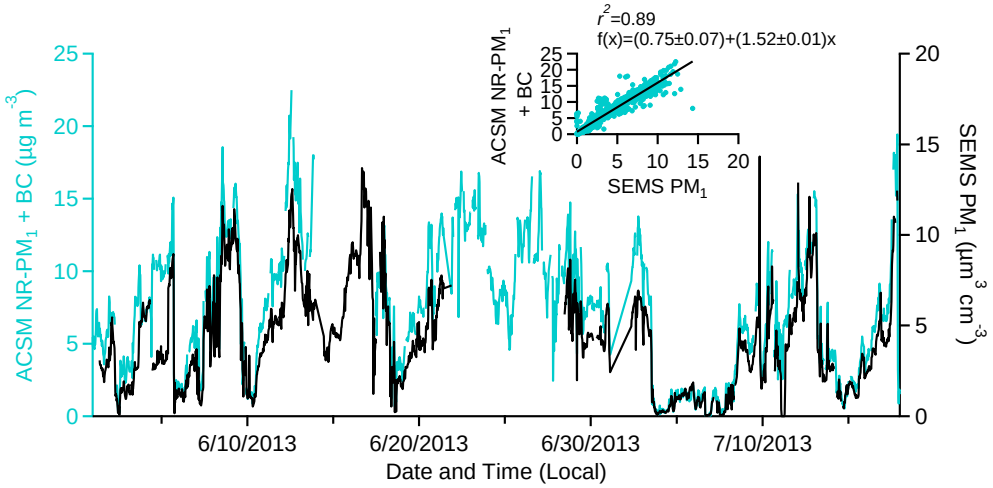

Figure ~~S1~~S3. Comparison of PM_1 mass concentration from ACSM and black carbon measurements with PM_1 volume concentration from SEMS suggests a strong correlation. Slope shown in insert suggests an estimated aerosol density of 1.52 g cm^{-3}.

~~B.~~C. PMF Analysis

Table S2. Summary of PMF solutions obtained for 2013 SOAS campaign dataset.

# Factors	FPEAK	SEED	$Q/Q_{expected}$	Solution Description
1	0	0	0.27262	One-factor (OOA) resulted in large residuals at some time periods and *m/z*'s.
2	0	0	0.23717	Two-factor (IEPOX-OA and LV-OOA) is significantly reduced residuals. LV-OOA factor time trends and mass spectrum seem to be a mixture of less- and more-oxidized OA.
3	0	0	0.21338	Three-factor (IEPOX-OA, LV-OOA, and 91Fac) seems like an optimum solution. The 91Fac appears to share some similarities in time trend and mass spectrum to IEPOX-OA and LV-OOA but with a distinct *m/z* 91.
3	-0.2 to 0.2	0	0.2134-0.21447	In this range, factor ~~MS~~mass spectra and time series are changing suggesting possibility of optimum solution.
3	**-0.09**	**0**	**0.2137**	**Optimum number of factors (IEPOX-OA, LV-OOA, and 91Fac) and FPEAK. All three factors have distinctive time trends and mass spectra, and compare well with independent particle and/or gaseous measurements, and reference ~~MS~~mass spectra from database and/or experiment in this study.**
3	0	0-100 in steps of 5	0.21336-0.21353	For 3-factor, time trends and mass spectra are nearly identical at different starting points.
4 to 10	0	0	0.19965-0.16295	Q/Q_{exp} is reduced but OOA factor is split into more factors that do not compare well with reference ~~MS~~mass spectra.

Table S3. Correlation of PMF 2-, 3-, and 4-factor solutions at Fpeak 0 with collocated measurements and reference mass spectra.

	2-factor		3-factor			4-factor			
	Fac1	Fac2	Fac1	Fac2	Fac3	Fac1	Fac2	Fac3	Fac4
~~r^2 TS~~ r^2 Time Series									
CO	0.41	0.33	0.37	0.44	0.28	0.37	0.45	0.34	0.29
NO_x (=NO+NO_2)	0.02	0.01	0.03	0.01	0.02	0.03	0.01	0.00	0.05
NO_y	0.15	0.22	0.14	0.21	0.20	0.13	0.22	0.17	0.22

	2-factor		3-factor			4-factor			
	Fac1	Fac2	Fac1	Fac2	Fac3	Fac1	Fac2	Fac3	Fac4
NO_z	0.15	0.22	0.14	0.21	0.21	0.13	0.21	0.17	0.23
O_x (=NO_2+O_3)	0.18	0.21	0.15	0.30	0.13	0.14	0.32	0.16	0.16
SO4	0.37	0.16	0.35	0.31	0.14	0.35	0.33	0.19	0.17
ACSM SO_4	0.62	0.34	0.59	0.53	0.31	0.59	0.55	0.39	0.33
ACSM NO_3	0.75	0.73	0.72	0.80	0.70	0.70	0.79	0.74	0.68
ACSM NH_4	0.61	0.41	0.57	0.59	0.36	0.57	0.61	0.44	0.37
~~r^2 MS~~ r^2 Mass Spectra									
HOA	0.11	0.05	0.17	0.03	0.57	0.18	0.02	0.35	0.29
LV-OOA	0.97	0.97	0.83	0.93	0.32	0.80	0.91	0.67	0.52
SV-OOA	0.55	0.41	0.64	0.32	0.88	0.64	0.28	0.91	0.44
BBOA	0.46	0.28	0.64	0.20	0.69	0.66	0.17	0.69	0.34
82Fac	0.89	0.71	0.94	0.60	0.47	0.94	0.56	0.68	0.38
91Fac	0.54	0.42	0.60	0.32	0.80	0.58	0.27	0.67	0.69
IEPOX-OA	0.81	0.65	0.89	0.56	0.53	0.89	0.52	0.84	0.33
Lab IEPOX SOA	0.55	0.32	0.80	0.24	0.38	0.83	0.21	0.53	0.19

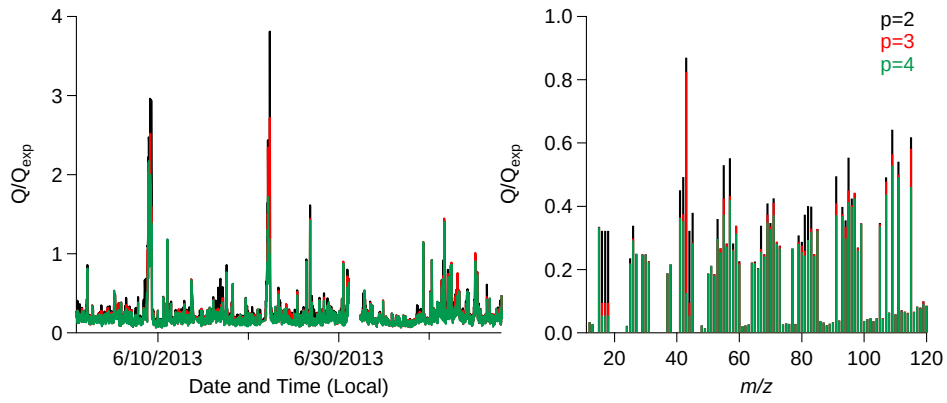

Figure ~~S2~~S4. Time series and mass spectra of Q/Q_{exp} for 2-,3-, and 4-factor solutions are used to determine the optimum number of factor in PMF analysis. The 3-factor solution time series and mass spectra of Q/Q_{exp} suggest that adding the third factor reduces Q/Q_{exp} substantially. The 4-factor solution does not significantly reduce time series and mass spectrum of Q/Q_{exp} compared to those of 3-factor solution.

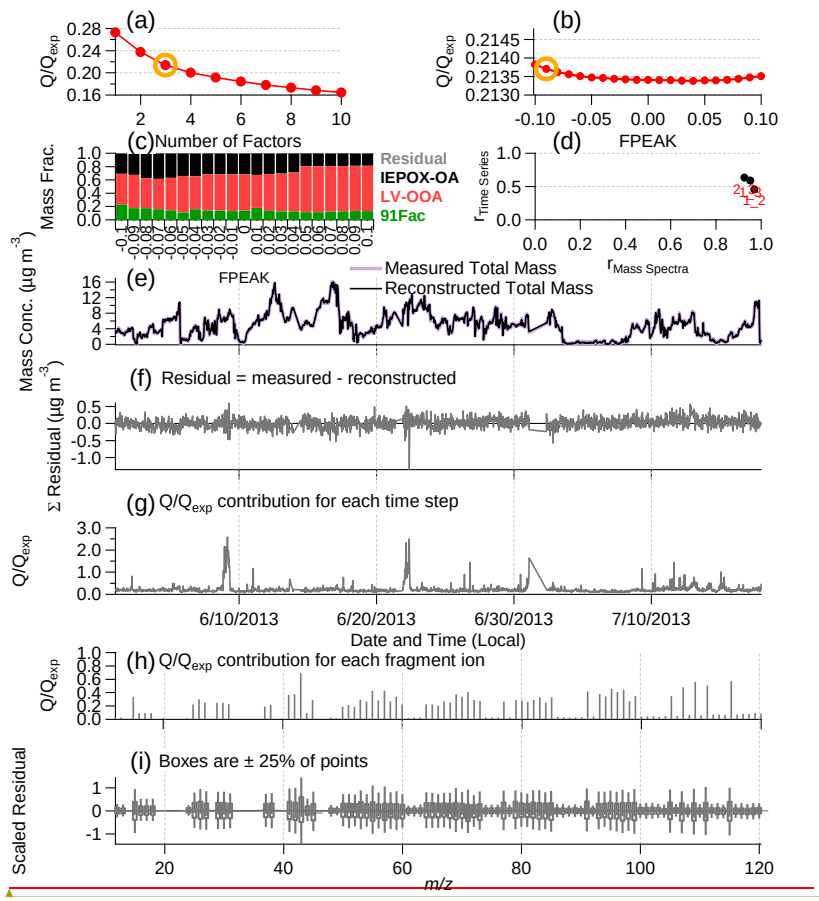

Formatted: Style Arial 16 pt Bold Kern at 14 pt, Font: (Default) Arial, Font color: Auto, English (U.S.), Check spelling and grammar

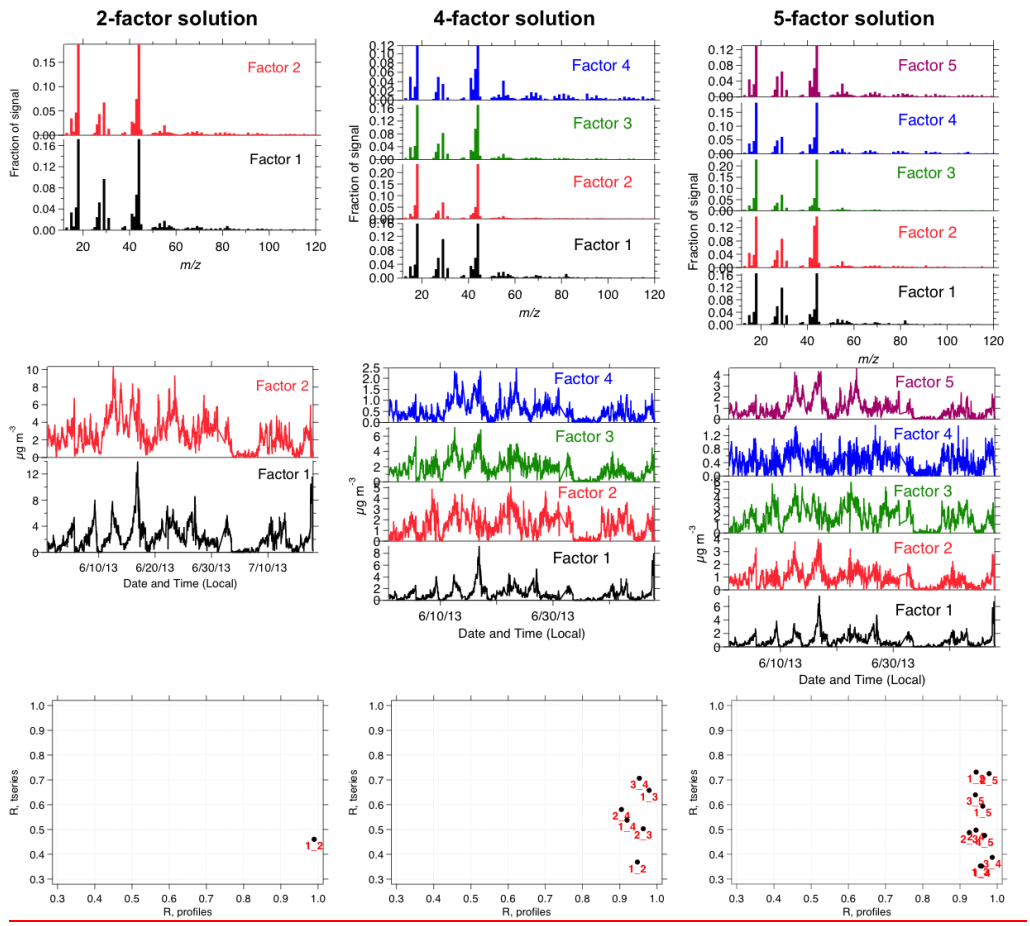

Figure ~~S3~~S5. Time series, mass spectra, and factor correlation plots for 2-, 4-, and 5-factor solutions.

Formatted: Font: Not Bold

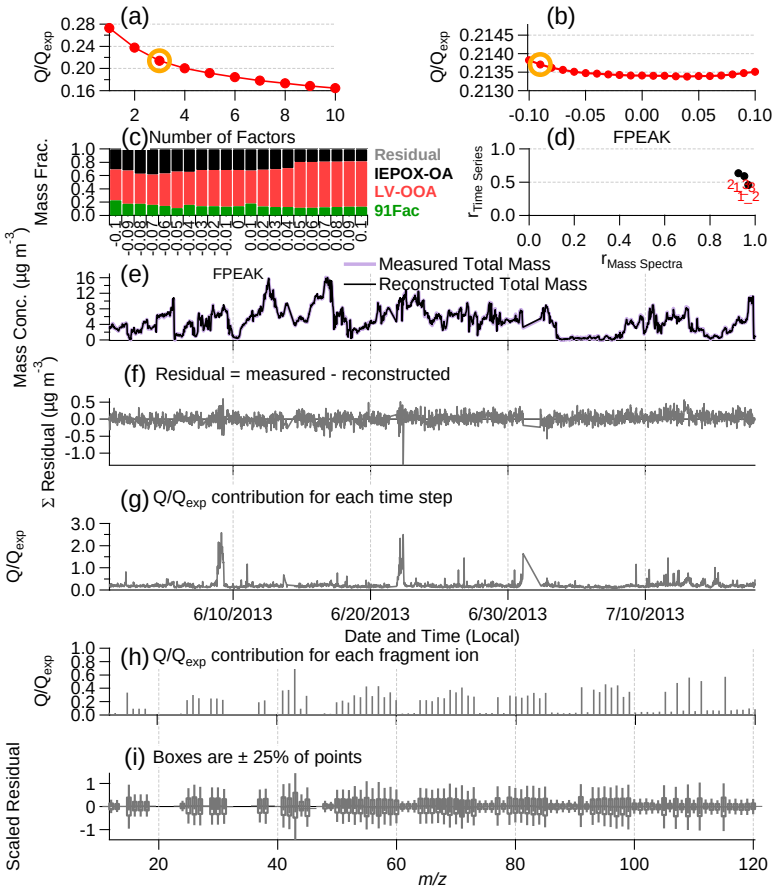

Figure S6. Diagnostic plots for ~~PMF analysis of~~3 factor solution resolved from 2013 SOAS campaign dataset: (a) Q/Q_{exp} as a function of number of factors (p), (b) Q/Q_{exp} as a function of FPEAK selected for the chosen number of factors, (c) fractional contribution of OA factors for each FPEAK, (d) correlation among PMF factors based on factor ~~TS~~time series and ~~MS~~mass spectra, (e) TS of the measured OA mass and the reconstructed OA mass, (f) variation of the residual of the fit, Q/Q_{exp} for each point in time (g) and for each *m/z* (h), and the box and whisker plot of the scaled residuals for each *m/z*.

Formatted: Style Arial 16 pt Bold Kern at 14 pt, Font: (Default) Arial, Font color: Auto, English (U.S.), Check spelling and grammar

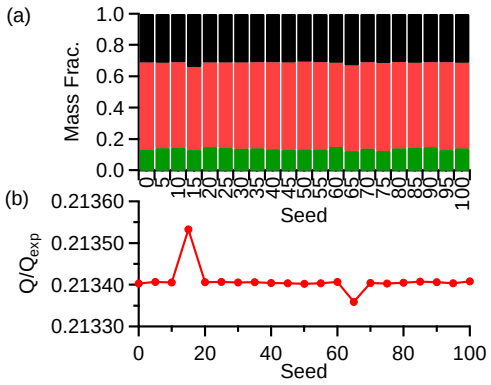

Figure ~~S4~~S7. Diagnostic plots for seed analysis of PMF three factor solution: (a) fractional contribution of OA factors for each seed, and (b) Q/Q_{exp} as a function of seed selected for the chosen number of factors. Changes in mass fraction contribution of each factor are negligible (< 1%) over seed range. Similarly, *Q/Qexp* values at different seed are nearly identical with very small changes (< 1%).

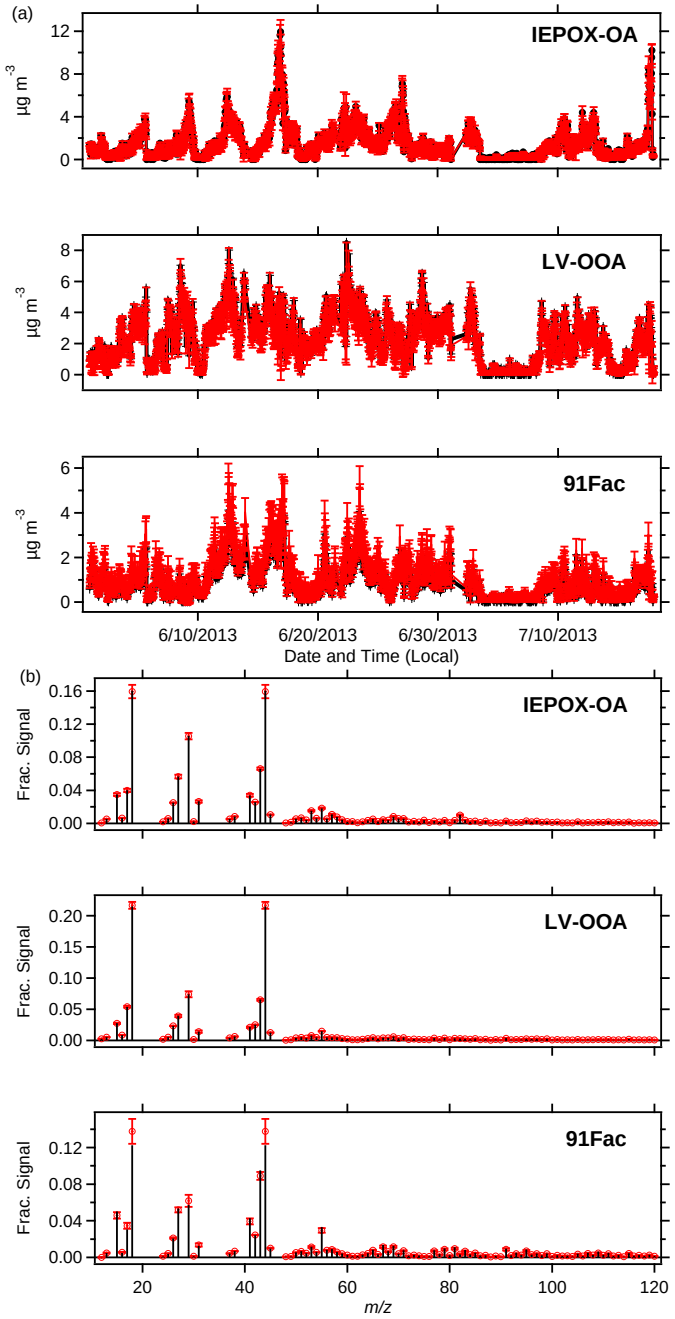

Figure ~~S5~~S8. Results from bootstrapping analysis of the three factor solution of the 2013 SOAS campaign dataset. Average (a) time series and (b) mass spectra are shown in black with 1-σ error bars in red. All four factors show some uncertainty in their mass spectra and time series, which are nonetheless small compared to the general factor profile and contribution.

~~C.~~D. Filter Sampling Methods and Analysis

FLEXPART Model

The intensive filter sampling periods were selected on the basis of the FLEXPART Lagrangian particle dispersion model v. 9.02 (Stohl et al., 2005), driven by analytical data (every 6 hours) and 3 hour forecasts of the Global Forecast System (GFS) of the National Centers for Environmental Prediction (NCEP). Back-trajectory calculations were conducted on a 0.1 x 0.1 degree grid by releasing 10000 air parcels every 3 hours at each SAS field site and following parcels back in time for 72 hours. The resulting 3-hour surface residence time fields (concentration of parcels at a given time between 0 and 100 m above ground) were convolved with emission inventories and then spatially integrated to estimate total emissions injected into the air parcel during each 3-hour interval. This allowed estimation of (1) total emissions load of an air mass sampled at LRK (as well as the other ground sites), (2) the mixture of different emission source types (mobile, biogenic VOCs, biomass burning, etc.), and (3) the age (and hence amount of chemical processing) emissions experienced prior to arrival at LRK. NO_x and SO_2 concentrations were estimated from the National Emission Inventory (NEI), biomass burning emissions from the Fire Inventory from NCAR (FINN, Wiedinmyer et al., 2011) and biogenic VOC emissions were based on results of a MOZART global model (Emmons et al., 2010) simulation using the Model of Emissions of Gases and Aerosols from Nature (MEGAN, Guenther et al., 2006).

Filter Analysis

Table S4. Temperature program and purge gas type used in OC/EC analysis of particle-laden filter punches.

Step	Gas	Hold time (s)	Temperature (°C)
1	He	60	310
2	He	60	480
3	He	60	615
4	He	90	900
5	He	30	Oven off
6	He	8	550
7	He/O_2	35	600
8	He/O_2	45	675
9	He/O_2	45	750
10	He/O_2	45	825
11	He/O_2	120	920

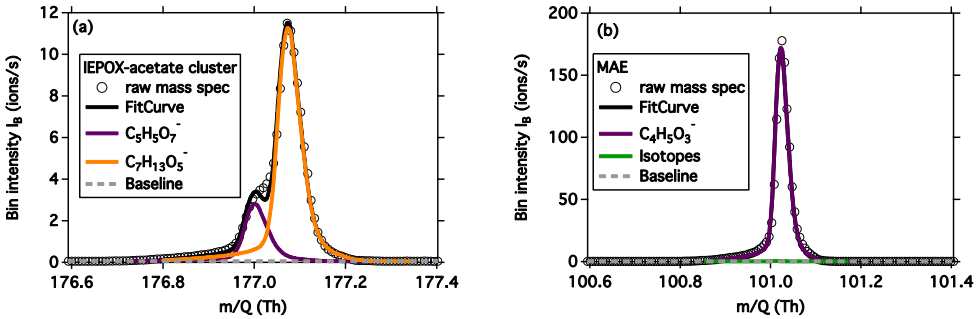

Figure ~~S6~~S9. Typical high-resolution fitting of (a) IEPOX as an acetate cluster, and (b) MAE as a deprotonated ion from HR-ToF-CIMS measurement at LRK site.

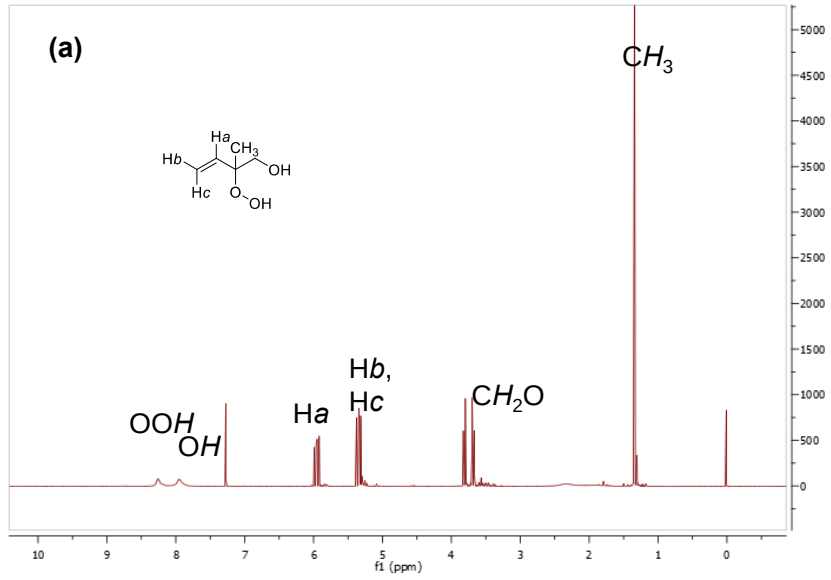

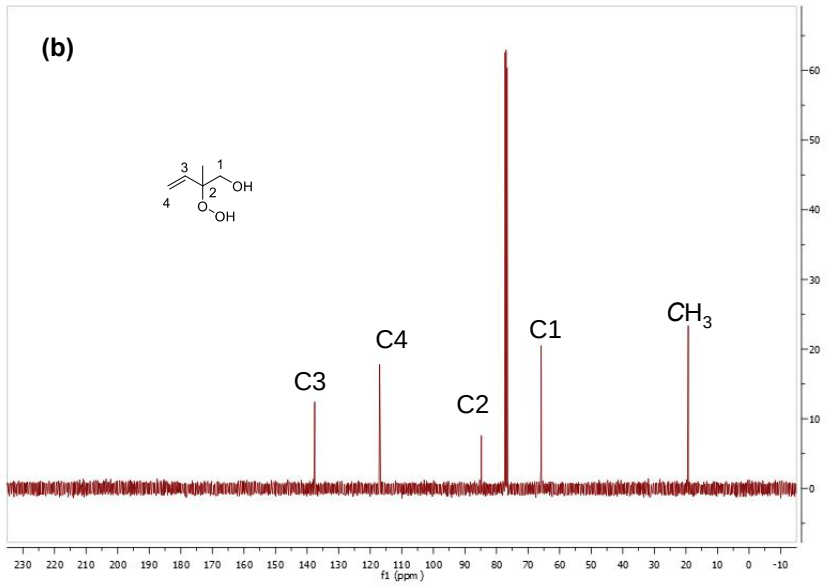

Figure S10. Spectrum of ISOPOOH (2-hydroperoxy-2-methylbut-3-en-1-ol) from (a) ^{1}H NMR (400 MHz, $CDCl_3$); and (b) ^{13}CNMR (100 MHz, $CDCl_3$).

Formatted: Font: Bold, Font color: Auto, Kern at 14 pt

Formatted: Font: Bold, Font color: Auto, Kern at 14 pt

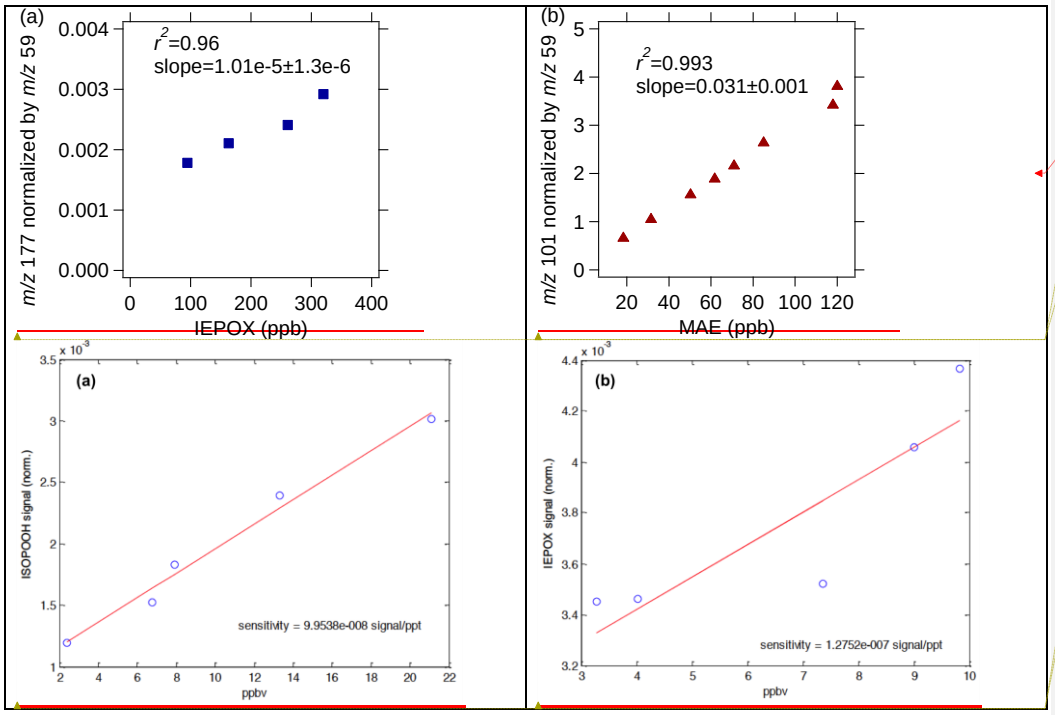

Figure ~~S7~~S11. Response factors of CIMS toward (a) ISOPOOH and (b) IEPOX measured after 2013 campaign. IEPOX response factor is lower compared to that measured in 2013. This is likely due to changes in voltages setting and repairs done after 2013 SOAS campaign.

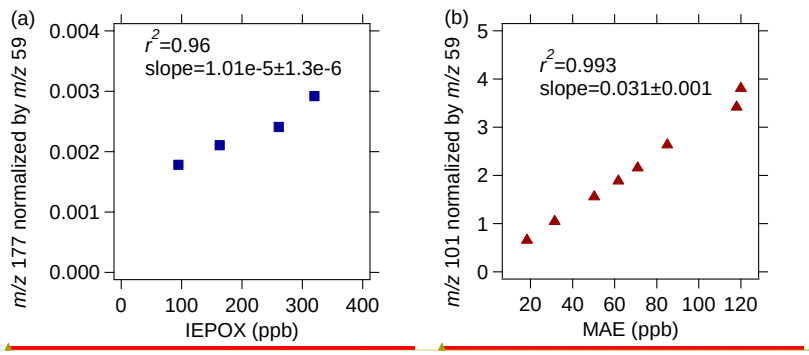

Figure S12. Calibration factors of (a) IEPOX and (b) MAE from HR-ToF-CIMS with acetate ion chemistry conducted before 2013 SOAS campaign.

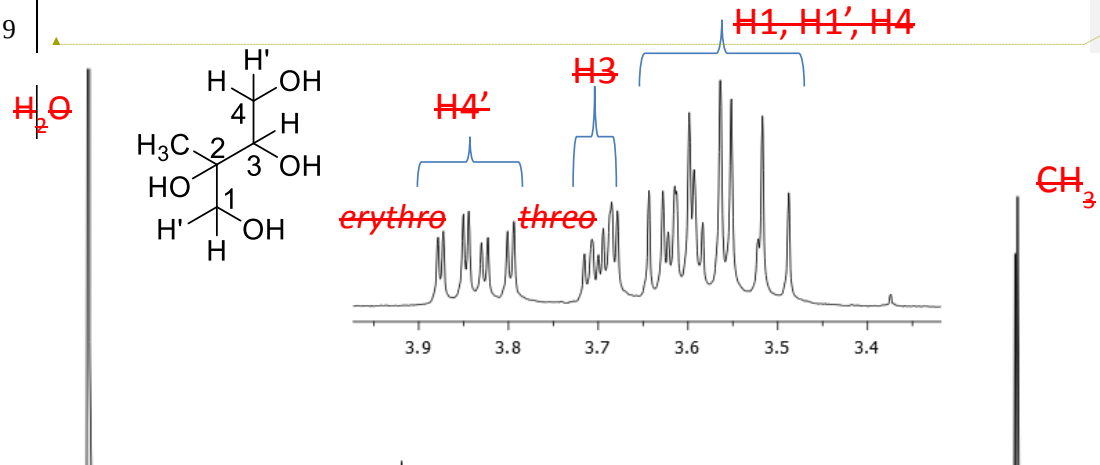

Formatted: Style Style Arial 16 pt Bold Kern at 14 pt + Arial Auto, English (U.S.), Check spelling and grammar

Formatted Table

Formatted: Style Style Arial 16 pt Bold Kern at 14 pt + Arial Auto, English (U.S.), Check spelling and grammar

Formatted: Font: Bold, Font color: Auto, Kern at 14 pt

Formatted: Font: Bold, Font color: Auto, Kern at 14 pt

Formatted: Style Style Arial 16 pt Bold Kern at 14 pt + Arial Auto, Font: Not Bold

Formatted: Style Style Arial 16 pt Bold Kern at 14 pt + Arial Auto, English (U.S.), Check spelling and grammar

Formatted: Style Style Arial 16 pt Bold Kern at 14 pt + Arial Auto, English (U.S.), Check spelling and grammar

Formatted: Font: 16 pt, Bold, Font color: Auto, Kern at 14 pt

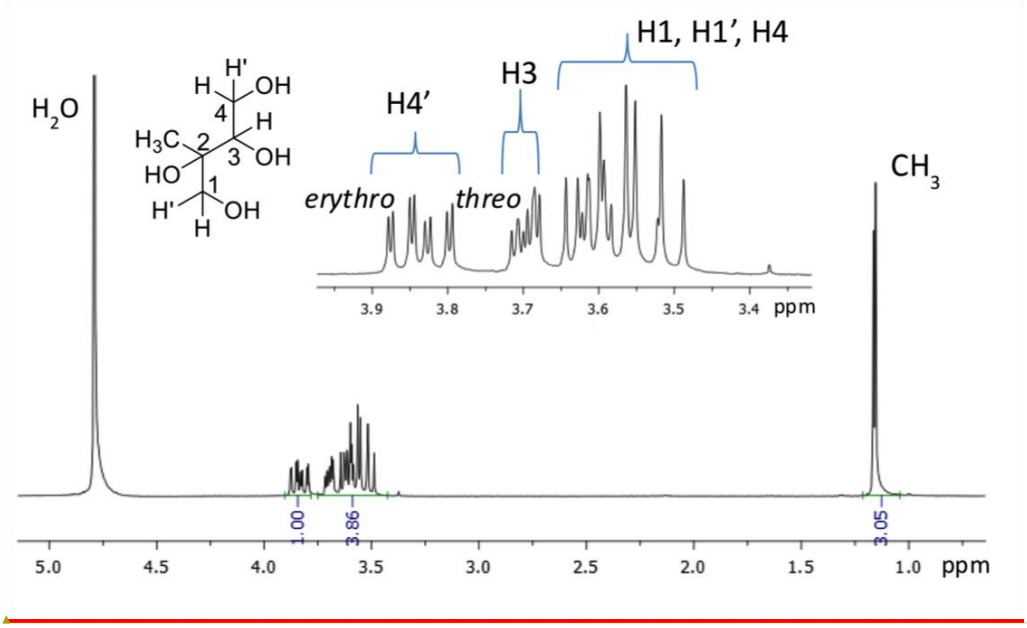

Figure ~~S8~~S13. ^{1}H NMR spectrum (D_2O, 400 MHz) of 2-C-methylerythritol and 2-C-methylthreitol mixture.

Formatted: Font: 16 pt, Bold, Font color: Auto, Kern at 14 pt

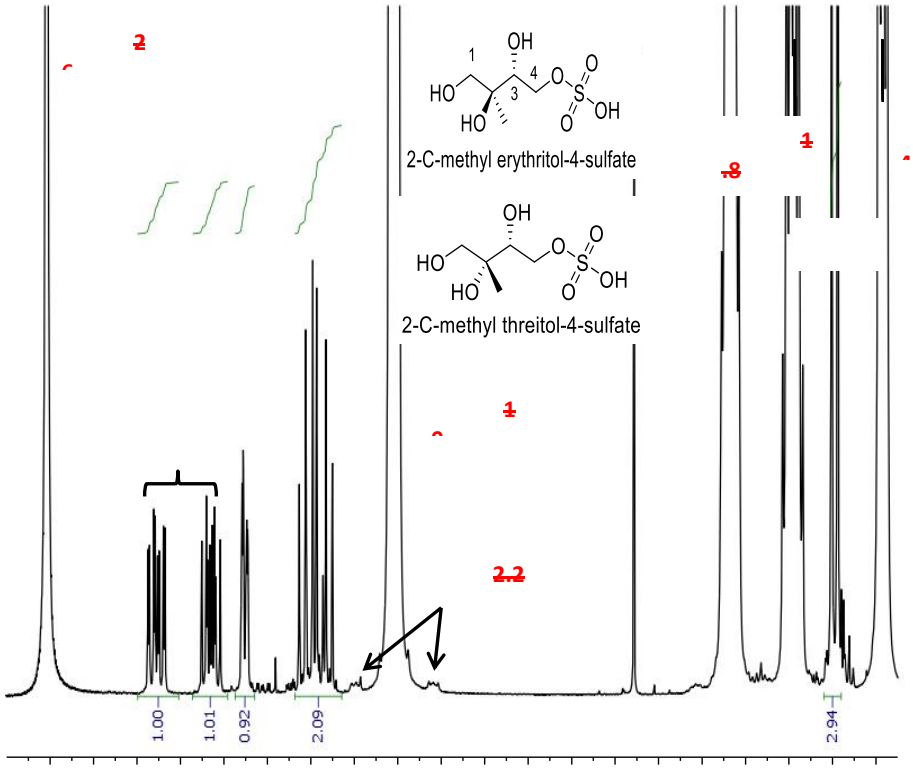
2-C-methyl erythritol-4-sulfate
2-C-methyl threitol-4-sulfate
1.00
1.01
0.92
2.09
2.94

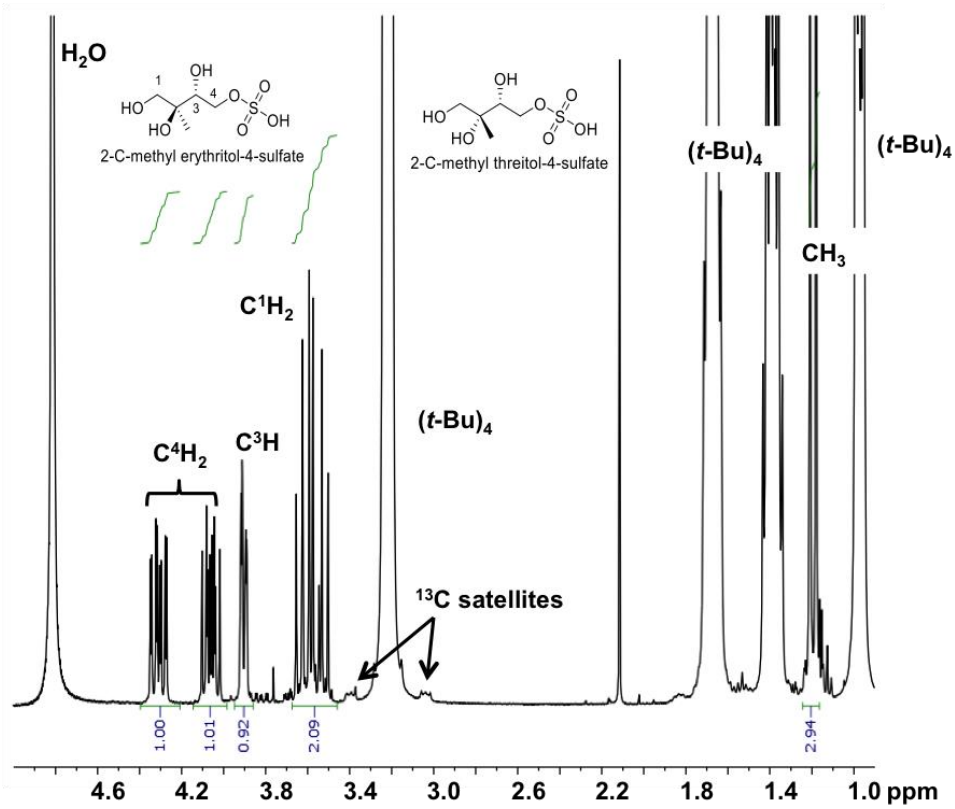

Figure ~~S9~~S14. ^{1}H NMR spectrum (D_2O, 400 MHz) of 2-C-methyltetrol sulfate ester mixture.

Formatted: Line spacing: 1.5 lines

~~D.~~E. Gas- and Particle-phase Analysis

Table S5. Correlation of PMF Factors with collocated measurements and reference mass spectra.

	IEPOX-OA	LV-OOA	91Fac
$r^2_{Time\ Series}$			
CO	0.29	0.38	0.18
NO_x (=NO+NO_2)	0.03	0.00	0.03
NO_y	0.09	0.19	0.16
NO_z	0.08	0.16	0.15
O_x (=NO_2+O_3)	0.07	0.36	0.06
SO_4	0.31	0.23	0.07
ACSM SO_4	0.58	0.39	0.18
ACSM NO_3	0.55	0.62	0.55
ACSM NH_4	0.47	0.48	0.23
CIMS MAE	0.27	0.30	0.33
CIMS IEPOX	0.24	0.31	0.37
PTR-MS Isoprene	0.01	0.08	0.05
PTR-MS MVK+MACR	0.36	0.37	0.47
PTR-MS Acetonitrile	0.12	0.09	0.07
PTR-MS Monoterpenes	0.00	0.02	0.01
LWC	0.00	0.06	0.00
pH	0.05	0.08	0.02
WSOC	0.37	0.28	0.27
$r^2_{Mass\ Spectra}$			
HOA[a]	0.11	0.05	0.24
LV-OOA[a]	0.97	0.97	0.92
SV-OOA[a]	0.55	0.41	0.75
BBOA[a]	0.46	0.28	0.56
82Fac[b]	0.89	0.71	0.82
91Fac[b]	0.54	0.42	0.75
IEPOX-OA[c]	0.81	0.65	0.83
Lab IEPOX SOA[c]	0.55	0.32	0.49

References: (a) Ng et al. (2011), (b) Robinson et al. (2011), and (c) Budisulistiorini et al. (2013)

Table S6. Correlation of isoprene-derived SOA tracers measured by GC/EI-MS and UPLC/DAD-ESI-HR-Q-TOFMS with collocated measurements.

r^2	MeTHF	MeTetrol	Triol	2-MG	IEPOXOS	IEPOXOSdimer	MAEOS
CO	0.07	0.34	0.29	0.45	0.36	0.1315	0.2625
NO_x (=NO+NO_2)	0.03	0.00	0.01	0.03	0.00	0.04	0.00
NO_y	0.16	0.11	0.12	0.38	0.1315	0.02	0.2223
NO_z	0.29	0.17	0.23	0.35	0.2528	0.1012	0.3537
O_x (=NO_2+O_3)	0.05	0.01	0.01	0.00	0.04	0.0203	0.05
SO_4	0.06	0.36	0.31	0.35	0.34	0.1415	0.2826
ACSM SO_4	0.09	0.36	0.31	0.31	0.3935	0.2422	0.3531
ACSM NO_3	0.17	0.41	0.38	0.46	0.4240	0.32	0.4441
ACSM NH_4	0.07	0.32	0.27	0.32	0.3430	0.2018	0.3430
CIMS MAE	0.45	0.26	0.33	0.37	0.3231	0.2423	0.4847
CIMS IEPOX	0.41	0.21	0.28	0.30	0.2625	0.2019	0.4241
PTR-MS Isoprene	0.06	0.03	0.03	0.09	0.0809	0.0405	0.0506
PTR-MS MVK+MACR	0.15	0.24	0.26	0.29	0.3432	0.2221	0.21
PTR-MS Acetonitrile	0.01	0.20	0.18	0.33	0.30	0.17	0.1113
LWC	0.02	0.00	0.01	0.02	0.0305	0.0102	0.0002
pH	0.07	0.05	0.06	0.06	0.1113	0.0708	0.0506
WSOC	0.06	0.33	0.31	0.29	0.3840	0.2830	0.2122

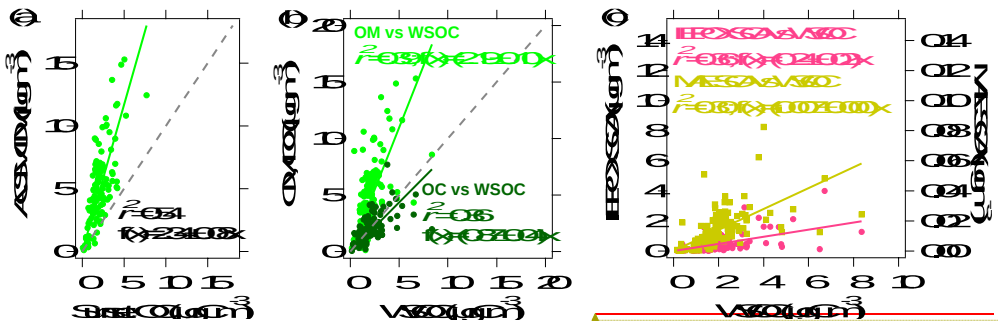

Formatted Table

Formatted: Font: 16 pt, Bold, Font color: Auto, Kern at 14 pt

Formatted: Font: Bold

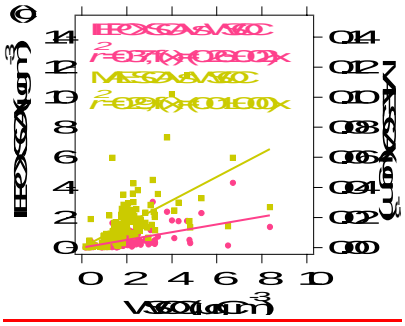

Figure ~~S10~~S15. Comparisons of organic ~~aerosol~~matter (OM) by ACSM with organic carbon (OC) by Sunset OC/EC (a) and water soluble organic carbon (WSOC) measurements (b). OM:OC ratio was estimated to be 2.34. Comparisons of WSOC with SOA tracers (c) indicate that IEPOX- and MAE-derived masses might explain 25% and 0.5% of the WSOC mass, respectively.

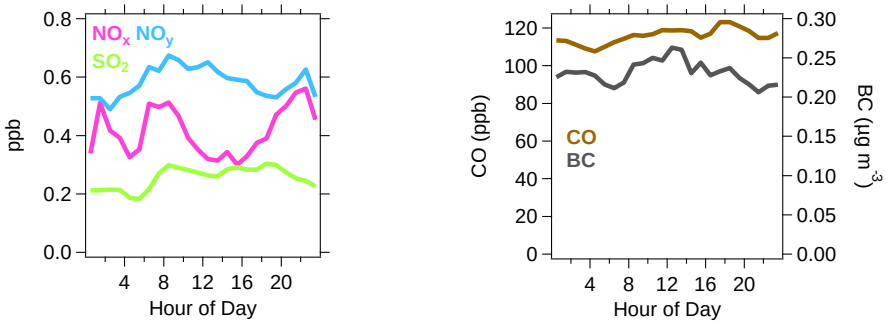

Figure ~~S11~~S16. Diurnal variation of NO_x, NO_y, and SO_2 (left) and CO and BC (right). Overall, concentration of primary tracers (i.e., NO_x, SO_2, CO, and BC) are small.

Potential Source of 91Fac

The source of 91Fac is currently a matter of speculation. Aged biomass burning aerosol (Robinson et al., 2011) has been suggested because of the similarity of the profile to that of biomass burning aerosols, except for absence of prominent ions at *m/z* 60 and 73 expected from levoglucosan (Alfarra et al., 2007). A more recent study proposed that fresh BVOC (i.e., monoterpene) oxidation products are a possible source based on chamber experiments (Chen et al., 2014). At LRK, 91Fac correlates moderately with sulfated and nitrated species of monoterpene SOA, i.e., $C_{10}H_{16}O_7S$ (r^2 = 0.37; Fig. 5) and $C_9H_5NO_8S$ (r^2 = 0.41), but weakly with acid species, i.e., terpenylic acid ($C_8H_{12}O_4$, r^2 = 0.36). Good correlation between LRK 91Fac and aerosol nitrate (r^2 = 0.55) and weak association (r^2 < 0.2) with NO_x, NO_y, and CO (Table S5) are indicative of an aged aerosol that may be associated with nitrate radical chemistry or as yet unidentified pathways.

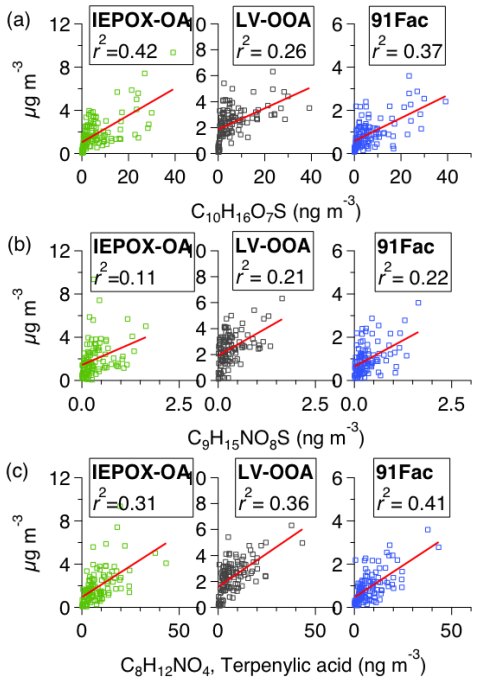

Figure S17. Correlation of PMF factors with α-pinene derived organosulfate, $C_{10}H_{16}O_7S$ (a), nitrated organosulfates, $C_9H_{15}NO_8S$ (b), and terpenylic acid $C_8H_{12}NO_4$ (c).

HYSPLIT model

Atmospheric transport during the ~~2014~~2013 SOAS field study was analyzed by computing air trajectories using the HYSPLIT Model (http://ready.arl.noaa.gov/HYSPLIT.php) from the Air Resources Laboratory of the National Oceanic and Atmospheric Administration (NOAA). Wind fields from the NOAA-NCAR Global Reanalysis data set were used as input to HYSPLIT for trajectory calculations. Vertical air parcel motion was determined from estimated vertical velocities in the input data set. Air trajectories were computed 24 hours backward in time from Look Rock in one-hour time steps with ending heights at Look Rock of 100, 500 and 1500 m above ground level. Each trajectory arrived at Look Rock at midnight (EST) or 01:00 EDT.

To further examine the influence of NO_x emissions as well as aerosol acidity, we examined where air masses originated from to our site using back trajectory (HYSPLIT model) analysis. Figs. ~~S12~~S18 and ~~S13~~S19 present the back-trajectories of air mass arrived at the LRK site at 01:00 local time (00:00 EST) of the date on each plot. During periods (10 – 16 June 2013) of high levels of IEPOX-derived SOA mass, the model shows that air masses were coming from the south at the beginning and slowly shifted from the west for the next three days (Fig. ~~S12~~S18). Throughout periods when IEPOX-derived SOA is low (2 – 8 July 2013), air masses were coming from the south and southeast. Considering that the site is located at about 800 m above sea level, it is less likely that the air masses (at 100 m above the surface) carried NO_x from nearby sources. Air masses at 500 m and 1500 m above the surface might carry some NOx, however, it might have been diluted during the transport.

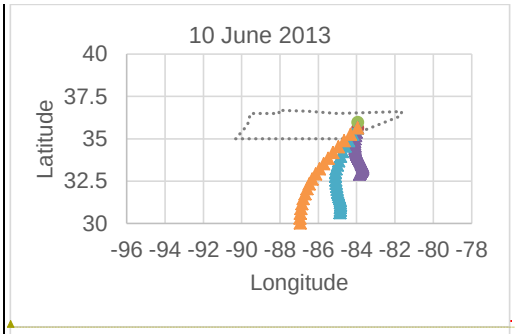

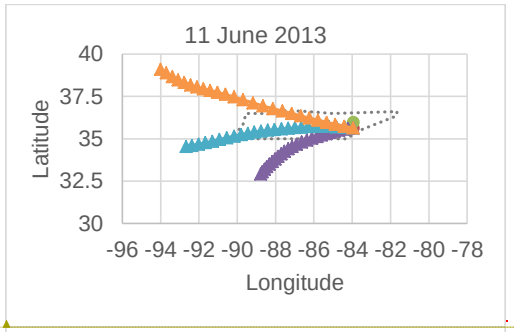

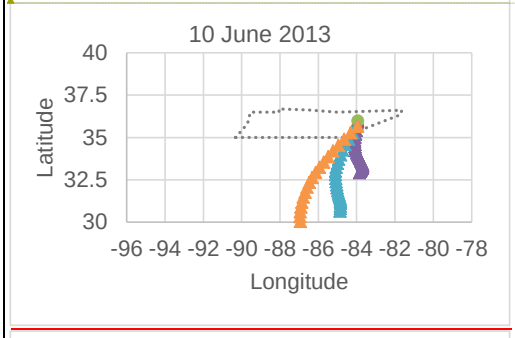

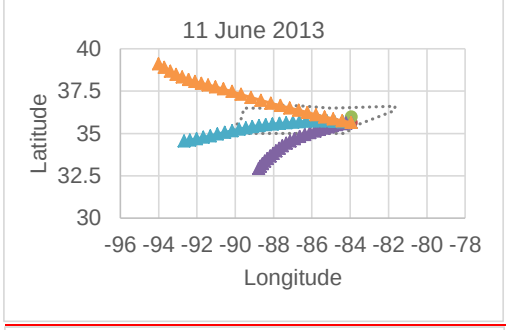

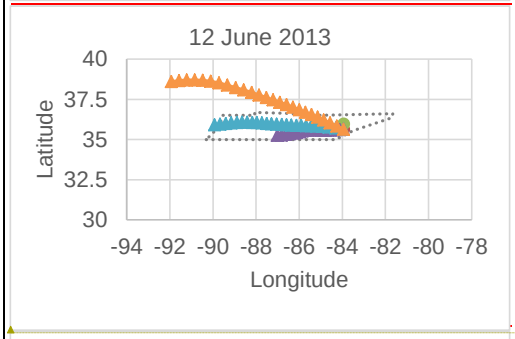

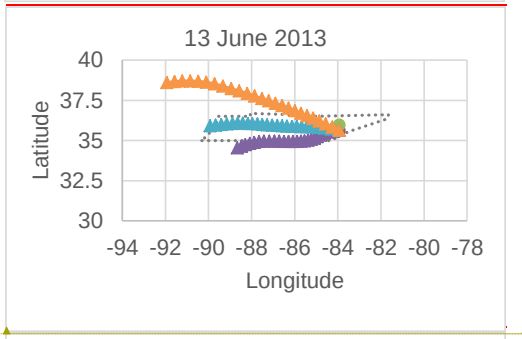

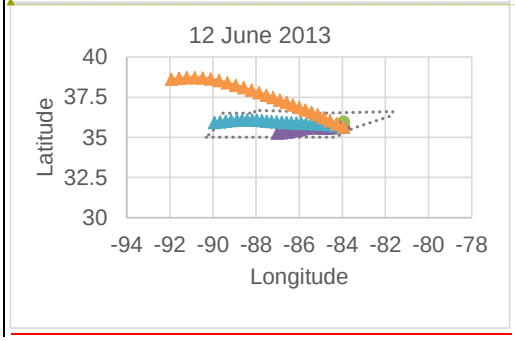

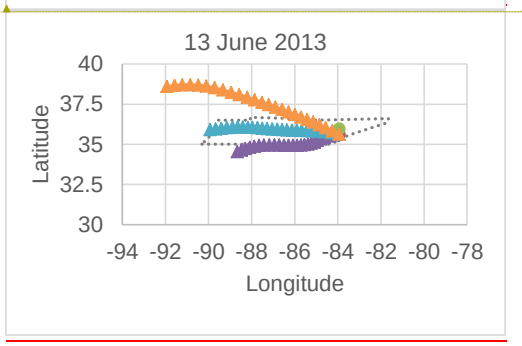

Formatted: Font: (Default) Arial

Formatted: Font: (Default) Arial

Formatted: Font: (Default) Arial

Formatted: Font: (Default) Arial

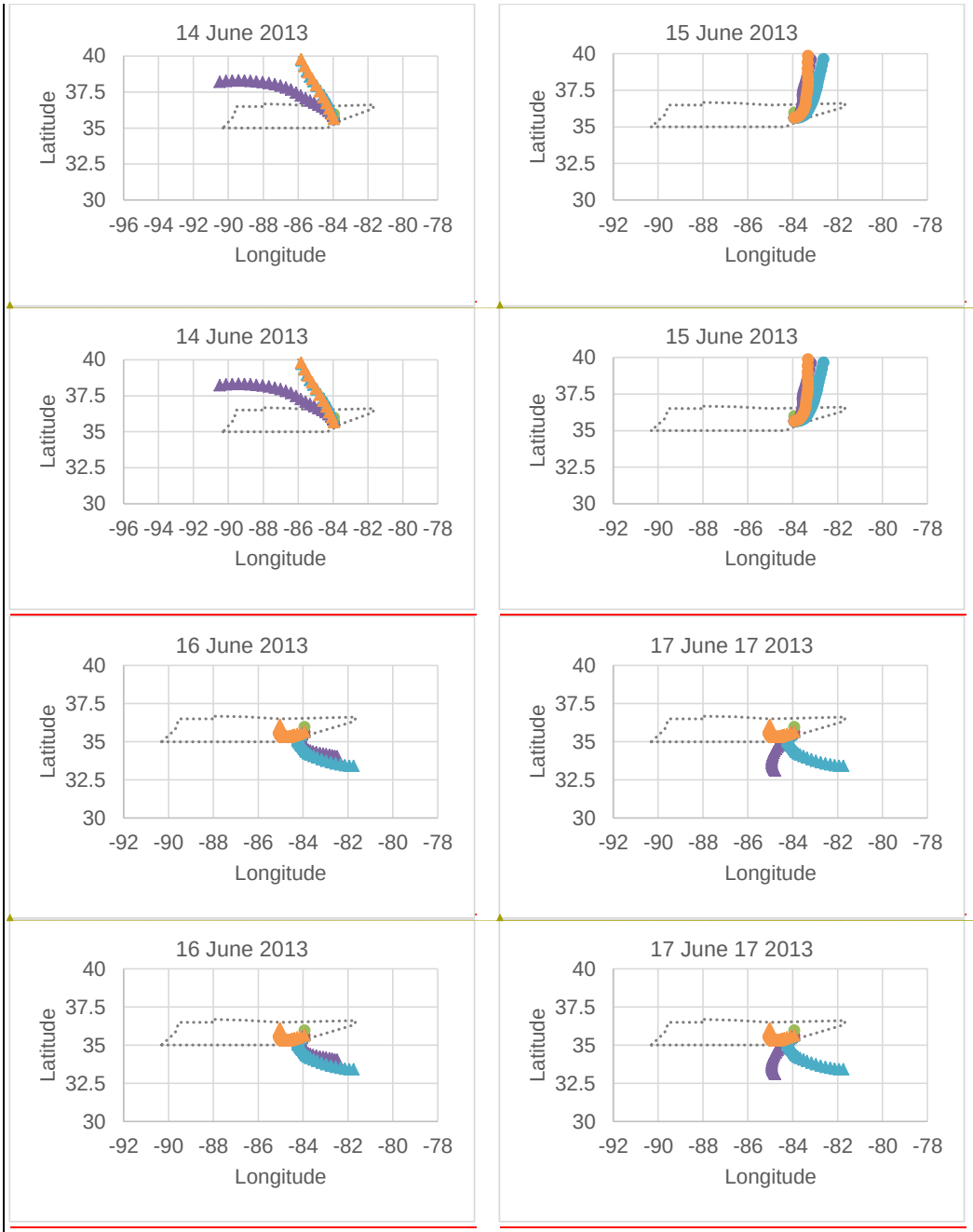

Formatted: Font: (Default) Arial

Formatted: Font: (Default) Arial

Formatted: Font: (Default) Arial

Formatted: Font: (Default) Arial

Figure ~~S12~~S18. Air mass back trajectories from HYSPLIT 24-hr model ~~duringthe~~during the first and second intensive filter sampling periods when high IEPOX-derived SOA formation was observed. The backtrajectories were estimated at elevation of 100 m (orange), 500 m

(turqoise), and 1500 m (purple) above the site. Concentration of IEPOX-derived SOA started to decrease on June 17, 2013.

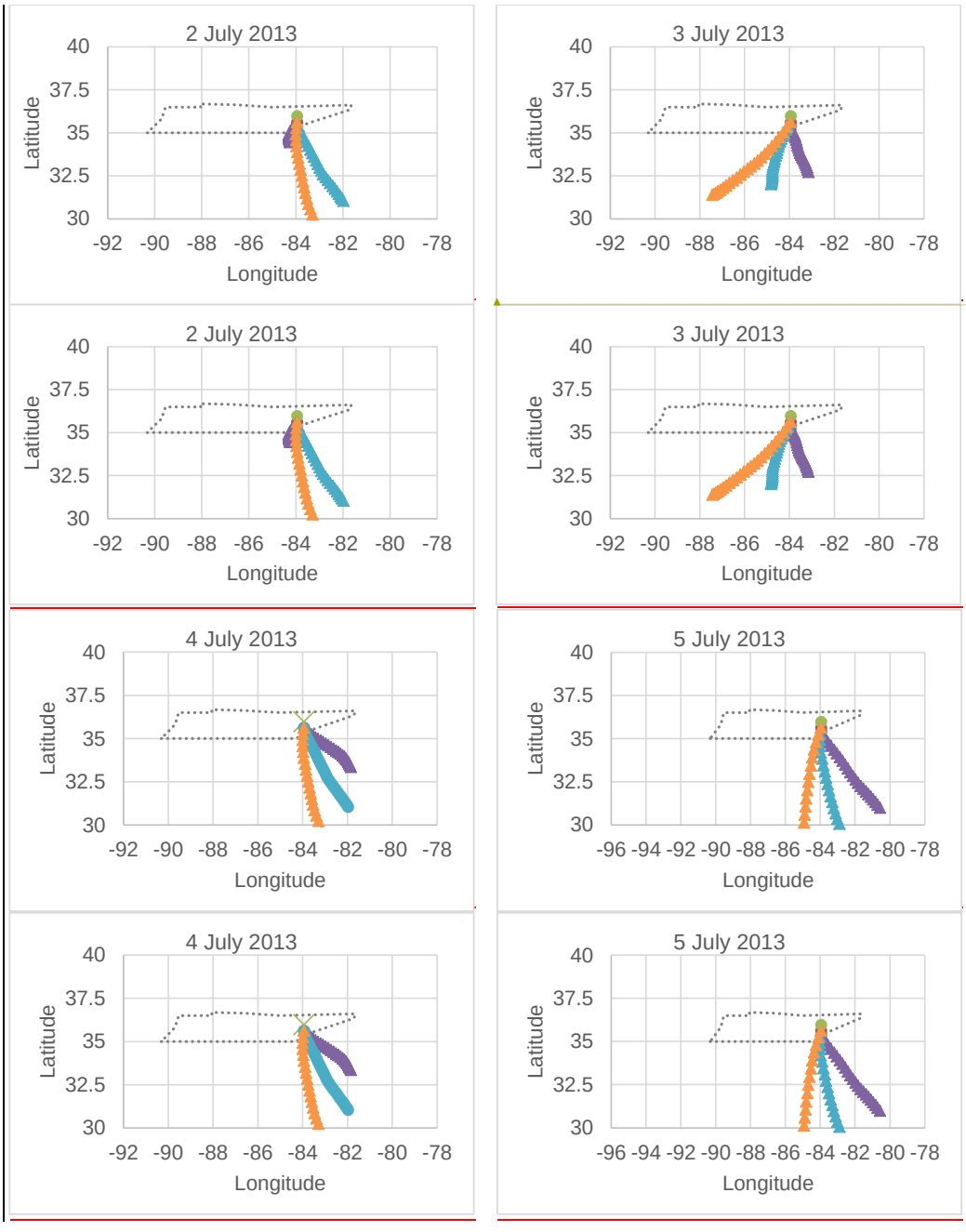

Formatted: Font: 10 pt

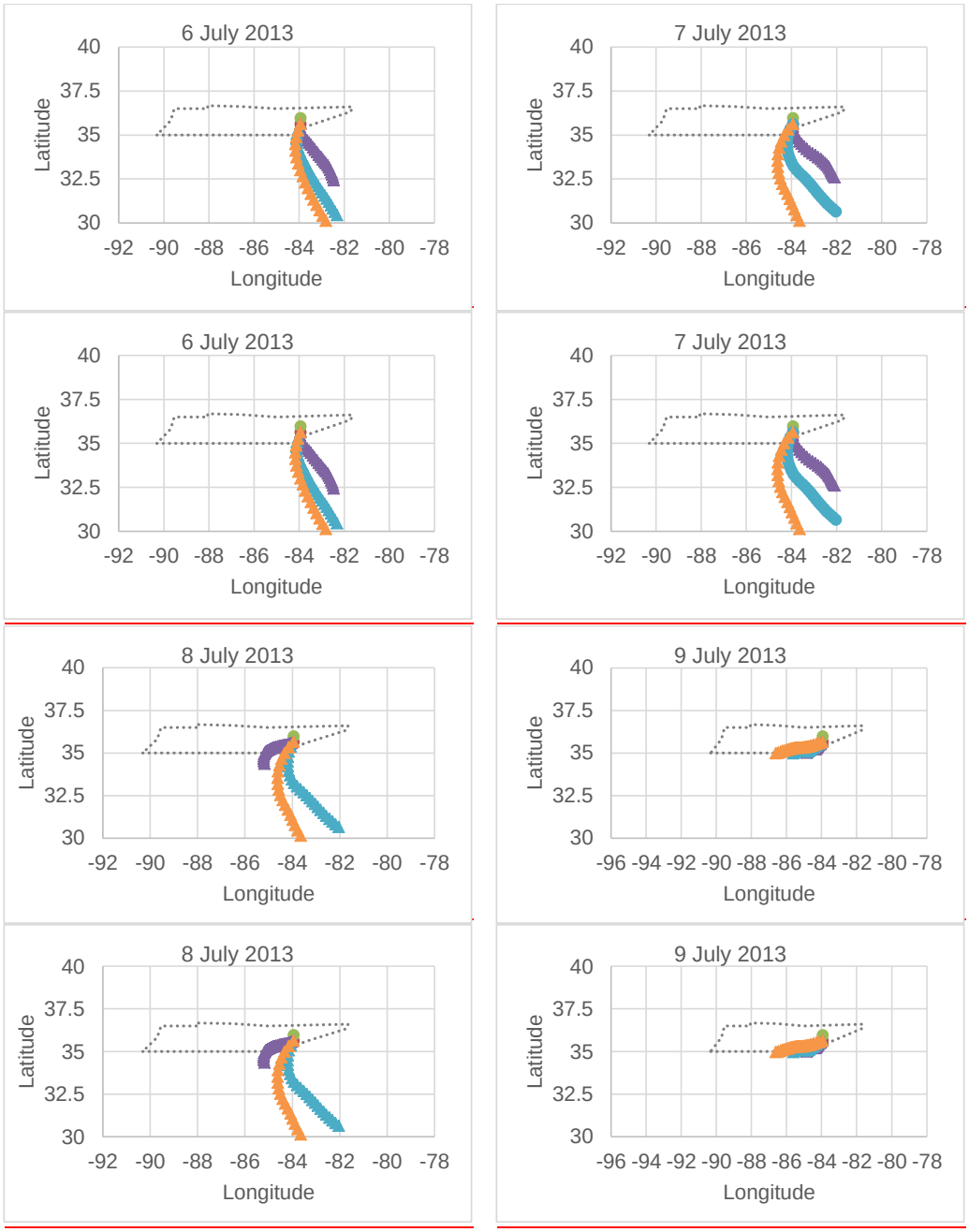

Figure ~~S13~~S19. Air mass back trajectories from HYSPLIT 24-hr model during low IEPOX-derived SOA formation of 2 – 8 July 2013. 9 July 2013 was the beginning of the fourth intensive period. The backtrajectories were estimated at elevation of 100 m (orange), 500 m (turquoise), and 1500 m (purple) above the site.

Results from simpleGAMMA

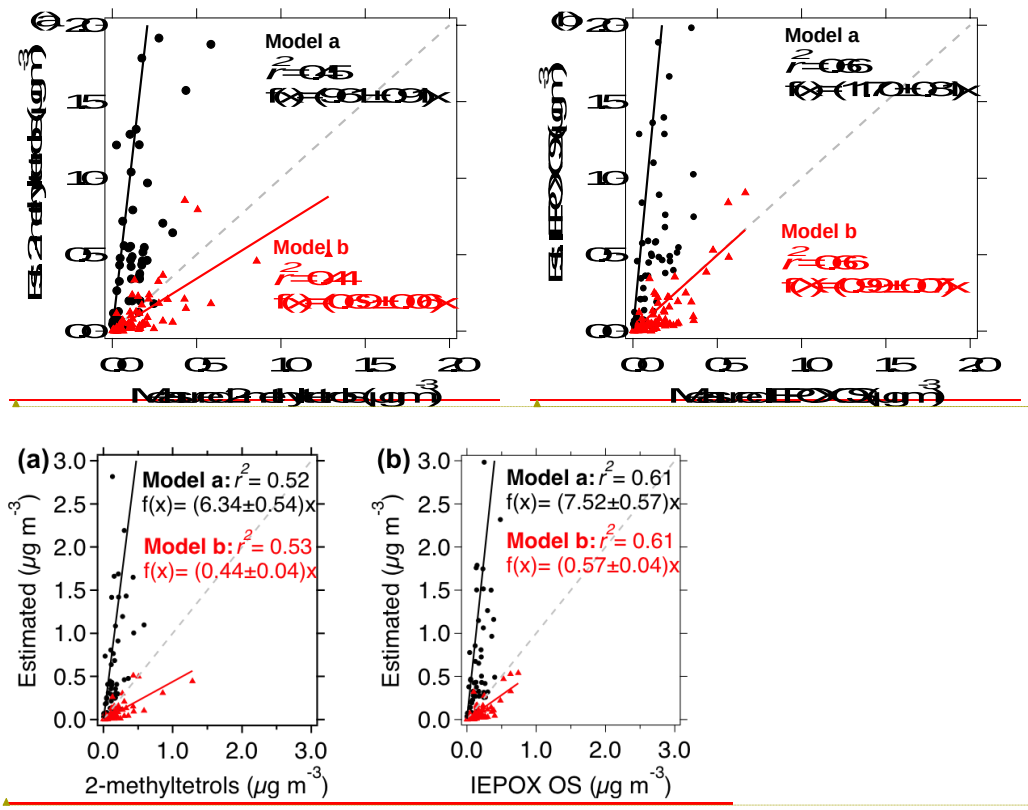

Figure ~~S14~~S20. Correlation of (a) 2-methyltetrols and (b) IEPOX-derived organosulfate (IEPOX OS) estimated by simpleGAMMA by assumming H* of 3.0 × 10^7 (Nguyen et al., 2014) (model a) and 2.7 × 10^6 (Pye et al., 2013) (model b).

Formatted: Font: Bold

Formatted: Font: Bold

Formatted: Font: Bold